The Effects of Nanopattern Surface Technology and Targeted Metabolic Therapies on Orthopaedic Implant Related Infections

Donald Hansom

MRCS, MBChB, BSc (Hons)

Submitted in fulfilment of the requirements for the Doctor of Medicine

School of Medicine College of Medical, Veterinary and Life Sciences

University of Glasgow

August 2016

Abstract

Bacterial biofilm infections cause significant morbidity in orthopaedic joint replacement. One of the most common bacteria in orthopaedic prosthetic infections is *Staphylococcus aureus*. Infection causes implant failure due to bacterial adherence and subsequent biofilm production. Nanotopography refers to the topography of a surface at the nanometre level and has major effects on cell behaviour. Studies suggest that surface nanotopography impacts the differential ability of staphylococci species to adhere, and may reduce orthopaedic implant infection rate. This research thesis focuses on bacterial adhesion on nanofabricated materials, and investigates the related metabolic changes and possible interventions.

Staphylococcus aureus growth and quantification methods were optimised, with regard to growth media, incubation time and lysozyme incubation time. Both polystyrene and titanium (Ti) nanosurfaces were studied. Adhesion analysis was performed using fluorescence imaging, quantitative PCR, and bacterial percentage coverage. Metabolomic analysis was conducted by substitution with 'heavy' labelled glucose into growth medium, thus allowing for bacterial metabolomic analysis and identification of up-regulated, labelled metabolites and pathways.

Bacterial growth was optimal using DMEM + supplement media, with adhesion occurring after 1hr bacterial incubation. Optimal lysozyme incubation for bacterial quantification using qPCR was 2hr. These parameters were used for all subsequent experimentation. Surface topography affects cell behaviour, bacterial adhesion and long term implant survival can be affected. This study found reduced bacterial adhesion on the SQ and HEX polystyrene patterns. While not found to be significant, this trend was supported by a lower average percentage bacterial coverage on both the SQ and HEX patterns ($P=0.05$ and $P=0.01$, respectively). It may be that the SQ and HEX nanopatterns are the optimal nanopit orientation required to prevent bacteria microcolony formation, keeping the bacteria in small, isolated clusters. In addition, this series of investigations showed an increase in bacterial concentrations on both the 2.5Hr ($P<0.05$) and 3Hr ($P<0.01$) treated Ti nanowire discs when compared to the

polished Ti control disc, suggesting nanoroughness increases are associated with elevated bacterial adhesion. This theory was further supported by average percentage coverage, being significantly higher on the 2.5Hr and 3Hr treated discs ($P<0.001$). If, however, a disordered NC Ti nanopattern, hexagonal in nature, is used bacterial adhesion is significantly reduced when compared to a polished, control surface ($P<0.05$). The bacterial percentage coverage was also noted to be significantly lower on the NC surfaces, with over a 10-fold reduction when compared to the control surface. It is postulated that this reduction is through similar mechanisms to those described by Ivanova *et al*, and primarily related to altered surface interactions. Metabolomic analysis demonstrated increased intensity counts for key metabolites (pyruvate, aspartate, alanine and carbamoyl aspartate) involved in bacterial aggregation, proteoglycan and DNA synthesis. These pathways are also known to be important in bacterial biofilm production. Therapeutic targeting of these pathways (CA and ß-CLA) was found to result in significantly reduced bacterial adhesion.

This study shows that by altering nanotopography bacterial adhesion, and therefore, biofilm formation can be affected. Specific nanopatterned surfaces may reduce implant infection associated morbidity and mortality. The identification of metabolic pathways involved in adhesion allows for a targeted approach to biofilm eradication in S. *aureus*. This is of significant benefit to the patient, the surgeon and the NHS, and may well extend far beyond the realms of orthopaedics.

Table of Contents

List of tables

List of figures

List of publications and presentations based on thesis

Hansom D, Tsimbouri M, Ramage G, Burgess K, Dalby M, Meek D and Clarke J. 'Nano-topographical modulation of cells and bacteria for next generation orthopaedic implants.' Centre of Cell Engineering – Glasgow Orthopaedic Research Initiative, December 2014.

Hansom D, Ramage G, Burgess K, Gadengaard N, Millar N, Clarke J. 'The Effects of Nanopattern Surface Technology on Orthopaedic Joint Replacement Infection.' Bone & Joint Journal Orthopaedic Proceedings Supplement, 2015. 97-B(SUPP 3): p. 2.

Hansom D, Ramage G, Burgess K, Meek D, Clarke J. 'Nano-topographical modulation of cells and bacteria for next generation orthopaedic implants.' El-Minia University Hospital Scientific Day, Egypt, February 2015.

Hansom D, Ramage G, Burgess K, Meek D, Clarke J. 'The Effects of Nanopattern Surface Technology on Orthopaedic Joint Replacement Infection.' Glasgow Meeting of Orthopaedic research, March 2015.

Hansom D, Ramage G, Burgess K. 'The Effects of Nanopattern Surface Technology on Orthopaedic Joint Replacement Infection.' British Orthopaedic Association congress, Liverpool, UK, September 2015.

Hansom D, Ramage G, Burgess K. 'The Effects of Nanopattern Surface Technology on Orthopaedic Joint Replacement Infection.' European Federation of National Associations of Orthopaedics and Traumatology, Geneva, Switzerland, June 2016.

Acknowledgements

Throughout the course of this research I have had the opportunity to work with a multitude of people, all of whom have in some way contributed to this research.

First and foremost, I'd like to thank Professor Gordon Ramage for his guidance and support. I am truly grateful for the time you spent explaining the intricacies of medical research to a clinician. Without these foundations this research would not have been possible let alone credible. Additionally, your help with proof reading this work was invaluable. I'd also like to thank Dr Karl Burgess for his guidance both during the initial planning and subsequent metabolomic aspect of this research. Both my supervisors have been extremely patient, and for that I am appreciative.

I would like to acknowledge my collaborators, Professor Nikolaj Gadegaard for his help in polystyrene nanofabrication and imaging advice and Dr Monica P Tsimbouri, for her help in securing titanium nanopatterns. This collaboration was vital to this research and much appreciated. In addition, I acknowledge my research funders, AOUK and GLAMOR for their financial support towards this research.

I would also like to thank Dr David Lappan for his technical and statistical advice. Thanks also to the other students at both the Glasgow University Dental School and the Department of metabolomics. Dr Laurence Stipetic, thank you for your help in both demonstrating and explaining metabolomic laboratory methods and being available for general advice and frustration venting! Thanks also to Ranjith Rajendran, Lindsay O'Donnell and Leighann Sherry for your help and advice at the Dental School laboratory, without which I'm sure this research would have taken considerably longer.

Finally, I'd like to thank my amazing wife Laura. Your steadfast support and encouragement in all aspects of our life have helped me complete this research, and for that, I cannot thank you enough.

Author's Declaration

I declare that I have carried out the work described in this thesis unless otherwise acknowledged or cited, under the supervision of Professor Gordon Ramage, Dr Karl Burgess and Mr Neal Millar. I further declare that this thesis has not, in whole or in part, been submitted for any other degree.

Donald Hansom

Abbreviations

AGR:	Accessory gene regulator
ANOVA:	Analysis of variance
ATP:	Adenosine triphosphate
Bap:	Biofilm-associated protein
ß-CLA:	Beta-chloro-L-alanine
BHI:	Brain heart infusion
CA:	Carbamoyl-aspartate
CE:	Capillary electrophoresis
CEW:	Chloroform, ethanol and water
ClfB:	Clumping factor D
CS:	Cysloserine
CFU:	Colony forming units
CoCR:	Cobalt chrome
CoNS:	Coagulase negative staphylococcus
CRP:	C-reactive protein
Ct:	Cycle threshold
CV:	Crystal violet
CWA:	Cell wall anchored proteins
dH_2O:	Distilled water
DNA:	Deoxyribonucleic acid
DMEM:	Dulbecco's modified eagle's media

D-MEM:	Dulbecco's modified eagle medium
DSQ:	Disorganised square
DW:	Dry weight
ECM:	Extracellular matrix
eDNA:	Extracellular DNA
EDTA:	Ethylenediaminetetraacetic acid
EPS:	Extracellular polymeric substances
ESR -	Erythrocyte sedimentation rate
FCS:	Foetal calf serum
FnbpA/B:	Fibronectin-binding proteins A/B
HA:	Hydroxyapatite
HEX:	Hexagonal
HCL:	Hydrogen chloride
ICA:	Intercellular adhesion
LB:	Luria Bertoni
LC:	Liquid chromatography
MHB:	Mueller Hinton broth
MIB:	Meat infusion broth
MIC:	Minimum inhibitory concentration
MS:	Mass spectrometry
MSCRAMM:	Microbial surface components recognising adhesive matrix molecules
MSC:	Mesenchymal stem cells

NB:	Nutrient Broth
NC:	Nanocauseway
NCTC:	National collection of type cultures
NG:	Nanograss
NHS:	National health service
NW:	Nanowire
OD:	Optical density
PBS:	Phosphate buffered saline
PCR:	Polymerase chain reaction
PMMA:	Polymethylmathacrylate
PTFE:	Polytetrafluoroethylene
PTSAgs:	Pyrogenic toxic superantigens
qPCR:	Quantitative polymerase chain reaction
RNA:	Ribonucleic acid
rpm:	Revolutions per minute
RT:	Reverse transcription
SD:	Standard deviation
SdrC:	Serine-aspartate repeat protein C
SEM:	Scanning electron microscopy
SQ:	Square
TE:	$T_{10}E_1$ buffer
THR:	Total hip replacement

Ti:	Titanium
TJA:	Total joint arthroplasty
TKR:	Total knee replacement
TSB:	Tryptic soy broth
TSS:	Toxic shock syndrome
TSST-1:	Toxic shock syndrome toxin-1
UHMWP:	Ultra-High Molecular Weight Polyethylene
UV:	Ultraviolet

Chapter 1

Introduction

1.1 Implantable medical devices

The history, development and current usage of medical implants will now be discussed, with emphasis on orthopaedic joint replacement surgery and the materials used therein.

1.1.1 Medical implants

Implantable medical devices or biomaterials are used extensively in modern medicine. They are defined as substances other than food or drugs that are contained in therapeutic or diagnostic systems (Peppas and Langer 1994). They have been used throughout history, playing an important role in the treatment of disease and improvement of health care (Langer and Tirrell 2004). Historically, biomaterials such as gold were used in dentistry by the Romans, Chinese and Aztecs, and recorded history highlights the use of wooden teeth and glass eyes (Ratner 2004). Since the development of synthetic materials at the turn of the nineteenth century, biomaterials have become increasingly used in health care. Polymethylmathacrylate (PMMA) was found to evoke only a mild foreign body reaction, and was subsequently used in dentistry in the 1930s, and later by Sir John Charnley in the 1960s as the basis for the cement used in total hip joint replacements (THR) (Ratner 2004). He suggested that the bone cement was used as a ‘grout’ rather than an ‘adhesive’, and that fixation was achieved by interlocking. This allowed the body weight to be more evenly distributed and dispersed over a larger surface area, signalling a turning point in THR (Charnley 1960). In addition to cement, Charnley also developed the use of polytetrafluoroethylene (PTFE) as a synthetic cartilage, designed to line the acetabulum of the pelvis. However, despite promising laboratory predictions PTFE showed significant wear within the first few years, resulting in high volumes of wear debris that elicited an intense foreign body reaction. Following this catastrophic failure, Charnley began to use Ultra High Molecular Weight Polyethylene (UHMWP), which at the time was used in the impact bearings of mechanical looms, and he found this biomaterial to have superior wear properties to that of PTFE (Gomez and Morcuende 2005). The qualities that made this particular biomaterial the ideal choice for THR were, excellent wear

resistance, low friction and high impact strength, attributes that remain similar even today (Kurtz, Muratoglu et al. 1999). In addition to orthopaedics, biomaterials are used throughout the field of medicine. For instance cardiothoracic heart valve replacements can be fabricated from a variety of substances, such as carbons, metals, elastomers, fabrics and natural products (i.e. porcine). These can dramatically improve cardiac function following implantation leading to a rapid improvement in symptoms (Ratner 2004). Dental implants have been previously mentioned in relation to PMMA; however, the widespread use of titanium implants to form artificial roots for crown fixation has transformed implantology. Titanium has been found to provide a tight seal (via osseointegration) against bacterial invasion, and appears to form a tight apposition with the bone in the jaw improving implant longevity (Ratner 2004). Intraocular lenses made from PMMA or silicone are used to replace the natural lens of the eye when damaged or cataractous (Lloyd, Faragher et al. 2001). Good vision can be restored almost immediately and the success rate is reported at over 85% (Foster, Fong et al. 1989).

It is clear from the above examples that biomaterial science is an ever expanding, important and useful area of development that has the ability to significantly improve patient morbidity and mortality. Simple interventions, such as intra-venous cannulas right through to complex orthopaedic prosthetic replacements, all have their foundations in biomaterial science. As previously mentioned, a wide variety of biomaterials have been used throughout history and in numerous medical sub-specialities. One of the largest demands on biomaterials today is from the orthopaedic community.

1.1.2 Hip and knee joints

1.1.2.1 The Hip joint

The natural hip joint is a multi-axial ball and socket type synovial joint as shown in Figure 1-1. It consists of an articulation between the femoral head and the acetabulum of the pelvis, and with the addition of multiple ligaments, labral tissue and an articular capsule creates a highly mobile yet stable joint (Moore, Agur et al. 2002).

Figure has been removed due to Copyright restrictions

Figure 1-1 The native hip joint adapted from (System 2003)

1.1.2.2 The Knee Joint

In comparison, the knee joint is a hinge type synovial joint as shown in Figure 1-2. It consists of 3 articulations, the lateral and medial articulations between the femoral and tibial condyles and the articulation between the patella and the femur anteriorly (Moore, Agur et al. 2002). In contrast to the hip joint, the bony geometry of the knee is inherently unstable and relies on a collection of strong ligaments for stability as well as a strong fibrous joint capsule.

Figure has been removed due to Copyright restrictions

Figure 1-2 The native knee joint. Adapted from (System 2003)

Both joints, however, rely on intact articular cartilage for a smooth, pain free range of motion. Hyaline (meaning 'glass-like') cartilage covers articular surfaces of synovial joints and functions to distribute weight-bearing forces and reduce friction. It is entirely avascular, aneural and alymphatic and relies solely on diffusion from synovial fluid for nourishment (Ramachandran 2006). The primary constituent of cartilage is water (around 80% of total wet weight). The water is held in place by proteoglycans, which hold a negative charge and constitute 20% total wet weight. The water present in cartilage is primarily intermolecular and is able to move when a load or pressure is applied. This movement is however restricted by the frictional drag of macromolecules present within the cartilage. These decrease water flow and stiffen the cartilage, allowing greater resistance to higher loads. This allows the cartilage to 'change' its properties with load/compression and is known as a biphasic material that is visco-elastic (Ramachandran 2006). Additionally, cartilage is also anisotropic; having different mechanical properties depending on the direction it is loaded. This is due to the collagen fibres also present in cartilage (primarily type II collagen), which constitutes around 10-15% total wet weight. The collagen is arranged in a strong, mesh like arrangement due to multiple

crosslinks and collagen-proteoglycan interactions. When under tension, the structure of the articular cartilage, organisation of collagen fibres and cross-links are altered. Cartilage is essentially pulled apart, allowing an influx of water and a decrease in compressive stiffness (Ramachandran 2006).

Collectively, all of the above properties result in a material that is approximately ten times more effective as a shock absorber than bone and has an extremely low coefficient of friction (0.002). This is around 30 times smoother than most modern artificial joint replacements and represents a gold standard bearing (Ramachandran 2006).

1.1.3 Prosthetic joint replacements

Orthopaedic surgery plays a major role in the treatment of arthritis. Once medical management fails and symptoms are not controlled, joint replacement (arthroplasty) often provides the only treatment. Most total joint arthroplasty (TJA) involves the knee or the hip. In the United Kingdom in 2014 there were around 89,000 primary total hip replacement carried out and around 91,000 total knee replacements, the majority of which were carried out for arthritic conditions (Scottish-Arthoplasty-Project 2014).

Joint replacement refers to the artificial replacement of the natural joint. In general, joint replacements can either have both components cemented (cemented implant), neither component cemented (un-cemented implant) or have one component cemented and one un-cemented (femoral component cemented - hybrid implant, acetabular component cemented – reverse hybrid implant). The choice of implant is dependent on a variety of factors including surgeon preference, patient demographics and implant availability. Implant composition will be discussed in a later section. Figure 1-3 and Figure 1-4 represent simplified diagrams of both a primary total knee replacement and primary total hip replacement respectively.

Figure has been removed due to Copyright restrictions

Figure 1-3 Primary THR, adapted from (Morphopaedics 2004).

Figure has been removed due to Copyright restrictions

Figure 1-4 Primary TKR (Surgeon 2013)**.**

1.1.4 Orthopaedic biomaterials

Many synthetic materials are utilised in TJA, and to be successful must fulfil certain primary criteria:

- A high level of biocompatibility in order to avoid any inflammatory or toxic response beyond an acceptable tolerable level.

- Appropriate mechanical properties, with a Young's modulus of elasticity (a measurement of the stiffness of a material) similar to that of bone.

- Economically viable manufacturing and processing methods.

Implant selection is complex and depends on a variety of different parameters, such as patient age, reason for replacement and surgeon preference and will not be addressed in this project. A multitude of different materials are used in arthroplasty such as metals, ceramics, polymers and composites, which will now be briefly discussed.

1.1.4.1 Metals

Historically, metals have been used for centuries as a substitute for damaged human bones due to their superior mechanical properties, namely strength. Originally made from stainless steel, due to its ease of manufacture, corrosion resistance and increased strength, excessive loosening and increased friction were documented. This was likely due stainless steel's high Young's modulus of elasticity, causing increased stress shielding and ultimately implant failure (Learmonth, Young et al.), which forced a change to cobalt chrome. Whilst demonstrating improved corrosion resistance and biocompatibility, Young's modulus of elasticity was also found to be significantly raised increasing overall strength (Ramachandran 2006). These femoral components of the THA are around 5-6 times stiffer than bone and therefore suffer from problems relating

to stress-shielding. The regenerative and remodelling processes in bone are directly triggered by loading, i.e. bone subjected to loading or stress regenerates and bone not subjected to loading results in atrophy (Wolff's law (Ramachandran 2006)). Therefore, a much stiffer implant reduces the load on the bone and results in stress shielding (Katti 2004). This is a problem associated with Co-Cr and stainless steel, which are known to have a higher elastic modulus (230GPa and 190GPa respectively) than that of the most commonly used titanium alloys Ti-6A1-4V (110GPa) (Ramachandran 2006). Additionally, titanium alloys also show good wear characteristics, excellent biocompatibility and fatigue resistance, the downside being the relative expense (Learmonth, Young et al.), costing up to five times as much per kilogram than stainless steel. Titanium alloy implants are favourable materials for orthopaedic implants and are commonly used. They will therefore be the focus of this study.

1.1.4.2 Acetabular components (UHMWP)

The first acetabular components were also made from stainless steel, but suffered problems with fit in relation to articulating surfaces, high friction moments and excessive wear of the bearing surfaces (Chan, Bobyn et al. 1999). Charnley developed the use of PTFE and subsequently UHMWP as previously mentioned, which is still the most commonly used material for the acetabular component of THA today (Long and Rack 1998). UHMWP is however not without its risks and is known to wear with time when used in conjunction with a metal femoral head. This has led to the introduction of ceramics, both for the femoral and acetabular bearing surfaces. Current research is focusing mainly on different prosthetic combinations that will reduce contact stresses and therefore wear (Santavirta, Böhler et al. 2003, Katti 2004), however this relates to the joint surface only and not the bone-implant interface, and therefore will not be discussed in depth.

1.1.4.3 Bone-implant interface

When considering the bone-implant interface perhaps one of the most important advances was made in the 1960s, again by Charnley when he introduced PMMA as a bone cement (Ratner 2004). As previously mentioned Charnley suggested that bone cement should be used as a 'grout' rather than an 'adhesive', and that

fixation was achieved by interlocking (Charnley 1960). This allowed the body weight to be more evenly distributed and dispersed over a larger surface area, thus reducing stress shielding and improving implant survival. Whilst national joint registry results continue to show that cemented implants are being used (33% of all THR in 2012), un-cemented implants are increasing in usage (43% of all THR in 2012). It has been suggested this increase in usage is due to a superior outcome in younger patients (Eskelinen, Remes et al. 2006, Hooper, Rothwell et al. 2009) with improved osseointegration, specifically relating to the femoral component (Willert and Buchhorn 1998). The Swedish joint registry data suggests that un-cemented femoral components perform better than cemented stems, with the primary cause of un-cemented THR failure being due to loosening and wear-related problems of the acetabular component (Hailer, Garellick et al. 2010). This would go some way to support the increase in reverse hybrid total hip replacements in the UK in the most recent national joint registry data (20% of all THR in 2012). In contrast, a recent meta-analysis suggested that cemented implants have a better short term clinical outcome than un-cemented devices, however overall implant survival rates are similar between prosthesis (Abdulkarim, Ellanti et al. 2013). Evidently the optimal method for fixation remains controversial, however it is recognised that if osseointegration can be achieved between implant and bone in un-cemented implants, then overall outcome improves as loosening is prevented. One approach to this is to coat implants with bioactive material (hydroxyapatite) that can promote osseointegration. Titanium lends itself well to such coating, resulting in significantly improved implant lifespans (Katti 2004). A comparison of current materials used in arthroplasty is shown in Table 1.

Prosthesis	**Advantage**	**Disadvantage**
Metal-on-polyethylene	Predictable lifespan, cost effective	Potential for high wear rate leading to aseptic loosening
Ceramic-on-ceramic	Low friction, low debris, inert.	Expensive, can produce noise on movement

Metal-on-metal	Reduced wear in comparison to metal-on-polyethlene. Increased stability with large diameter heads.	Metallosis due to metal ions, potential carcinogenic effect, aseptic lymphocyte dominated vasculitis-associated lesions (ALVAL)
Ceramic-on-polyethylene	Lower wear rate than metal-on-poly	Expensive

Table 1 Comparison of materials used in arthroplasty, adapted from (Knight, Aujla et al. 2011, Cash and Khanduja 2014).

1.2 Arthroplasty problems

The various complications associated with arthroplasty with now be discussed, with focus on infection, current diagnostic methods and treatment strategies.

1.2.1 Associated problems with Orthopaedic biomaterials

Despite joint arthroplasty being one of the most successful and cost effective interventions in modern medicine, it is not without its complications. Improvements in surgical technique and implant design have contributed to a marked reduction in mortality after TJA (Parvizi, Holiday et al. 1999, Parvizi, Johnson et al. 2001). However, due to advances in preventative medicine, modern medical care and an aging population, overall patient survivorship is on the increase. This has resulted in arthroplasty being performed in older patients with significant comorbidities (Boettcher 1992, Pagnano, McLamb et al. 2003, Kreder, Berry et al. 2005). In addition, as osteoarthritis incidence increases with age, the overall number of arthroplasties being performed is also on the increase and current estimations suggest that by 2030, the demand for THR and TKR in the United States will increase by 174% and 673%, respectively (Kurtz, Ong et al. 2007). It is therefore suggested that a higher overall number of complications associated with TJA will be observed in the future.

Complications associated with TJA can broadly be divided into systemic (medical) and local (orthopaedic).

1.2.1.1 Systemic Complications

Systemic complications can be further subdivided into either major or minor depending on their severity according to study by Parvizi *et al*, 2001, that prospectively analysed over 30,000 THA over a 28-year period (Parvizi, Johnson et al. 2001). Major complications constituted complex medical/surgical interventions, life threatening circumstances or a resultant functional impairment. Minor complications were defined as requiring a period of observation or medical treatment. They found the major systemic complication rate in TKA to be 4.9% and the minor rate to be 3.4%. Most life-threatening complications were cardiovascular in nature with the main constituent being that of pulmonary embolism (~1.8% overall incidence). The major complication rate in THA was 2%, with a minor rate of 3.1%. Again the most life-threatening complication was found to be pulmonary embolism with an overall incidence of 1.5%.

1.2.1.2 Local Complications

These include infection, dislocation, peripheral nerve injury, periprosthetic fracture and vascular injury (Parvizi, Johnson et al. 2001). The most recent data taken from the Scottish arthroplasty report (Scottish-Arthoplasty-Project 2014) suggests that the most common complication is that of infection. Currently the risk of infection is around 1-1.5% at one year for large joint arthroplasty in the general population (Antti-Poika, Josefsson et al. 1990). The National Joint Registry data from the UK also supports the above documented risks, with 22% of TKR revisions and 12% of THR revisions being carried out because of infection in 2012 (NJR 2013). Infection as a cause for revision was topped only by aseptic loosening (40% in THR and 32% in TKR) (NJR 2013).

Infection of a prosthetic replacement is a serious postoperative complication, and continues to persist despite the use of prophylactic measures that include peri-operative systemic antibiotics, strict hygiene protocols and sterile laminar flow theatres (Belt, Neut et al. 2001). Even though infection appears to be implicated in a small percentage of operations, arthroplasty is so common (1

million/year worldwide (Neut, van Horn et al. 2003)) that a significant number of patients are affected. If infection is confirmed, the results can be devastating to both the patient and society. It can lead to severe consequences such as bone destruction, arthroplasty failure, amputation and even death due to general sepsis (Górecki and Babiak 2009). It is therefore associated with an increased morbidity, which significantly increases hospital length of stay and overall impact to the health care system, with the total cost estimated at around £450million worldwide annually (Sculco 1992).

1.2.1.3 Diagnosing arthroplasty infection

The aforementioned costs are based on confirmed bacterial infection by way of culture of intra-operative samples or joint aspiration. Unfortunately this may be misleading and the real extent of bacterial infection may be underestimated. Bacteria have been suggested to play a role in a proportion of the supposed aseptic loosening of prostheses. Josefsson *et al* (1990) noted that perioperative measures against infection not only lead to a decreased infection rate, but also the incidence of aseptic loosening (Josefsson, Gudmundsson et al. 1990). As methods of infection detection improve, the above theory is further supported (Neut, van Horn et al. 2003). At present the standard method for diagnosing bacterial infection is through isolation of responsible pathogens via culture of intra-operative or intra-articular samples. Problems with this method, such as diagnostic delay and sensitivity have been widely publicised (Hoeffel, Hinrichs et al. 1999). Whilst some cultures can be easily grown in a matter of days, some bacteria (especially anaerobes) often take considerably longer (Tunney, Patrick et al. 1999). In addition, small colonies of bacteria may not be isolated by the laboratory leading to false negative result. In addition concurrent antibiotic therapy in patients may also lead to false negative microbiological results (Neut, van Horn et al. 2003). It has therefore been suggested that standard culture techniques may not be identifying bacteria that are colonising orthopaedic implants (Dupont 1986). Indeed if diagnosis of infection was based on non-culture techniques such as PCR or fluorescence scanning microscopy, then the reported incidence of infection has been shown to be higher when compared to the cultures alone (Lonner, Desai et al. 1996, Tunney, Patrick et al. 1999, Zimmerli, Trampuz et al. 2004). It is therefore concluded that, whilst current data suggests the infection rate in TJA is approximately 1-2%, in reality this

figure may be considerably higher and thus the importance of preventative measures in arthroplasty is clear.

1.2.2 Orthopaedic implant infection

Infection is able to reach prosthetic devices in two ways. Firstly from direct contamination intra-operatively (endogenous spread), usually from the patient or surgeons skin flora, from contaminated air in the operating room or contaminated instruments (Gristina, Hobgood et al. 1987). It is suggested that 95% of arthroplasty infections occur within the 1st year following implantation (Lidwell, Lowbury et al. 1983) and that up to 63% of operations show contamination in the field of operation (primarily indirect surgical instruments such as sucker tips, light handles and gloves) (Davis, Curry et al. 1999). Further studies have cultured viable micro-organisms from instruments and tissue that have been in direct contact with the site of the prosthesis in 30% of all cases (Maathuis, Neut et al. 2005).

The second way by which infection may reach prosthetic implants is via the bloodstream (Gristina, Hobgood et al. 1987). Haematogenous infection occurs after a pathogen is transported via the bloodstream or lymphatic system to the prosthesis. The original source is often distant to the prosthesis, such as a urinary tract infection, periodontal abscess or pneumonia. This haematogenous infective spread is thought to play a minor role in arthroplasty infection representing around 0.3-7% of all arthroplasty infections (Ainscow and Denham 1984, Ahnfelt, Herberts et al. 1990). Bacteria isolated from orthopaedic infections are frequently the *Staphylococcus* species, namely coagulase-negative staphylococci (*S. epidermidis*) and *S. aureus* (Garvin, Hinrichs et al. 1999, Nickinson, Board et al. 2010). While some studies report that *S. epidermidis* and *S. aureus* are collectively responsible for 42-62% of all confirmed prosthetic joint infections (Trampuz and Widmer 2006), more recent epidemiological studies looking at almost 800 orthopaedic isolates from prosthetic infections, found that up to 79% of all infections were the result of Staphylococci, with two thirds (52%) being the result of either *S. aureus* or *S. epidermidis*, using culture techniques alone (Campoccia, Montanaro et al. 2006). Other bacterial species were found to represent around 22% of all prosthetic infections as summarised in Figure 1-5. These figures have further been supported by Ribeiro *et al* (2012),

whose review found that *S. aureus* and *S. epidermidis* collectively accounted for two thirds of all confirmed prosthetic joint infections in orthopaedics (Ribeiro, Monteiro et al. 2012).

Figure has been removed due to Copyright restrictions

Figure 1-5 Frequency of pathogenic species amongst orthopaedic clinical isolates of implant-associated infection (Campoccia, Montanaro et al. 2006).

Infected prosthetic joints can be classified into three types. This was presented in 1975 by Coventry *et al* and is still relevant today (Coventry 1975):

- Acute infection: - usually occurs within 3 weeks of the index procedure and represents a prosthesis that was infected from the outset, either with a wound did not heal or a haematoma.

- Delayed infection: - Present after 3 weeks. Patient generally has a healed wound but continues to have problems, primarily pain, associated with the prosthesis.

- Late haematogenous infection: - as mentioned previously, this is a secondary infection that arises from a remote site months to years after the index procedure.

Most prosthetic joint infections are a result of delayed infection (Hernigou, Flouzat-Lachianette et al. 2010) and therefore this will be the focus of this study. Once confirmed, prosthetic infections can be treated in various ways. Current practice in most countries, in the case of early infection, is surgical debridement with the exchange of mobile components of the prosthesis and application of antibiotics (local +/- systemic) (Górecki and Babiak 2009). Treatment of late/haematogenous infection is more varied and generally dependant on the patient, anatomic location of infection and surgical preference. In general, one of the below treatments are offered:

- 1-stage replacement
- 2-stage replacement
- Permanent removal of prosthesis

- Suppressive antimicrobial therapy

Current literature suggests that 1-stage revision with cement and antibiotics controls infection in 83% of cases, whilst 2-stage replacement with cement and antibiotics controls infection in 91-97% of cases and is viewed by some as the gold standard (Callaghan, Katz et al. 1999, Buttaro, Pusso et al. 2005). Treatment is therefore controversial, and whilst infection may be more effectively controlled by 2-stage revision, the individual patient still requires two operations increasing overall operative risk. It must however be remembered that, as with most medical problems, prevention is the best strategy (Jahoda 2009).

1.3 Bacteria and Biofilms

Specific bacteria and biofilms associated with arthroplasty will now be discussed, in addition to current treatment strategies, the role of osseointegration and altered implant surface topography.

1.3.1 Bacteria associated with arthroplasty

Staphlococci are a genus of gram-positive bacteria and include around 40 different species. Under the microscope they appear round (cocci) and form in grape-like clusters (Ryan and Ray 2004). The majority are found on the skin and mucous membranes of humans and other organisms, and can broadly be divided into their ability to produce coagulase, an enzyme causing blood clot formation (Rogers, Fey et al. 2009).

S. epidermidis is coagulase negative species and is widely recognised as an opportunistic pathogen of foreign bodies, especially prosthetic cardiac valves (Blouse, Lathrop et al. 1978, Hammond and Stiver 1978, Christensen, Simpson et al. 1982), intravascular catheters (Bender and Hughes 1980, Gristina, Hobgood et al. 1987) and orthopaedic implants (Patterson and Brown 1972, Ainscow and Denham 1984, Ahnfelt, Herberts et al. 1990). In recent studies coagulase negative staphylococcus (CoNS) has been found to account for almost half of all TJA infections, of which *S. epidermidis* makes up almost 70%, meaning this is the causative organism in 32% of all orthopaedic implant-related infections

(Campoccia, Montanaro et al. 2006). Nosocomial infections represent the most frequent types of infection caused by *S. epidermidis* however in contrast to *S. aureus* these infections usually do not cause sepsis in non-compromised patients (Vuong and Otto 2002). The main reason for this being that *S. epidermidis* has only one primary toxin associated with it, the haemolytic peptide δ-toxin (often associated with necrotizing enterocolitis in neonates)(Overturf, Sherman et al. 1990). This toxin causes lysis of erythrocytes by forming pores in the cytoplasmic membrane and is thought to be involved in the construction, growth and subsequent detachment of the biofilm (McKevitt, Bjornson et al. 1990). It is also suggested that the δ-toxin forms an inflammatory polypeptide which in turn modulates cytokine and nuclear factor κB expression in macrophages (Mehlin, Headley et al. 1999). As a result *S. Epidermidis* is usually associated with chronic infections, typically in the immunocompromised patient, or when foreign bodies such as implantable orthopaedic devices are involved. Given its relative non-toxic nature, *S. epidermidis* relies heavily on its ability to form biofilms, specifically its adherence to surfaces (Vuong and Otto 2002). This biofilm forming ability is considered to be *S. epidermidis's* main virulence factor (Raad, Alrahwan et al. 1998). Additionally, it also produces exoenzymes, primarily a metalloprotease and a cysteine protease, which have demonstrated an ability to degrade host matrix proteins and components of the immune system in vitro (Sloot, Thomas et al. 1992), thought to be through the actions of elastase (Teufel and Götz 1993).

Virulence factor regulation is similar between *S. epidermidis* and *S. aureus*, with the accessory gene regulator (AGR) locus being key (Recsei, Kreiswirth et al. 1986). This is a quorum-sensing system, thus the AGR-regulated target expression is cell-density dependant. In brief, when cell density is low, surface proteins are expressed allowing tissue colonisation. As cell density increases, AGR becomes active, surface protein production stops and extracellular exoenzymes and toxins are produced (Novick and Muir 1999). Other regulatory loci such as SAR and sigB have also been indicated (Cheung, Koomey et al. 1992, Deora, Tseng et al. 1997) and likely form a complicated network of regulatory loci that govern virulence factors both in *S. epidermidis* and *S. aureus* (Kuroda, Ohta et al. 2001).

S. aureus is a coagulase positive organism and is an important nosocomial pathogen, able to cause a variety of human disease conditions. It is commonly found as part of the normal skin flora in the anterior nasal nares especially, with 20% of the general population being long-term carriers (Kluytmans, Van Belkum et al. 1997). When cutaneous/mucous barriers are breached, significant infection can ensue ranging from simple cellulitis through to pneumonia, meningitis, bacteraemia and sepsis (Bowersox 1999). Campoccia *et al* (2006) found *S. aureus* to be the responsible organism for 34% of all orthopaedic implant-associated infections, constituting the chief causative organism (Campoccia, Montanaro et al. 2006). In comparison to *S. epidermidis*, *S. aureus* has a wide variety of toxins that improve its ability to colonise and cause disease, including haemolysins, nucleases, proteases, lipases and collagenases (Bernheimer and Bey 1986, Dinges, Orwin et al. 2000). In addition some strains are known to produce toxic shock syndrome toxin-1 (TSST-1) (Monday and Bohach 1999), staphylococcal enterotoxins (Bernheimer and Bey 1986), exfoliative toxins and leucocidin (Colin, Mazurier et al. 1994). Collectively these toxins are thought to affect the cells of the immune system, primarily inhibiting the host immune responses to *S. aureus* (Dinges, Orwin et al. 2000). More specifically TSST-1 and the staphylococcal enterotoxins are known as pyrogenic toxic superantigens (PTSAgs). In addition to *S. aureus*, *Streptococcus pyogenes* has also been found to produce these PTSAgs (Monday and Bohach 1999). This PTSAg group are known to enhance endotoxin lethality, with staphylococcal enterotoxins being potent emetic agents (Schlievert, Jablonski et al. 2000) and have an association with significant myocardial necrosis (Schwab, Watson et al. 1955). TSST-1's in comparison show an increased ability to cross the mucosal surfaces (Davis, Kremer et al. 2003) and increases the effect of endotoxin on renal tubular cells (Keane, Gekker et al. 1986). The exact causative mechanism for emesis is not fully understood, however it is thought to be an inflammatory response to staphylococcal enterotoxins, and symptoms have been correlated to the generation of a number of inflammatory mediators such as prostaglandin E_2, leukotriene B_4 and 5-hydroxyeicosatetraenoic acid (Jett, Neill et al. 1994). Ultimately these result in stimulation of the medullary emetic centre in the brain stem through vagal and sympathetic transmission (Dinges, Orwin et al. 2000). Whilst usually self-limiting, if it is associated with toxic shock syndrome (TSS), morbidity is usually significantly higher. TSS is an acute, and sometimes

fatal, syndrome characterised by high fever, erythematous rash, hypotension, and multi-organ involvement (Davis, Chesney et al. 1980, Shands, Schmid et al. 1980, Lee, Deringer et al. 1991, Davies and Geesey 1995). Acute respiratory distress syndrome and disseminated intravascular coagulation are common and potentially life threatening complications of TSS (Shands, Schmid et al. 1980, Arko, Rasheed et al. 1984). In addition, *S. aureus* is also known to produce a number of cytotoxic molecules, namely haemolysins and leukocidin. Of the haemolysins, Alpha-haemolysin has been researched most thoroughly and is common in a high percentage of *S. aureus* strains (Dinges, Orwin et al. 2000). It is dermonecrotic and neurotoxic and it thought to cause osmotic swelling by breaking down cell integrity and increasing intravascular permeability (Bhakdi, Bayley et al. 1996). Coded by the *hla* gene, alpha-haemolysin is one of the most potent cytotoxins, with levels as low as 1µg being lethal following intravenous injections in rabbits (Freer and Arbuthnoti 1982, Bhakdi, Bayley et al. 1996). Other cytotoxins such as beta, gamma and delta haemolysin and leucocidin are known to be involved with *S. aureus*, in particular immune response mediation, however, the exactly mechanisms are not fully understood (Dinges, Orwin et al. 2000).

1.3.2 The Biofilm

Bacteria have been identified in fossils dating back over 4.5 billion years (Sochart 2012). Most research into bacterial infection was historically based on acute infection, which has now been largely combatted by the development of modern vaccines, antibiotics and infection control measures (Bjarnsholt 2013). In the 20th century these diseases have been supplemented by a new type of chronic infection, caused by bacteria growing in slime-enclosed aggregates known as biofilms. Biofilms were first described by Antonie Van Leeuwenhoek who examined the “animalcules” in the plaque on his own teeth in the seventeenth century (Donlan and Costerton 2002) and in the 1930-40’s were described as ‘colonies in which microbes of different varieties and shapes congregate as they attach to some surface’(Heukelekian and Heller 1940, Tresse, de Wit et al. 2008). It is unlikely these scientists fully appreciated what they were describing or indeed what a profound difference biofilms would make to modern microbiology and medicine. It was not until the 1980’s when Costerton demonstrated the role of the biofilm in prosthetic joint infections (Sochart

2012). It has become increasingly clear, primarily through natural environmental studies, that biofilms are commonplace and consist of communities of sessile organisms embedded in a hydrated matrix of extracellular polymeric slime with polysaccharides, proteins (Costerton, Stewart et al. 1999) and nucleic acids (Fux, Stoodley et al. 2003). Biofilms were further recognised to prefer inert surfaces, such as stones in a stream, or indeed prosthetic implants and other medical devices (Costerton, Stewart et al. 1999).

Biofilms are composed primarily and characteristically adhere to surfaces (Sochart 2012). A biofilm can contain one or more bacterial or fungal strains and species and can be defined by a number of characteristics (Costerton, Stewart et al. 1999, O'Toole, Kaplan et al. 2000, Fux, Stoodley et al. 2003). A biofilm is a community of bacterial cells that form a consortium that is surrounded and protected by a matrix produced and secreted by the bacteria. This 3D biofilm structure is a dynamic process and involves a series of co-ordinated molecular events, controlled primarily through quorum sensing and inter-bacterial communication (Fux, Stoodley et al. 2003). This extra-cellular matrix contains different extracellular polymeric substances (EPS) including proteins, DNA and polysaccharides. This can provide the biofilm with a protective coating, thus allowing the biofilm to withstand very high doses of particular antibiotics that would kill planktonic cells outright (Bjarnsholt 2013). In addition the biofilm allows a dramatic increase in tolerance to host defences providing the root of many bacterial infections (Fux, Stoodley et al. 2003). It is recognised that whilst antibiotic therapy typically reverses the symptoms caused by the release of planktonic cells from the biofilm, the biofilm itself remains alive and intact (Marrie, Nelligan et al. 1982). For this reason, biofilm infections are recognised to show recurring symptoms, after cycles of antibiotic therapy, until the sessile population is surgically removed (Lynch and Robertson 2008). Antibiotic resistance has been attributed to the restricted penetration of the anti-microbial and host defences into biofilms, and recent studies suggest that resistant biofilm phenotypes are emerging (Xu, McFeters et al. 2000). It should also be noted that the bacterial colony must be adherent to a surface, either inert (Costerton, Stewart et al. 1999), or biological such as in bacterial endocarditis, cystic fibrosis (Hoiby, Ciofu et al. 2010), the gastrointestinal tract (Macfarlane and Dillon 2007) or oral mucosa (Dongari-Bagtzoglou 2008).

Biofilm formation takes place in several stages depicted in Figure 1-6. Bacterial adhesion is the first stage and relies on the surface of the biomaterial undergoing changes on its surface after implantation. This is known as surface conditioning and occurs through physical, chemical and electrostatic mechanisms (Sochart 2012). This is the critical stage, or 'race to the surface' which is essentially a battle between tissue cell integration and bacterial adhesion to the same surface (Gristina, Hobgood et al. 1987). On contact with the surface, bodily fluids immediately coat the implant with host materials, namely serum proteins and platelets (Neut, van Horn et al. 2003). This coating, as well as preventing an autoimmune reaction to the implant, allows bacterial adhesion. Bacterial attachment is facilitated by adhesins (organism specific cell surface proteins or lipoproteins) and bacterial aggregation occurs where they become encased in EPS to form what is known as a biofilm (Costerton, Stewart et al. 1999). It has been suggested that during this attachment phase, possibly after micro-colony formation, the transcription of specific genes is activated. Studies with *P. aeruginosa* have shown transcription of genes that are required for the synthesis of EPS are activated on attachment to a solid surface (Davies and Geesey 1995). This suggests that by merely attaching to a solid surface, bacteria are able to immediately start forming EPS, thus creating a protective environment to thrive.

Once adhered and aggregated, bacteria begin to grow and enter the maturation phase. At this stage bacteria appear to develop coordinated social behaviour moving into differentiated micro-colonies. It is suggested that this gene expression and subsequent differentiation occurs through quorum sensing (Costerton, Stewart et al. 1999). This is a cell density-dependant control mechanism, such that when a critical bacterial density is reached, signalling molecules produced by the bacteria activate bacterial receptors and produce and release extracellular signals. This is a dedicated communication system that allows sharing of genetic information between bacteria by conjugation, transformation and transduction (Sochart 2012). This would go some way to explaining the development of antibiotic resistance in some biofilms.

Finally the last stage of the biofilm cycle is detachment and dispersal of planktonic cells from biofilms. During this stage pieces of biofilm break away and are dispersed into surrounding fluid. This permits spread of the bacteria and

allows it to colonise new surfaces. Again it appears that this process is initiated by a chemical cue, much like biofilm maturation. Studies of *P. aeruginosa* have shown that biofilm detachment is a result of alginate digestion by alginase (Hay, Gatland et al. 2009). While many antimicrobial therapies target bacteria systemically, this is often after adhesion has occurred. This study focusses on prevention of bacterial adhesion as a strategy against TJA infection. Utilising modern molecular techniques it has become increasingly clear that if bacterial adhesion can be restricted, then the subsequent stages of development can be prevented, blocking biofilm production. Without a protective biofilm environment, bacteria are almost one hundred times more susceptible to antimicrobial treatment (Olson, Ceri et al. 2002), thus by preventing bacterial adhesion, arthroplasty infection could be treated more effectively and overall incidence drastically reduced.

Figure has been removed due to Copyright restrictions

Figure 1-6 The stages of Biofilm formation (Jahoda 2009)

1.3.3 Biofilm treatment strategies

Before treatment strategies can be discussed, our ability to diagnose chronic infections due to biofilm formation needs to be understood. As previously mentioned, acute infections are generally easy to diagnose and treat. The problem, specifically with orthopaedics, lies with diagnosing chronic or delayed infection. Routine sampling at present relies either on a wound swab or biopsy via needle aspiration or tissue sample. Clearly if a deep seated infection is present, the wound if often clean and dry and causes no concerns, therefore a swab if of no use. Equally with a biopsy, given the heterogeneous distribution of bacteria there is a risk that a biopsy may fail to contain any bacteria (Bjarnsholt 2013). A diagnostic review by Trampuz and Zimmerli in 2005 suggested that a combination of laboratory, histopathology, microbiology and imaging achieves the highest sensitivity, specificity and accuracy for prosthetic joint replacement infection (Trampuz and Zimmerli 2005) (Table 2).

Investigation	Comment	Median Sensitivity	Median Specificity	References
Laboratory Tests • C-Reactive Protein • Synovial Fluid • ESR	Repeated increasing measurements post-operatively Leukocyte count >1.7 x 10^9/l Differential >65% neutrophils Elevated	95% 97% 83%	90% 98% 90%	(Widmer 2001, Trampuz, Steckelberg et al. 2003, Trampuz and Zimmerli 2005)
Histopathology	≥1 to ≥10 neutrophils per high powered field, averaged over 10 high powered fields	82%	96%	(Athanasou, Pandey et al. 1995, Widmer 2001, Trampuz, Steckelberg et al. 2003, Trampuz and Zimmerli 2005)
Microbiology • Preoperative Aspiration • Intraoperative specimen • Sonication of implants	Sterile, not on antibiotics Tissue Culture (Min. 3-6 samples) Material cultured in laboratory	86% 99.6% 78.5%	92% 86% 98.8%	(Atkins, Athanasou et al. 1998, Widmer 2001, Trampuz, Piper et al. 2007, Høiby, Bjarnsholt et al. 2015)
Imaging • Nuclear Medicine	Labelled WBC/IgG	95.5%	88%	(Widmer 2001, Trampuz and Zimmerli 2005)

Table 2 Adapted summary of diagnostic criteria for infected arthroplasty (Widmer 2001, Trampuz and Zimmerli 2005, Høiby, Bjarnsholt et al. 2015)

Even if a biofilm infection is diagnosed, the treatment is vastly different to that of an acute infection. Antibiotics may not penetrate the biofilm, leaving operative removal of the infected implant the only viable option followed by prolonged periods of combination antibiotic therapies (Høiby, Bjarnsholt et al. 2010). Current research focuses on substances that destroy the biofilm matrix, such as disperin-B (Donelli, Francolini et al. 2007), or altering quorum sensing by quorum quenching enzymes (Dong and Zhang 2005). Other angles to the biofilm problem involve electromagnetic fields to enhance antibiotic activity or substances that cause 'self-destruction' of the biofilm (Sochart 2012). Although these methods may well prove beneficial, it is the authors belief, and it is widely recognised that, the most efficient means of combatting biofilm infections is to prevent infection in the first place (Bjarnsholt 2013). Whilst in normality the human skin acts as a barrier against bacterial invasion, this barrier is compromised by surgery and the insertion of implants. One aspect of prevention is therefore aimed at surgical technique and hygiene. The aseptic technique, first introduced by Joseph Lister, is of extreme importance. In addition the use of ultra-clean theatres with laminar flow, sterile instruments, garments and implants are paramount in the avoidance of contamination (Babb, Lynam et al. 1995, Chow and Yang 2004) and must be combined with administration of prophylactic antibiotics (Høiby, Bjarnsholt et al. 2010).

As mentioned previously, the two main problems that contribute to arthroplasty revision are failure of bone-implant interface and arthroplasty infection. A great deal of research continues to look at improving the former, with titanium being used for implants due to its ability to form an oxide layer over the implant, thus improving biocompatibility and bioactivity (Wang, Ouyang et al. 2011). Despite this however, osseointegration is often not sufficient, resulting in mechanical instability and ultimately implant failure. Research at present is focusing on controlling this bone-implant interface and is aimed at producing a surface that is both osteoconducive (a surface that allows bone growth (Albrektsson and Johansson 2001)) and osseointegrative regardless of implantation site or bone quality (Puleo and Nanci 1999). It is certainly recognised that tissues act mainly with the outermost layers of an implant, in an area known as the 'primary interaction zone' which measures approximately 0.1-1nm in thickness (Kasemo 1998). It would therefore be reasonable to assume that by altering this area, the

interactive ability of the implant, be it osseointegrative or its effect on bacterial adherence, may be altered.

Osseoinduction was first described by Brånemark *et* al in 1977 (Branemark, Hansson et al. 1977) and defined by Albrektsson *et al* (1981) as direct contact between living bone and implant (at light microscope magnification) (Albrektsson, Brånemark et al. 1981). In the context of bone/implant interactions, osseointegration involves the recruitment of immature, undifferentiated mesenchymal stem cells and their subsequent stimulation to allow osteoblast development (Albrektsson and Johansson 2001). This stimulation is dependent on the particular implant biomaterial, with metals such as copper and silver performing poorly in relation to osseointegration, whilst titanium is significantly more osseointegrative (Albrektsson, Brånemark et al. 1981). Despite the widespread use of titanium, oral prosthetic studies have suggested that 17 years after implantation, average bony contact was only 70-80% (Albrektsson, Eriksson et al. 1993). A great deal of research has therefore focussed on improving osseointegration by altering the implant surface. Perhaps the most publicised and commercially available coating is that of hydroxyapatite (HA) which is suggested to improve osseointegration (de Groot, Geesink et al. 1987, Geesink, de Groot et al. 1987). HA provides a source of calcium and phosphate, similar to that of the host's bone, which allows osteoblasts to form osteoid directly onto the HA surface coating increasing new bone formation and the bone/implant interface (Soballe 1993). Research into HA coating continues to evolve, with the integration of bioactive molecules and growth factors in an attempt to further improve implant longevity (Choi and Murphy 2010, Saran, Zhang et al. 2011, He, Huang et al. 2012).

Biomimetic molecules such as collagen have been shown to improve implant integration (Rammelt, Illert et al. 2006, Mathews, Bhonde et al. 2011), whilst coating implants with growth factors improve their ability to modulate cell functions such as enhancing stem cell differentiation and decreasing inflammation (Liu, de Groot et al. 2005, Macdonald, Samuel et al. 2011). Smaller molecules, such as peptides, derived from protein molecules, have also been shown to increase cellular functions such as adhesion and bone formation (Auernheimer, Zukowski et al. 2005, Wojtowicz, Shekaran et al. 2010). Whilst

the encouragement of osseointegration is of clear importance to implant survival, the mitigation of infection must also be addressed.

Infection resistant coatings can be categorized as passive or active. Passive coatings do not release bactericidal agents to the surrounding tissues, while active coatings release pre-incorporated bactericidal agents such as antibiotics, antiseptics, silver ions and growth factors/chemokines/peptides to down regulate infection (Goodman, Yao et al. 2013). Current arthroplasty practice involves the routine administration of prophylactic antibiotics and, depending on implant, the use of antibiotic loaded bone cement. First popularised by Buchholz *et al* (1970) the incorporation of antibiotics into PMMA cement can reduce deep infection rates in conjunction with systemic antibiotics (Engesaeter, Lie et al. 2003). The use of antibiotic loaded bone cement has decreased, particularly in the United States, with the increased use of cementless implants worldwide (Goodman, Yao et al. 2013). This provides an opportunity for the development of new antibacterial technologies. Such advances include the incorporation of broad-spectrum antibiotics such as gentamicin into HA coatings on titanium implants, significantly reducing implant related infection (Alt, Bitschnau et al. 2006). This however relates to acute implant infection, with 80-90% of the antibiotics being released within the first 60 minutes following implantation, therefore their role in chronic infection remains unclear (Alt, Bitschnau et al. 2006). An optimal antibiotic delivery system should release antibiotics at an optimal bactericidal level, for a sufficiently long period of time and then stop to prevent antibacterial resistance and tissue integration side effects (Antoci, Adams et al. 2007). Clearly this requires a complex and advanced implant coating that currently is not available.

The surface characteristics of implants, however, can be altered to provide a passive approach to preventing infection. Modification of the properties of the implant surface provides a relatively simple way to prevent bacterial adhesion. Increasing surface 'wetability' through UV light exposure (Yu, Ho et al. 2003, Gallardo-Moreno, Pacha-Olivenza et al. 2009), hydrophilic PMMA implant coatings and protein resistant polyethylene glycol have been applied to titanium implants and reduced bacterial adhesion (Harris, Tosatti et al. 2004, Del Curto, Brunella et al. 2005). There is however debate as to whether these surface alterations impair osseointegration.

1.3.4 Biofilms and Topography

Whilst the above advances are undoubtedly important, the physical aspect of the material surface in relation to bacterial adhesion is an area of research that has long been neglected. When looking at bacteria, this material topography is assessed at the nanometre scale. Recent research has shown that alterations in the surface topography at the nanoscale can have major effects on cell behaviour (McMurray, Gadegaard et al. 2011), bacterial adhesion (Xu and Siedlecki 2012) and ultimately long term implant survival (Sjöström, Brydone et al. 2013). Dental research has shown that particular nanopatterns show biocompatible responses and are capable of inducing osteoblastic cell adhesion, spreading and propagation (Pelaez-Vargas, Gallego-Perez et al. 2011). Research regarding bacterial adhesion has shown that submicron surface textures on polyurethane can significantly reduce bacterial adhesion when looking at S. *aureus* and S. *epidermidis*, with a subsequent reduction in biofilm formation (Xu and Siedlecki 2012). Due to challenges associated with fabricating surfaces at the nanoscale, the majority of research to date has been performed on surfaces other than titanium. This project therefore focuses on bacterial adhesion, and subsequent biofilm formation of nanofabricated titanium. It is postulated that by controlling particular nanosurface parameters, bacterial adhesion can be effectively regulated.

1.3.5 Bacterial metabolomics

While multiple mechanical theories as to the mechanism behind bacterial adhesion exist (De Beer, Stoodley et al. 1994, Fuchs, Haritopoulou et al. 1996, Baty, Eastburn et al. 2000, Edwards, Bond et al. 2000), it has been suggested that adhesion is mediated by surface proteins (Hussain, Herrmann et al. 1997), extracellular proteins (Heilmann, Schweitzer et al. 1996), adhesins (McKenney, Hübner et al. 1998) and autolysins (Heilmann and Götz 1998) to name a few. The metabolomic pathways associated with such compounds and therefore bacterial adhesion remains relatively under-researched.

Metabolomics is defined as ‘the quantitative measurement of the dynamic multi-parametric metabolic response of living systems to pathophysiological stimuli or genetic modification’ (Nicholson, Lindon et al. 1999). Metabolomics is the study

of a complete complement of small molecules (known as metabolites) within a system, known as the metabolome. The metabolome was first described by Oliver *et al* in 1998 (Oliver, Winson et al. 1998) whilst studying the yeast genome, and resultant metabolomics development is often referred to as metabonomics (Nicholson, Lindon et al. 1999) or metabolic profiling (Niwa 1986) by some groups. The ability to provide a 'snap-shot' of cell metabolism is emerging as a useful tool across a multitude of disciplines, ranging from plant physiology to human disease, nutrition and drug discovery, but has only become possible as a result of recent technological breakthroughs in small molecule separation and identification (Wishart 2008).

Stable isotope labelling allows the targeting of specific compounds that are predicted to be involved in specific metabolomic pathways, and relies on the incorporation of labelled isotopes (such as ^{13}C) into metabolite pools (Birkemeyer, Luedemann et al. 2005). These compounds can subsequently be traced 'downstream', highlighting any specific pathways demonstrating increased metabolic activity. Another equally important aspect of metabolomics is a compiled database containing descriptive and spectral information of all constituent chemicals found in different metabolomes (Smith, O'Maille et al. 2005, Cotter, Maer et al. 2006, Moco, Bino et al. 2006, Wishart, Tzur et al. 2007). The relatively recent production and widespread availability of such databases has allowed the detection and characterisation of multiple metabolomes in a matter of minutes (Dunn, Bailey et al. 2005, Moco, Bino et al. 2006, Wishart 2008).

Currently bacterial metabolomics has focused mainly on the classification (Hettick, Green et al. 2008) and understanding of normal bacterial metabolism. Schaub *et al* (2008) found altered glycolysis dynamics under differing growth rates and glucose availability in *E. coli* (Schaub and Reuss 2008), whilst Koek *et al* (2006) found a time-related progression of metabolites with bacterial growth (Koek, Muilwijk et al. 2006). While interactions between surface topography and bacterial adhesion are documented, the effects of targeting bacterial metabolism therapeutically are not and remain a novel area of research in metabolomics and thus an additional focus of this study.

1.4 Hypothesis

It is hypothesised that by altering the surface topography at the nanometre level, bacterial adhesion can be altered. This thesis therefore aims to compare bacterial adhesion on different nanopatterned topographies, both through quantification and imaging. Metabolomic analysis will provide valuable information relating to bacterial adhesion pathways and therefore allow specific therapeutic targeting.

Objectives that need to be overcome include biofilm growth optimisation, reproducibility of results, and factors such as incubation time, temperatures, growth phase application to surfaces and culture densities will have to be addressed. Additionally, a novel method for identifying upregulated adhesion metabolites and pathways is proposed. Expected problems include labelled compounds incorporation, metabolomics sample preparation and associated analysis. These issues will be addressed by utilising and adapting similar methodologies to those described by Birkemeyer *et al* (2005) and sample preparation to that of Stipetic *et al* (2015) (Birkemeyer, Luedemann et al. 2005, Stipetic, Hamilton et al. 2015, Stipetic, Dalby et al. 2016).

By overcoming the objectives above, this research aims to test the hypothesis that different nanosurfaces affect bacterial adhesion and that targeted therapeutic metabolomics can directly inhibit bacterial adhesion pathways. Ultimately this would be of benefit to the patient, the NHS and society and provide a new wave of orthopaedic implant combined with targeted bacterial inhibition at the metabolomic level.

Chapter 2

Staphylococcal Biofilm Growth Optimisation

2.1 Introduction

Adhesion and subsequent biofilm growth of both *S. aureus* and *S. epidermidis* is complex and influenced by numerous well-defined virulence factors. Virtually any surface can be colonised by bacteria, whether biotic or abiotic and includes all biomaterials (Dunne 2002). The process of bacterial attachment, as outlined in Chapter 1, and thus subsequent biofilm formation is dictated by a number of different variables (Dunne 2002), which must be considered when optimising bacterial adhesion *in vitro*.

Principally, for adhesion to occur both the bacteria and surface must come into close contact. This critical proximity has been suggested to be around 1nm (Dunne 2002), however, proximity is not the only factor involved in adhesion. It has been shown to be dependent on a variety of different forces that exist between the inert surface and bacteria (Oliveira 1992). These are primarily Van der Waals attraction forces, electrostatic forces and hydrophobic interactions. Van der Waals forces are usually attractive and act over a relatively large separation distance (<50nm) (Fletcher 1996), but are relatively weak (Busscher, Cowan et al. 1992). In comparison electrostatic forces work at a much closer separation distance (10-20nm) and opposing surfaces must have opposite net surface charges to allow attraction. When considering bacteria and a potential attachment surface, the net surface charges are often negative, resulting in repulsion and prevention of adhesion (Carpentier and Cerf 1993, Fletcher 1996). *In vitro* this repulsion force is overcome by sufficient electrolyte concentrations, thus increasing the ionic strength of the medium and eliminating the electrostatic repulsion barrier (Fletcher and Loeb 1979). The most controversial force affecting bacterial adhesion is that of hydrophobicity. A number of studies have found that adhesion is directly related to surface hydrophobicity, with increased quantity (Fletcher and Loeb 1979, Paul and Loeb 1983), rate (Paul and Loeb 1983) and strength (Rijnaarts, Norde et al. 1993) of bacterial attachment occurring with hydrophobic surface forces. In contrast, however, other studies have observed no difference in bacterial adhesion when comparing hydrophobic and hydrophilic surfaces (Pedersen 1990, Busscher, Cowan et al. 1992). It should be recognised however, that *in vitro*, primary contact usually occurs between an

organism and a conditioned surface. This surface conditioning can significantly affect surface hydrophobicity and therefore adhesion (An, Dickinson et al. 2000, Dunne 2002). Any material surface exposed to an aqueous medium will almost immediately become conditioned or coated by polymers from that medium, which will then affect the rate and extent of microbial attachment (Donlan 2002). First described by Loeb *et al* (1975) these conditioned films are found to form within minutes of exposure and are found both in the natural environment (George I and Rex A 1975) and bodily secretions such as blood, tears, urine, saliva and intravascular fluid (Sand 1997). Certainly, Wang and colleagues (1995) study on *S. epidermidis* adhesion demonstrated increased adhesion to polyethylene discs in the presence of surface-activated platelets (Wang, Anderson et al. 1995). Successive studies have shown plasma protein treated PMMA increases bacterial adhesion (Herrmann, Vaudaux et al. 1988). The above-mentioned factors are widely recognised as the first stage of adhesion (Wang, Anderson et al. 1995, Fletcher 1996, Sand 1997, Dunne 2002), the longevity of which is dependent on the sum total of these variables.

The second stage of adhesion is the 'anchoring' or 'locking' phase, and this relates to binding between specific adhesins and the surface (Dunne 2002). This represents irreversible bacterial attachment to a surface and is usually regulated at a transcriptional level (An, Dickinson et al. 2000). *S. epidermidis* is known to produce a polysaccharide intracellular adhesion (PIA), allowing for cell-to-cell adhesion and subsequent biofilm formation (Heilmann, Gerke et al. 1996, Heilmann, Schweitzer et al. 1996, Heilmann and Götz 1998), while *S. aureus* possess designated microbial surface components recognising adhesive matrix molecules (MSCRAMM), which are thought to play a major role in adhesion (Lowy 1998).

In addition to understanding bacterial adhesion, culture conditions are also important in bacterial growth optimisation. A multitude of different growth media's are available for bacterial culture (Fletcher 1976, Christensen, Simpson et al. 1982, Park, Kim et al. 1998, Allan, Newman et al. 2001, Vieira and Nahas 2005). As a general rule, growth media must contain a source of energy, carbon, nitrogen and minerals all of which are required bacterial growth and metabolism (Fred and Waksman 1928). The addition of a standardised bacterial concentration is also an important factor to consider, when discussing bacterial

growth, based on optical densities (OD), as this remains proportional to bacterial density (Monod 1949). Whilst providing a representation of bacterial concentration suitable for standardisation, this method does not provide an exact quantification. Quantification based on colony forming units (CFU) is a method used to estimate the number of viable bacteria or fungal cells in a sample. It is essentially a visual representation of bacterial growth, and requires each colony to be counted to provide a result. Whilst relatively simple to carry out, this method is time consuming and cannot ascertain whether a colony arose from one cell or a group of cells. For this reason, this method often results in an underestimation of bacteria (Parkinson, Gray et al. 1971). This is certainly likely to be the case with S. *aureus* and *S. epidermidis*, as they are both known to grow in clusters rather than homogenous planktonic cells (Goldman and Green 2008). In comparison, a real-time polymerase chain reaction (qPCR) can be used to amplify and simultaneously quantify targeted bacterial DNA. Currently, qPCR is recognised by some as the quantification method of choice for the detection and quantification of microorgansims (Postollec, Falentin et al. 2011). It is quicker, more sensitive and more specific than culture based methods and does not carry the associated problems (Nolan, Hands et al. 2006). qPCR techniques have been described extensively (Heid, Stevens et al. 1996, Kubista, Andrade et al. 2006). In brief, qPCR consists of a succession of amplification cycles resulting in an exponential increase of DNA amplification products that can be monitored at every cycle using a fluorescent reporter. Fluorescence values obtained from each amplified product are recorded throughout the cycled reaction. There is an inverse relationship between the amount of DNA and the cycle number, thus a higher amount of DNA present at the beginning of the reaction, correlates to a fewer number of cycles being required to reach the cycle threshold (Ct). The Ct value is a level at which the fluorescence measured is statistically higher than background readings (Gibson, Heid et al. 1996), and is found during the exponential phase of amplification (Higuchi, Fockler et al. 1993). This study will utilise both methods described above to quantify bacteria.

Accurate bacterial quantification also relies on adequate bacterial removal from a surface. While bacteria in liquids are relatively easy to quantify via the methods described above, bacteria attached to a surface are somewhat more troublesome. Explanted prostheses can be sonicated and the resultant fluid used

for quantitative analysis and culture (Monsen, Lövgren et al. 2009). Ultrasound disrupts the bacterial biofilm on the prosthetic material and when used as an addition to conventional culture, has been shown to improve the sensitivity of prosthetic joint infection microbiological diagnosis (Trampuz, Piper et al. 2007, Piper, Jacobson et al. 2009). This technique will therefore be utilised in this study.

2.2 Chapter Aims

It was the hypothesis of this study that surface property impacts the differential ability of staphylococci species to adhere. Therefore, the aim of this initial pilot investigation was to undertake optimisation experiments to define conditions and media for qualitative and quantitative assessment of staphylococcal adhesion upon biologically important substrates in downstream analyses. Work from this chapter has been published in:

Hansom D et al *THE EFFECTS OF NANOPATTERN SURFACE TECHNOLOGY ON ORTHOPAEDIC JOINT REPLACEMENT INFECTION*. Bone & Joint Journal Orthopaedic Proceedings Supplement, 2015. **97-B**(SUPP 3): p. 2.

Work from this chapter has been presented at the following conferences:

Hansom D, Tsimbouri M, Ramage G, Burgess K, Dalby M, Meek D and Clarke J. 'Nano-topographical modulation of cells and bacteria for next generation orthopaedic implants.' Centre of Cell Engineering – Glasgow Orthopaedic Research Initiative, December 2014.

Hansom D, Burgess K, Meek D, Clarke J, Ramage G. 'The effects of nanopattern surface technology on orthopaedic joint replacement.' Glasgow Meeting of Orthopaedic research, March 2015.

Hansom D, Burgess K, Meek D, Clarke J, Ramage G 'Nano-topographical modulation of cells and bacteria for next generation orthopaedic implants.' El-Minia University Hospital Scientific Day, Egypt, February 2015.

Hansom D, Burgess K, Gadengaard N, Millar N, Clarke J & Ramage G. 'The effects of nanopattern surface technology on orthopaedic joint replacement.' European Federation of National Associations of Orthopaedics and Traumatology, June 2016.

Hansom D, Burgess K, Gadengaard N, Millar N, Clarke J & Ramage G. 'The effects of nanopattern surface technology on orthopaedic joint replacement.' British Orthopaedic Research Society, September 2016.

2.3 Materials and Methods

2.3.1 Bacterial Culture and Standardisation

2.3.1.1 Staphylococcal strain collection

Four different strains staphylococci were used in this study. *S. aureus* Newmans strain (Duthie and Lorenz 1952), an orthopaedic clinical isolate from the Southern General Hospital, Glasgow (Stipetic, Hamilton et al. 2015)), NCTC 11047, and one well characterised biofilm forming strain of *S. epidermidis* (RP62A - ATCC 35984 (Gill, Fouts et al. 2005)). The clinical isolate was selected based on a positive hip aspirate obtained in theatre of a THR in a 75-year-old female. All strains were stored in the culture collection facility at the University of Glasgow Dental School at -80^{o}C. These were maintained for *in vitro* experiments by streaking for single colonies onto Luria Bertoni (LB) agar (Vitko and Richardson 2013) and incubating for 24 h at 37^{o}C, after which time growth was visually confirmed. Plates were stored intermittently at 4^{o}C until required. A loopful of each isolate was inoculated into 10mL of tryptic soy broth (TSB) solution (casein peptone 17 g/L, dipotassium hydrogen phosphate 2.5 g/L, glucose 2.5 g/L, sodium chloride 5 g/L, Soya peptone 3 g/L [Sigma-Aldrich, Dorset, UK]) and placed in an orbital shaking incubator at 150rpm at 37^{o}C overnight.

2.3.1.2 Bacterial standardisation

Following overnight growth, the samples were washed by centrifugation at 3000rpm for 5 min. Supernatant was discarded and the pellet washed with 10ml of phosphate buffered saline (PBS [Sigma-Aldrich, Dorset, UK]). This was

centrifuged for a further 5 min at 3000rpm, after which the supernatant was removed and the pellet re-suspended in PBS. This was then vortex mixed to ensure homogenous sample mixing, and the optical density 590nm (OD_{590}) prepared. All samples were standardised to an OD_{590} of 0.6 = $1x10^8$ cfu/ml. These samples were then further diluted 100-fold in appropriate growth medium (TSB, Brain heart infusion [BHI], Dulbecco's modified eagle medium [D-MEM], DMEM + supplements [10% foetal calf serum (FCS), 1% L-Glutamine, 1% sodium pyruvate and 1% non-essential amino acids] and FCS) to obtain a bacterial concentration of $1x10^6$ cfu/ml. Different FCS concentrations were used to ascertain optimal bacterial growth, and therefore biofilm formation (10%, 25%, 50% and 75%). Media selection was based on a range on growth conditions currently being used in different laboratories (Tranter, Tassou et al. 1993, Yarwood, Bartels et al. 2004).

2.3.1.3 Growth kinetics and optimal media selection

Following standardisation, 200µL of each sample was added to defined wells in a pre-sterilised, polystyrene 96-well, flat bottomed microtitre plate (Corning incorporated, NY, USA). The plate was incubated at 37°C for 24h with an OD_{590} read every hour, followed by shaking at 100rpm for 30 sec (FLUOstar Omega, BMG labtech). Negative controls containing no organisms were included for each growth media, and all testing was carried out in triplicate on three separate occasions.

2.3.2 DNA extraction and PCR analysis

2.3.2.1 Bacterial DNA extraction

Following standardisation (2.3.1), one ml of overnight bacterial culture was transferred to a 1.5 mL microfuge tube and centrifuged at 13,000 rpm for 10 min to pellet each sample. DNA was subsequently extracted using the MasterPure Gram Positive DNA Purification Kit (Epicentre®, Cambridge, UK). The supernatant was discarded and 150µL of TE Buffer (10mM Tris-HCL [pH 7.5], 1mM EDTA) was added to each sample to re-suspend the pellet and 1µL of lysozyme was added to break down the bacterial cells. Samples were incubated at 37°C for 2 h. Next, a cocktail containing 1µL proteinase K (50µg/mL) and 150µL Gram positive cell lysis solution was added to each sample, mixed thoroughly and

incubated at 75°C for 15 min. Samples were allowed to cool to 37°C and then stored on ice for 5 min before the DNA precipitation stage. To each lysed sample, 175µL of MPC protein precipitation reagent was added and vortexed for 10 sec. Samples were then centrifuged at 13,000 rpm for 10 min at 4°C with the resultant supernatant transferred to a clean microfuge tube with 1µL of RNase A (5µg/mL). All samples were incubated at 37°C for 30 min and 500µL of isopropanol added to each supernatant, which were then mixed by inverting each tube. The DNA was pelleted by centrifugation at 13,000 rpm for 10 min at 4°C. The pellet was washed with 70% ethanol and the DNA pellet was re-suspended in 35µL of TE buffer.

2.3.2.2 Nucleic acid quantification

Nucleic acid quantification was performed using the NanoDrop™ ND-100 spectrophotometer (Labtech International, Ringmer, East Sussex, UK). Before the DNA was quantified, TE buffer was used as a reference and concentrations recorded in ng/µL. Samples with a 260/280nm ratio of 1.8-2.2 were accepted as high quality and used for PCR reactions. DNA was stored at -20ºC until required.

2.3.2.3 Bacterial Quantification using DNA qPCR and standard curve production.

One µL of extracted DNA, as outlined in section 2.3.2.1, was added to a mastermix containing 10µL SYBR® GreenER™ (Invitrogen, Paisley, UK), 7µL of HyClone, nuclease free deionized distilled molecular biology grade water and 1µL of 10µM forward/reverse primers for *S. aureus* and 16S primers for *S. epidermidis* (Invitrogen, Paisley, UK) (Marchesi, Sato et al. 1998). Primers were chosen based on their known locus and ability to identify the selected bacteria. The sequences for each primer set used are shown in Table 3.

Target	**Primer sequence (5'-3')**
***S. aureus* (SAR0134)**	F – ATTTGGTCCCAGTGGTGTGGGTAT R – GCTGTGACAATTGCCGTTTGTCGT

***S. epidermidis* (16S)**	F – GGGCGGGGTACAAGGC R – CAGGCCTAACACATGCAAGTC

Table 3 S. epidermidis and S. aureus 16S primer sequences

All reactions were carried out in 96 well plates and sealed using caps (Agilent Technologies, Cambridge, UK). All samples were centrifuged to remove any air bubbles before qPCR was carried out. Three independent replicates were analysed in triplicate using an Applied Biosystems Step One Plus Quantitative PCR machine and Step One software (Foster City, California 94404, USA) (Biosystems 2010). The thermal profile consisted of 50°C for 2 min to allow for DNA polymerase activation. This was followed by 40 amplification cycles of 95°C denaturation for 15 sec and 60°C annealing for 60 sec. A non-template control (NTC) replacing DNA with sterile water was included to rule out the presence of contamination. The cycle threshold (Ct) was set automatically and Ct values for all samples of interest were used for the quantification of bacteria. Ct values were used as they allowed comparative analysis. Quantification was carried out by standardising each bacterial species to 1×10^8 CFU/mL followed by five-fold bacterial dilutions prepared ranging from 1×10^6 to 1×10^8 CFU/mL and finally DNA extraction and qPCR as described in section 2.3.2.1. Standard curves were constructed by plotting the Ct value against the equivalent $\log^{10}$ of the DNA concentration allowing unknown bacterial counts to be quantified. Each dilution of DNA was assessed in triplicate for each primer set. Trend lines were applied to all data sets and the R^2 value was used to assess how well the trend line fitted and the fraction of variance. An R^2 value of 1 represents a perfect fit between the trend line and the data points, and R^2 value of 0 represents no relationship. Only trend lines with a linear association of above 0.97 were deemed acceptable for inclusion in this study.

2.3.3 Biofilm Optimisation

2.3.3.1 Bacterial incubation optimisation

Standardised bacteria (2.3.1.2) in DMEM + Supplements were grown on 13mm plastic cover slips (Thermanox®, Rochester, NY, USA) in a 24 well plate for 30,

60 and 90 min time periods. Cover slips were used as Ti nanopattern and control surfaces were in limited supply, therefore all optimisation experiments were carried out on readily available materials.500µL of each bacterial sample was added to each well and the plates were incubated in a gentle shaking incubator at 37ºC for the allotted time frame. Following incubation, supernatant was removed and the coverslips were washed in PBS twice and sonicated for 10 min in 5ml of PBS. Each sample was then transferred to a 1.5ml microfuge tube and centrifuged at 10,000rpm for 8 min. The resultant supernatant was removed and the remaining pellet re-suspended in 150µL of TE buffer. DNA extraction and qPCR was then performed as described in section 2.3.2.3. This experiment was conducted in triplicate and repeated three times.

2.3.3.2 DNA extraction optimisation

All samples were prepared following standardised techniques described in section 2.3.1. The first stages of DNA extraction were performed as per section 2.3.2.1 and different lysozyme incubation times were implemented (60, 120, 180 and 240 min). The standard DNA extraction and quantification protocol was subsequently followed (sections 2.3.2.1 and 2.3.2.3). This allowed bacterial DNA quantification values to be obtained for different lysozyme incubation periods. Each experiment was carried out in triplicate and repeated 3 times.

2.3.4 Statistical Analysis

Graph production and statistical analysis were performed using GraphPad prism software (version 4; La Jolla, CA, USA). One way analysis of variance (ANOVA) was used to investigate significant differences between independent groups. If ANOVA revealed a statistical significance, a Dunnett's multiple comparison test was performed to determine statistical significance between groups. Statistical significance was achieved if $P<0.05$. Standard curve production, linear trend-line equations and R^2 values were achieved using Microsoft Excel, Microsoft Cooperation© (version 14.0.7128.500 32-Bit, 2010).

2.4 Results

2.4.1 Growth Kinetics

First, the growth kinetics of different clinical strains was examined. For all *S. aureus* strains tested, bacterial growth was noted to be significantly higher ($P<0.05$) in BHI, TSB and DMEM + supplements when compared to all FCS media (10%, 25%, 50% and 75%) (Figure 2-1). The clinical and Newman's strains were found to grow significantly better ($P<0.05$) in BHI, TSB and DMEM + supplements when compared to DMEM alone. The NCTC strain (Figure 2-1 [C]) was found to grow significantly better in BHI ($P<0.05$), but not TSB or DMEM + supplements when compared to DMEM alone. Of the media tested we focused on DMEM + supplements as this has been used extensively in cell culture experiments (Coelho, Cabral et al. 2000, Mandel and Tas 2010, Tsimbouri, McMurray et al. 2012, Tsimbouri, Gadegaard et al. 2014) and allows for future cell co-culture studies. No significant difference was found between bacterial growth in all strains when comparing DMEM + supplements and TSB media. When comparing different bacterial strains, the Newman's strain grew significantly better in DMEM + supplements when compared to the other *S. aureus* strains.

The biofilm control strain *S. epidermidis* was found to grow significantly better in TSB, BHI and DMEM + supplements when compared to 10%, 50% and 75% FCS medias ($P<0.001$) and 25% FCS media ($P<0.01$). Growth was also significantly better in TSB, BHI and DMEM + supplements when compared to DMEM alone ($P<0.001$) (Figure 2-1 [D]).

As illustrated, the optimal growth conditions that were clinically representative and reproducible were that of the Newman's strain in DMEM + supplements media. This was therefore the bacterial strain and media used for all subsequent experiments.

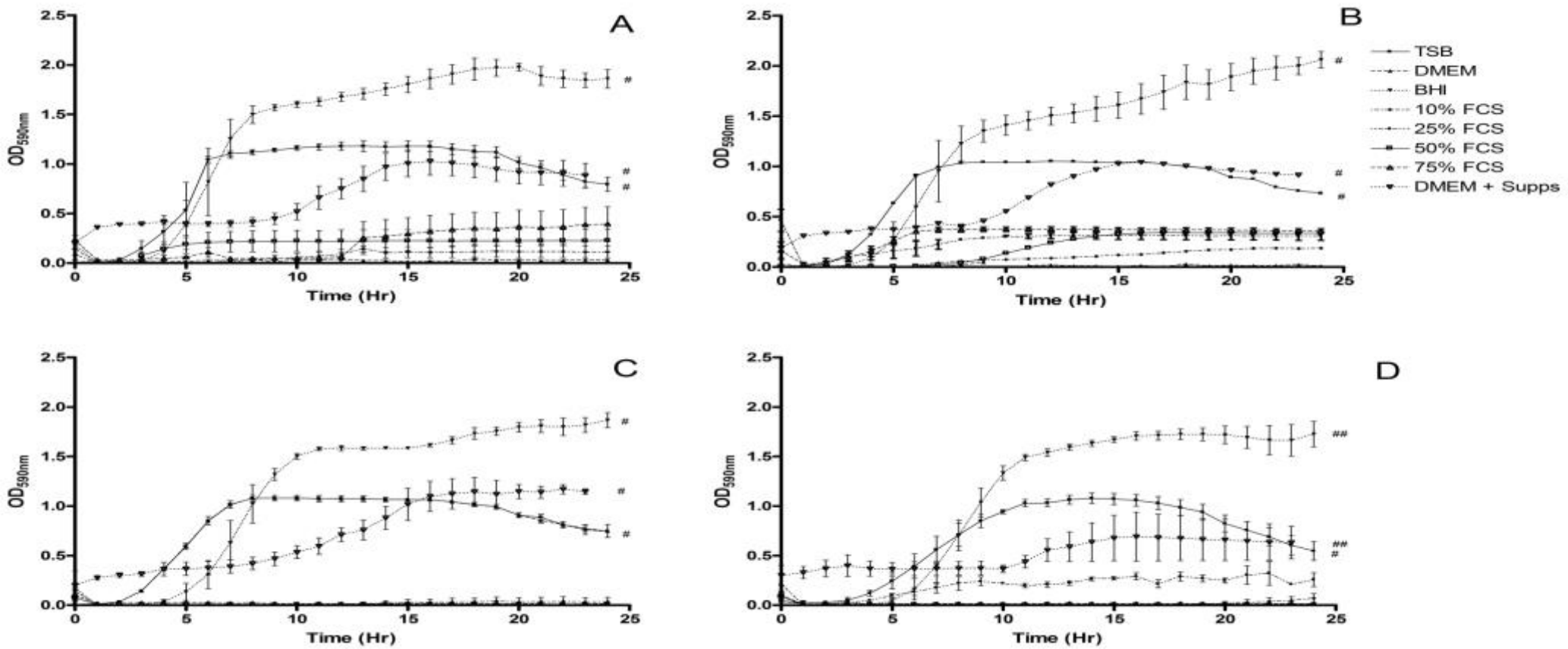

Figure 2-1 Bacterial growth curves.

All bacterial species and strains were standardised and grown in different media for a period of 24 h. (A) – Clinical strain. Growth was significantly better in TSB, BHI and DMEM + supplements when compared to all FCS concentration and DMEM ($^{\#}P<0.05$). (B) – Newman strain. Growth was significantly better in TSB, BHI and DMEM + supplements when compared to all FCS concentration and DMEM ($^{\#}P<0.05$). (C) – NCTC strain. Growth was significantly better in TSB, BHI and DMEM + supplements when compared to all FCS concentration and BHI when compared to DMEM ($^{\#}P<0.05$). (D) – S. *epidermidis*. Growth was significantly better in TSB, BHI and DMEM + supplements when compared to 10%, 50% and 75% FCS concentration and DMEM ($^{\#\#}P<0.001$). Growth was significantly better in DMEM + supplements when compared to 25% FCS ($^{\#}P<0.01$).

2.4.2 Standard curve production

Following the method described in section 2.3.2.3, standard curves were produced for all bacterial strains (Figure 2-2). The R^2 value was used to assess the fit of the trend line compared to the data points. All trend lines reached inclusion criteria and demonstrated a R^2 value of >0.97.

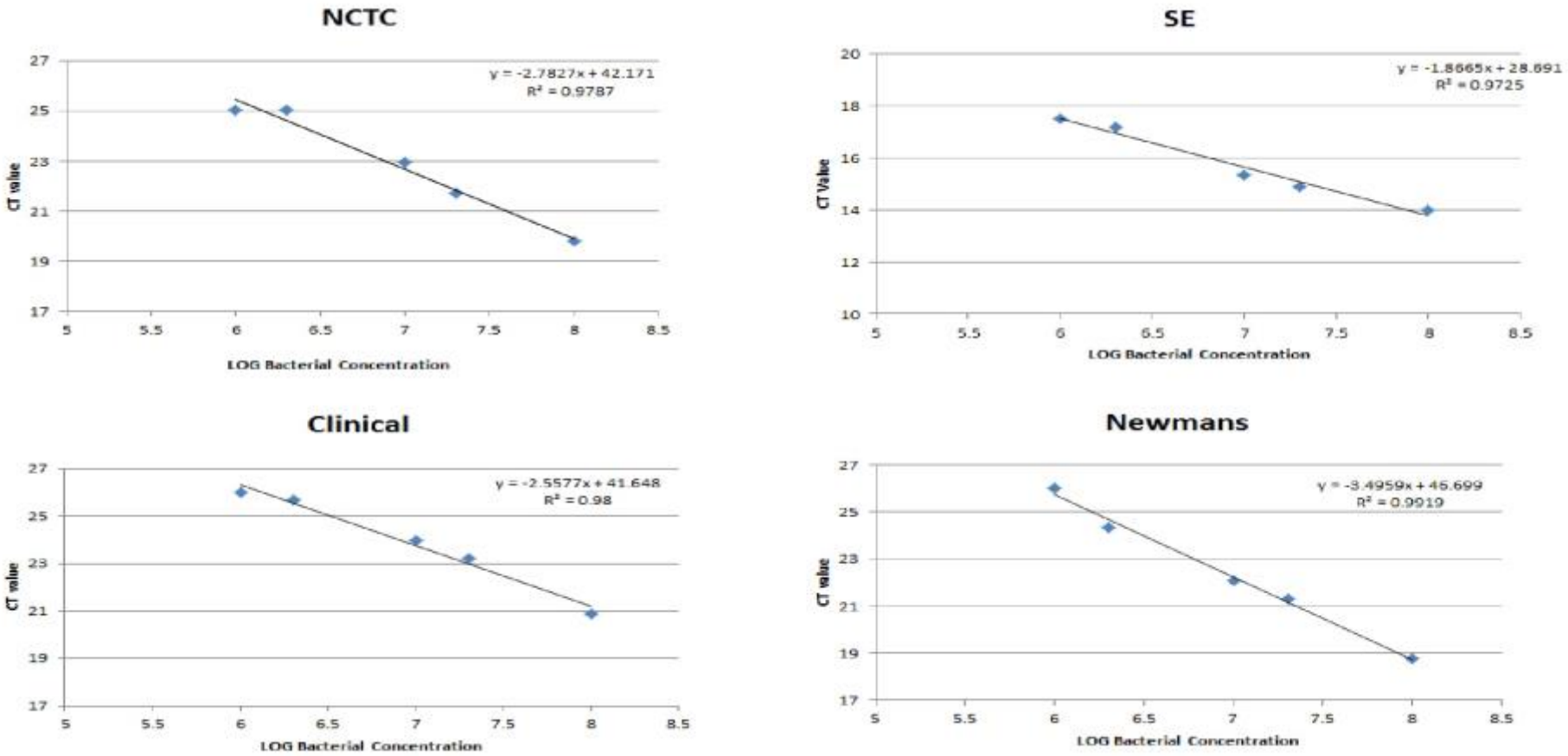

Figure 2-2 Standard curves for all bacterial species and strains.

Overnight cultures were standardised, and subsequently underwent 5-fold dilutions as per section 2.3.2.3. DNA was then extracted and qPCR performed as described in section 2.3.2.1. Average of all Ct values were plotted against the equivalent log10 of the DNA concentration and a linear trend line applied. The line equations allowed unknown bacterial counts to be quantified based on a single Ct reading. Each dilution of DNA was assessed in triplicate and repeated 3 times.

2.4.3 Optimal Bacterial Incubation

DNA extraction and qPCR (2.3.2) was used to identify the initial exponential increase in bacterial DNA concentration, illustrating the initial stages of biofilm development across all *S. aureus* strains. After 90 min incubation, bacterial concentration was found to be significantly higher when compared to 60 min ($P<0.01$) and 30 min ($P<0.001$) incubations in Newman's and clinical strains. There was no significant difference in bacterial concentration between 30 and 60 min incubations across all strains. 60 min was therefore used as the optimal incubation to isolate the adhesion phase of bacterial growth time (Figure 2-3), before exponential bacterial growth.

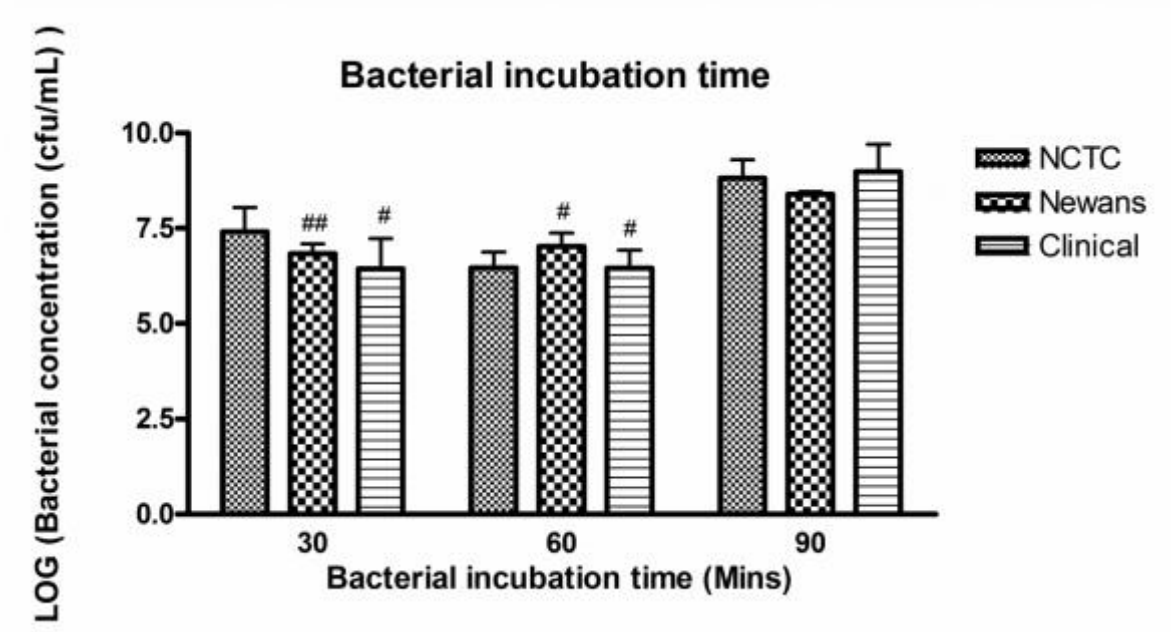

Figure 2-3 Optimised bacterial Incubation time.

S. aureus strains (NCTC, Newman's and clinical) were grown for 30, 60 and 90 min in DMEM + supplements media. Three replicates for each strain were used and carried out on 3 separate occasions. Data represents mean ± SEM. Significant differences were observed when comparing 90 min incubations to both 30 and 60 min incubations in Newman's and clinical (Stipetic, Hamilton et al. 2015) *S. aureus* strains. ($^{\#\#}P<0.001$, $^{\#}P<0.05$). No significant difference was noted between 30 and 60 min incubations in all strains.

2.4.4 Lysozyme incubation optimisation

Lysozyme incubation time was analysed in relation to the Newman's strain only (Figure 2-4). An incubation time of 120 min resulted in significantly more bacterial DNA being extracted when compared to 60 ($P<0.001$), 180 and 240 min ($P<0.01$). No significant difference was found between 60, 180 and 240 min. The optimal lysozyme incubation time of 120 min was used for all subsequent DNA extractions.

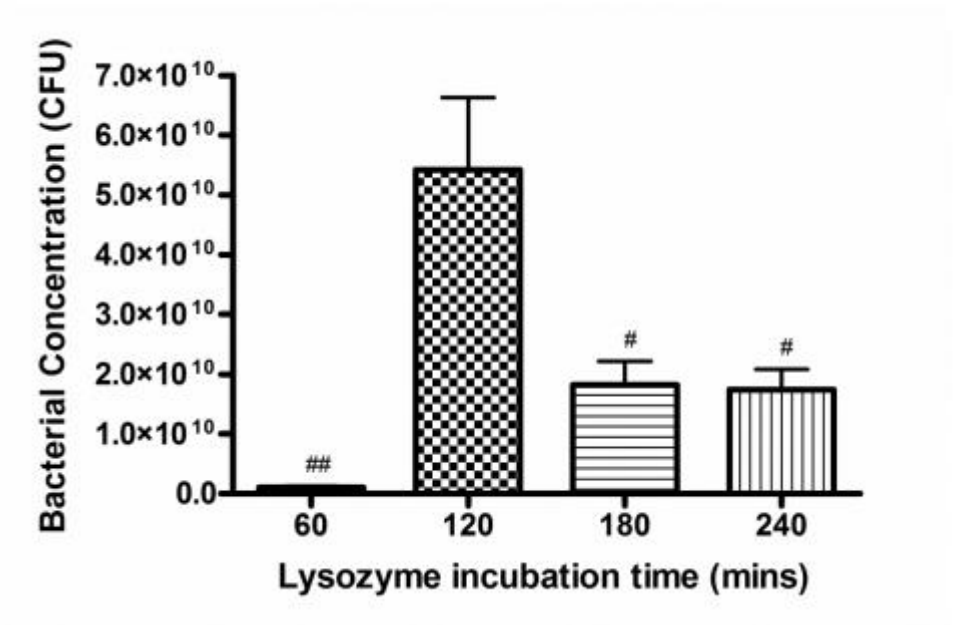

Figure 2-4 Optimal lysozyme incubation time.

Newman's strain was grown 60 min in DMEM + supplements media. Three replicates for each sample were used and carried out on 3 separate occasions. Data represents mean ± SEM. Significant differences were observed when comparing 120 min incubations to both 60 ($^{\#\#}P<0.001$) and 180 and 240 min incubations ($^{\#}P<0.01$). No significant difference was noted between 60, 180 and 240 min incubations.

2.5 Discussion

Implantable medical devices or biomaterials continue to be used extensively in modern medicine, specifically in orthopaedics (Charnley 1960, Ratner 2004, Gomez and Morcuende 2005, Kurtz, Ong et al. 2007). Orthopaedic implant infection represents a significant arthroplasty complication (Ainscow and Denham 1984, Ahnfelt, Herberts et al. 1990), with *S. aureus* and *S. epidermidis*

constituting up to 60% of all confirmed arthroplasty infections (Trampuz and Widmer 2006). Whilst a great deal of literature highlights the importance of these bacterial species in orthopaedic infections (Garvin, Hinrichs et al. 1999, Campoccia, Montanaro et al. 2006, Nickinson, Board et al. 2010), methods of standardising and optimising staphylococcal biofilm growth and quantification vary greatly (Bergamini, Bandyk et al. 1989, Atanassova, Meindl et al. 2001). Several bacterial quantification techniques are discussed in the literature (Alarcon, Vicedo et al. 2006, Stepanović, Vuković et al. 2007), however a generic method, used by the majority is not readily recognised. This chapter focuses on optimising biofilm growing conditions.

Firstly, we looked at growth media. Historically a multitude of different growth medias have been used for staphylococcal culture including; TSB, BHI, Nutrient Broth (NB) and Meat infusion broth (MIB) to name a few (May, Houghton et al. 1964, Christensen, Simpson et al. 1982, Safdar, Narans et al. 2003). Media composition is largely determined by the nature of the experiment and the properties and growth characteristics of the bacterial strains (Monod 1949). Whilst media such as BHI and TSB provide a nutritious environment for bacterial growth, the ability to incorporate future mesenchymal cell co-culture studies would be limited (Mandel and Tas 2010, Tsimbouri, McMurray et al. 2012, Tsimbouri, Gadegaard et al. 2014). Osteointegration is essential for long-term survival of TJR. The culture medium used in this study therefore had to be optimal for culture of mesenchymal stem cells as well as bacteria. DMEM + supplements (FBS, L-glutamine, Sodium Pyruvate and non-essential amino acids) has been used extensively in cell culture laboratories (Webber, Harris et al. 1985, Palmer, Schwartz et al. 2001, Dalby, Cates et al. 2004), therefore we used this media in the novel setting of bacterial culture to represent the clinical situation. Our results show that throughout all bacterial strains, DMEM + supplements caused significantly higher bacterial growth when compared to 10%, 25%, 50% and 75% FCS media (2.4.1). Additionally, in the majority of strains, DMEM + supplements was significantly better at supporting bacterial growth than DMEM alone. While more classical media such as TSB also promoted bacterial growth, it was not significantly more than DMEM + supplements. While DMEM + supplements did not produce the highest bacterial concentrations (BHI was significantly better for bacterial growth and culture when compared to all other

culture media), it did still promote bacterial growth and had the advantage of being a more clinically representative. It was therefore used as the optimal culture media for all subsequent bacterial biofilm experiments in this study.

Of the bacterial strains used, all were successfully cultured to produce standard curves as described in section 2.3.2.3. All R^2 values fell within our inclusion criteria (R^2 >0.97), and therefore provided a good linear association between Ct values and bacterial concentrations. As mentioned previously, all strains showed similar growth kinetics in relation to media selection. At this stage, due to time restraints, focus was applied to the Newman's strain. Initially isolated in 1952 from a human infection (thought to be osteomyelitis), this strain has been used extensively in animal models. In our study it provided the most reproducible results, with 100% of all overnight cultures being successful. It showed similar growth kinetics to the other 2 *S. aureus* strains, and was therefore felt to be suitable to represent the *S. aureus* family.

The majority of current bacterial quantification methods are based on the microtitre plate method described above. These can broadly be divided into biofilm biomass assays, viability assays and matrix quantification assays. Whilst all useful, each have drawbacks. Biomass assays are based on quantification of matrix as well as cells, the most common of which is crystal violet (CV). This method, first described by Christensen *et al*, 1985 (Christensen, Simpson et al. 1985), has been modified over the years, but still stains all cells and matrix. In addition it is usually only accurate after a prolonged period of bacterial growth (12-24h) and therefore has limited use in the identification of the early stages of biofilm development (Stepanović, Vuković et al. 2000). Viability assays count viable cells, but often rely on fluorogenic dyes, such as Syto9, to stain viable DNA (Boulos, Prevost et al. 1999). This method is used extensively in bacterial and yeast biofilm biomass quantification (Honraet, Goetghebeur et al. 2005, Honraet and Nelis 2006). Thus, given its widespread use, this method was trialled as a useable method. Unfortunately however, our experiments were restricted as our nanotopographies were imprinted on semi-transparent wells, which resulted in over-spill of fluorescence into neighbouring wells when measuring OD, causing inaccurate readings. Matrix quantification assays clearly measure only biofilm matrix and are therefore of limited use looking at bacterial adhesion, a stage that occurs before matrix production. Given the issues

described, qPCR was employed as a method of quantifying bacteria. Used extensively in dental (Williams, Trope et al. 2006) and medical (Larsen, Vogensen et al. 2010) fields, qPCR provides a real time quantification of bacterial DNA. Our analysis of the bacterial concentration following different bacterial incubation periods showed that after 90 min, bacterial concentrations were significantly higher when compared to both 30 and 60 min incubations in clinical and Newman's strains. When correlated with our bacterial growth curve, this suggests that at 90 min, the bacteria are in the exponential phase of growth and therefore adhesion/aggregation has already occurred. In contrast, no significant difference was noted between 30 and 60 min incubations, suggesting a pre-exponential growth phase environment representing the adhesion/aggregation phase of bacterial growth. Thus the optimal incubation time for bacteria adhesion was found to be 60 min.

The final area we optimised was the DNA extraction protocol used for qPCR. As per our methods (2.3.2), we focused on optimising the lysozyme incubation period. Our aim was to remove all adherent bacteria, and therefore achieve maximum DNA yields from each extraction and subsequent qPCR. Effective lysis is recognised as a key factor in the purification and extraction of bacterial DNA (Schutzbank and Kahmann). Lysozymes act primarily on the cell wall, causing enzymatic cell lysis by splitting polysaccharide (peptidoglycan) chains (Salazar and Asenjo 2007). Their action is therefore highly dependent on the cell wall constituents. Gram positive bacterial cell walls are composed of multiple layers of peptidoglycans which compromise around 90% of the cell structure (Sigma-Aldrich 2015). Lysozyme is therefore an extremely efficient agent for lysing gram positive bacteria. Of note, the specific lysozyme we used was ready-lyse lysozyme, which works at lower concentrations and over a larger pH range (Epicentre 2014). We found that significantly higher quantities of DNA were extracted at 120 min when compared to 60, 180 and 240 min. At 60 min incubation, it is likely that the lysozyme had not lysed all the cell walls resulting in a lower DNA concentration following qPCR. The lysozyme is clearly working at this stage, as DNA was extracted and quantified; therefore it seems that experimental conditions (as recommended by Epicentre®, Illumina®) were adequate. The cause of reduced DNA concentration following extractions at 180 and 240 min is less clear. It may be that following bacterial cell lysis, if left for a

prolonged time (i.e. >120 min), DNA degradation occurs resulting in a reduced DNA concentration following extraction. DNA is certainly known to degrade following cell apoptosis (Wyllie 1980, Jacobson, Weil et al. 1997), therefore is seems likely this occurs after forced bacterial cell lysis with lysozyme. The optimal lysozyme incubation time of 120min was therefore used for all subsequent experiments involving DNA extraction and qPCR. These optimisation experiments are summarised in the flow diagram below (Figure 2-5).

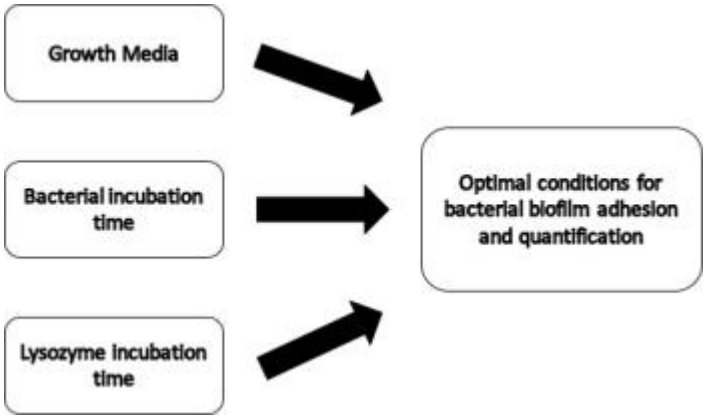

Figure 2-5 Optimisation experiment optimisation flow diagram.

In conclusion, this initial pilot study produced optimal, reproducible and quantifiable bacterial biofilms. Bacterial incubation in DMEM + supplement media for 60min was felt to represent the adhesion phase of biofilm development which is the focus of this study. Under these conditions, a lysozyme incubation period of 120min produced the highest DNA qPCR yields, and was thus felt to be optimal.

Chapter 3

Biofilms and Nanotopographies

3.1 Introduction

Adhesion is recognised as the first stage of bacterial biofilm development (Sauer, Camper et al. 2002, Hall-Stoodley, Costerton et al. 2004, Jahoda 2009). Whilst dependent on cell-surface interactions as described previously, alterations to the surface topography at a nanoscale has also been shown to have major effects on cell behaviour (McMurray, Gadegaard et al. 2011), bacterial adhesion (Xu and Siedlecki 2012) and ultimately long term implant survival (Sjöström, Brydone et al. 2013). Submicron surface textures on polyurethane has been shown to significantly reduce bacterial adhesion when looking at S. *aureus* and S. *epidermidis*, with a subsequent reduction in biofilm formation (Xu and Siedlecki 2012). Further studies have suggested that by changing the surface roughness of titanium, bacterial biofilm development can be altered. Ivanova *et al* 2009 found that as surface roughness is increased, bacterial attachment of S. *aureus* decreases (Ivanova, Truong et al. 2009). These results are however far from universal. Whilst some studies have shown a bacterial adhesion preference to trenches, known as contact guidance (Díaz, Schilardi et al. 2008), others have shown no preference to surface topography and disregarded surface roughness as factor in adhesion (Bos, van der Mei et al. 1999). The results of these contradictory studies are almost certainly due to differences in manufacturing methods and specific nanopatterns used. Studies looking at the effects of nano-roughness are based on the degree of roughness associated with a particular surface at the nanometre level (Ivanova, Truong et al. 2009). This is not a regulated nanopattern in the form of nanopits or nanowires, rather a roughened surface that is given an average 'roughness' value. To some extent therefore, the exact structure of the surface is unknown. In comparison, the research by Diaz *et al* 2003 provided continuous nano-channels in which bacteria preferentially grew (Díaz, Schilardi et al. 2008). It should be noted however that these channels were embedded, therefore could it be that the bacteria are simply settling into these channels and are unable to 'escape' and interact with other bacterial channels. There are clearly challenges and variations associated with fabricating surfaces at the nanoscale. Our study initially looked at nanopatterned polystyrene surfaces and subsequently focused on titanium nanosurfaces, each of which will now be introduced.

Synthetic plastics have been used in various nanotopography studies, due to their relatively low cost and ease of production (Sjöström, Dalby et al. 2009, Biggs, Richards et al. 2010, Sjöström, Brydone et al. 2013). Whilst not all plastics are commonly used directly in operative orthopaedics, their importance should not be underestimated. Chung *et al* found that catheter associated infections can be reduced by altering the nanotopography on the silicone elastomer Silastic® (Chung, Schumacher et al. 2007), whilst Xu *et al* found similar results on polyurethane (Xu and Siedlecki 2012). The former study created a nanotopography based on shark skin (aptly named Sharklet AF™) that consisted of rectangular ribs of varying lengths (4-16μm) with regular 2μm spacing. The protruding features of this topographical surface appeared to provide a physical barrier that prevented the expansion of small clusters of bacteria present within the recesses into microcolonies (Chung, Schumacher et al. 2007). Although prevention of bacterial adhesion is the focus of this study, the importance of an orthopaedic implant to osseointegrate must also be recognised. Surface topography is known to have effects on cell behaviour (McMurray, Gadegaard et al. 2011) as well as bacterial adhesion (Xu and Siedlecki 2012). Dalby *et al* demonstrated that highly ordered nanotopographies (supplied by the Gadegaard group, University of Glasgow) produce low cellular adhesion and osteoblastic differentiation whilst cells on random nanotopographies exhibited a more osteoblastic morphology (Dalby, Gadegaard et al. 2007, Hart, Gadegaard et al. 2007). This suggests that the use of disorder may be an effective strategy in promoting influence over at least mesenchymal stem cells (MSCs) for regenerative medicine and tissue engineering. Collaboration with both the Dalby and Gadegaard groups has allowed the use of these novel nanotopographies for our bacterial adhesion studies.

Our study initially focussed on polystyrene nanosurfaces that have previously shown osseointegrative properties in MSC research (Dalby, Gadegaard et al. 2007, Hart, Gadegaard et al. 2007), with the hypothesis that bacterial adhesion may also be affected. Subsequently we also looked at the more clinically relevant nanopatterned materials, Ti.

Titanium is the most commonly used metal in modern orthopaedic arthroplasty surgery (Ramachandran 2006). This is primarily due to its relative low Young's modulus of elasticity (110GPa) when compared with other metals used in

orthopaedics such as cobalt-chrome (230GPa) and stainless steel (190GPa) (Katti 2004). In addition, titanium alloys also show good wear characteristics, excellent biocompatibility and fatigue resistance, the only downside being the relative expense (Learmonth, Young et al.), costing up to five times as much per kilogram than stainless steel. Given titanium's widespread use in orthopaedic implant production, inclusion of nanopatterned titanium in our study was a novel and key feature. The titanium nanosurfaces were produced and supplied by our collaborators at the School of Oral and Dental Sciences, University of Bristol, Bristol, UK.

3.2 Chapter Aims

It was the hypothesis of this study that surface nanotopography affects the ability of staphylococci species to adhere. This chapter aims to investigate whether different materials and nanosurfaces, focussing on nanopits in polystyrene and nanowires, nanocauseways and nanograss in titanium, affect bacterial adhesion.

Work from this chapter has been published in:

Hansom D et al *THE EFFECTS OF NANOPATTERN SURFACE TECHNOLOGY ON ORTHOPAEDIC JOINT REPLACEMENT INFECTION*. Bone & Joint Journal Orthopaedic Proceedings Supplement, 2015. **97-B**(SUPP 3): p. 2.

Work from this chapter has been presented at the following conferences:

Hansom D, Tsimbouri M, Ramage G, Burgess K, Dalby M, Meek D and Clarke J. 'Nano-topographical modulation of cells and bacteria for next generation orthopaedic implants.' Centre of Cell Engineering – Glasgow Orthopaedic Research Initiative, December 2014.

Hansom D, Burgess K, Meek D, Clarke J, Ramage G. 'The effects of nanopattern surface technology on orthopaedic joint replacement.' Glasgow Meeting of Orthopaedic research, March 2015.

Hansom D, Burgess K, Meek D, Clarke J, Ramage G 'Nano-topographical modulation of cells and bacteria for next generation orthopaedic implants.' El-Minia University Hospital Scientific Day, Egypt, February 2015.

Hansom D, Burgess K, Gadengaard N, Millar N, Clarke J & Ramage G. 'The effects of nanopattern surface technology on orthopaedic joint replacement.' European Federation of National Associations of Orthopaedics and Traumatology, June 2016.

Hansom D, Burgess K, Gadengaard N, Millar N, Clarke J & Ramage G. 'The effects of nanopattern surface technology on orthopaedic joint replacement.' British Orthopaedic Research Society, September 2016.

3.3 Materials and Methods

S. *aureus* Newman strain was used for these experiments. Bacteria was collected, cultured and standardised under optimal growth conditions as per Chapter 2.

3.3.1 Polystyrene nanosurfaces

3.3.1.1 Production

Manufacture of polystyrene nanosurfaces was carried out by our collaborators at the Biomedical Interfaces at Glasgow Group, School of Engineering, University of Glasgow. 24 nanopattern surfaces were imprinted onto a polystyrene microscope slide. Each nanosurface was a circle with the same diameter as that found on a polystyrene 96-well, flat-bottomed microtitre plate (Corning incorporated, NY, USA). A purpose build well-type structure was then designed, and this was welded to the above-mentioned microscope slide containing different nanopatterns. These two sections were designed and made by our collaborators (Department of Electronics and Electrical Engineering, University of Glasgow, Glasgow, G12 8QQ, U.K), however, welding was carried out by the author. The microscope slide and well structure was welded together using an ultrasound welder (Standard 3000, Rinco Ultrasonics, Switzerland). Before welding, the correct orientation of microscope slide to well structure was checked, ensuring

each nanopattern was centred at the bottom of each well. The well layout is shown in Figure 3-1.

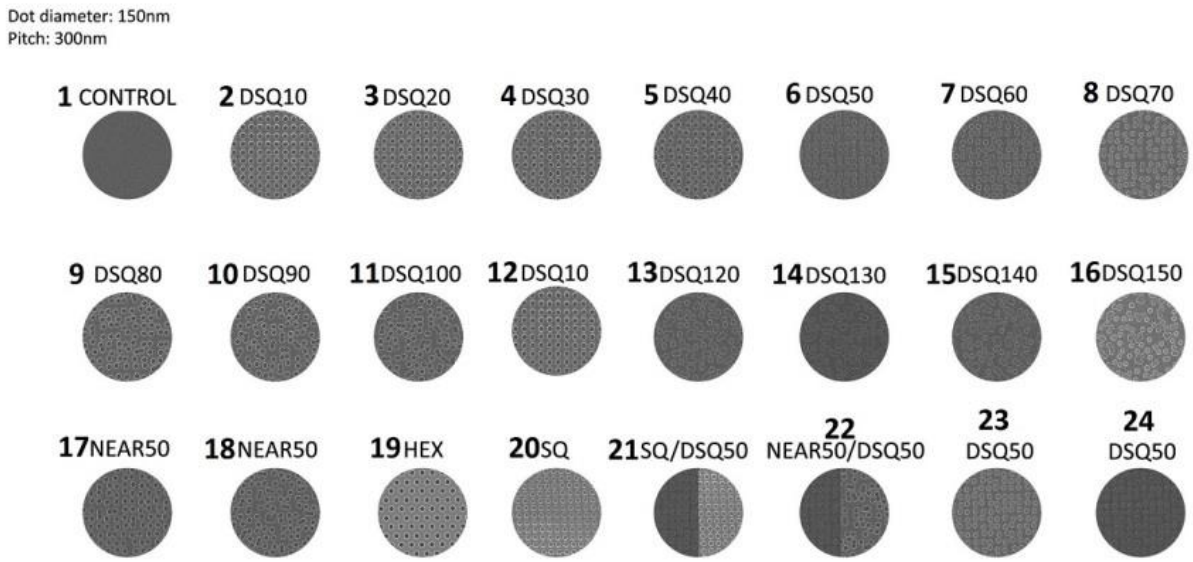

Figure 3-1 24 well polystyrene nanosurface layout

Diagrammatic representation of a 24-well nanosurface polystyrene plate where *DSQ* = disordered square, *HEX* = Hexagonal, *SQ* = Square, NEAR = near square. The number following each arrangement type represents the offset in nm from the true centre position.

Due to time constraints, only selections of the above nanopatterns were analysed. These were Control, DSQ10, DSQ50, DSQ100, DSQ150, NEAR50, HEX and SQ. It was felt that this gave a good representation of the different nanosurfaces available. If required at a later date, the remaining surfaces could be studied.

3.3.1.2 24-well plate sterilisation

Before bacterial work could commence all polystyrene 24-well plates were sterilised. Each well was filled with 200µL of 70% ethanol for 15min. Following this period, the ethanol was removed and the wells thoroughly washed out with PBS twice. The plates were then placed under a hood (Microflow biological safety cabinet, Astec, Hampshire, UK) until air-dried. Each plate was then sealed with Parafilm® to maintain sterility until required.

3.3.1.3 Bacterial growth quantification

S. *aureus* Newman strain was cultured, grown overnight and standardised as described in (2.3.1). Following standardisation in DMEM + supplement media, 150µL of each sample was added to defined wells in a pre-sterilised, polystyrene 24-well plate as previously described (3.3.1.2). The plate was incubated at 37ºC on a shaking platform for 1 hour. Following removal, supernatant liquid was removed and each well was gently washed with PBS to remove any non-adherent bacteria. At this stage, 150µL of TE buffer was added to each well in addition to 1µL of lysozyme, as per the DNA extraction protocol described (2.3.2). Following lysozyme incubation for 2 hours, each sample was transferred to a 1.5mL microfuge tube and DNA extraction and subsequent bacterial quantification using DNA qPCR was carried out (2.3.2.3). Previously obtained standard curves allowed bacterial concentrations to be calculated based on the Ct values obtained. All experiments were carried out in triplicate and repeated 3 times.

3.3.1.4 Imaging of bacteria

S. *aureus* Newman strain was cultured, grown overnight and standardised as described in (2.3.1). Following standardisation in DMEM + supplement media, 150µL of each sample was added to defined wells in a pre-sterilised, polystyrene 24-well plate as previously described (3.3.1.2). The plate was incubated at 37ºC on a shaking platform for 1 hour. Following removal, supernatant liquid was removed and each well was gently washed with PBS to remove any non-adherent bacteria. Samples were then allowed to air dry under a hood (Microflow biological safety cabinet, Astec, Hampshire, UK) and subsequently heat fixed. Each plate was then sealed with Parafilm® to maintain sterility until required. Polystyrene nanosurfaces were imaged using the EVOS® FL Auto cell imaging system (Life Technologies, Paisley, UK). A purpose build 24-well plate holder was designed to be used in conjunction with the above microscope. This allowed 10 randomly selected images to be taken of each polystyrene nanosurface. These images were then analysed using Cell Profiler® software (Carpenter, Jones et al. 2006), which provided a percentage bacterial coverage value for each surface. Percentage coverage values were then compared between surfaces. This experiment was carried out in triplicate.

3.3.1.5 Statistical analysis

Graph production and statistical analysis were performed using GraphPad prism software (version 4; La Jolla, CA, USA). One-way analysis of variance (ANOVA) was used to investigate significant differences between independent pattern groups. If ANOVA revealed a statistical significance, a Dunnett's multiple comparison test was performed to determine statistical significance between groups. Statistical significance was achieved if $P<0.05$.

3.3.2 Titanium nanowires, nanocauseways and nanograss

3.3.2.1 Production

Manufactured titanium and control surfaces were provided by our collaborators (School of Oral and Dental Sciences, University of Bristol, Bristol, UK). Ti nanowire (NW) production method was not the focus of this study, however in brief; each Ti surface was prepared from a 0.9 mm thick ASTM grade 1 Ti sheet (Ti metals Ltd, UK). The samples were polished to a mirror image and ultrasonically cleaned in water and ethanol. These polished samples were used as our control surface. For the nanowire formation, the Ti disks were immersed in 1M sodium hydroxide (NaOH) in a Polytetrafluoroethylene (PTFE) lined steel vessel (Acid Digestion vessel 4748, Parr Instrument Company, USA), which was placed in an oven at a temperature of 240°C. The vessel was removed from the oven and allowed to cool to room temperature after 2, 2.5 or 3hr's. Each NW surface was rinsed in water and ethanol, sequentially. To convert the $NaTiO_2$ to TiO_2 the samples were immersed in 0.6M Hydrogen Chloride (HCl) for 1 h, rinsed in water and ethanol, and finally heat treated at 600°C for 2 h. Examples of the Ti NW structures are shown in Figure 3-2. Samples were stored in sterile containers until required.

Manufactured Ti nanocauseway (NC), nanograss (NG) and control surfaces were also provided by our collaborators (School of Oral and Dental Sciences, University of Bristol, Bristol, UK). Their production differed slightly from the NW surfaces, which will be briefly highlighted. These surfaces were made from grade 5, Ti-6Al-4V (Ti64) (Ti-Tek (UK) Ltd) with a thickness of 1 mm. Ti64 squares ($10mm^2$) were cut, polished and ultrasonically washed in distilled water, and finally air dried. The squares were then placed inside a ceramic tube

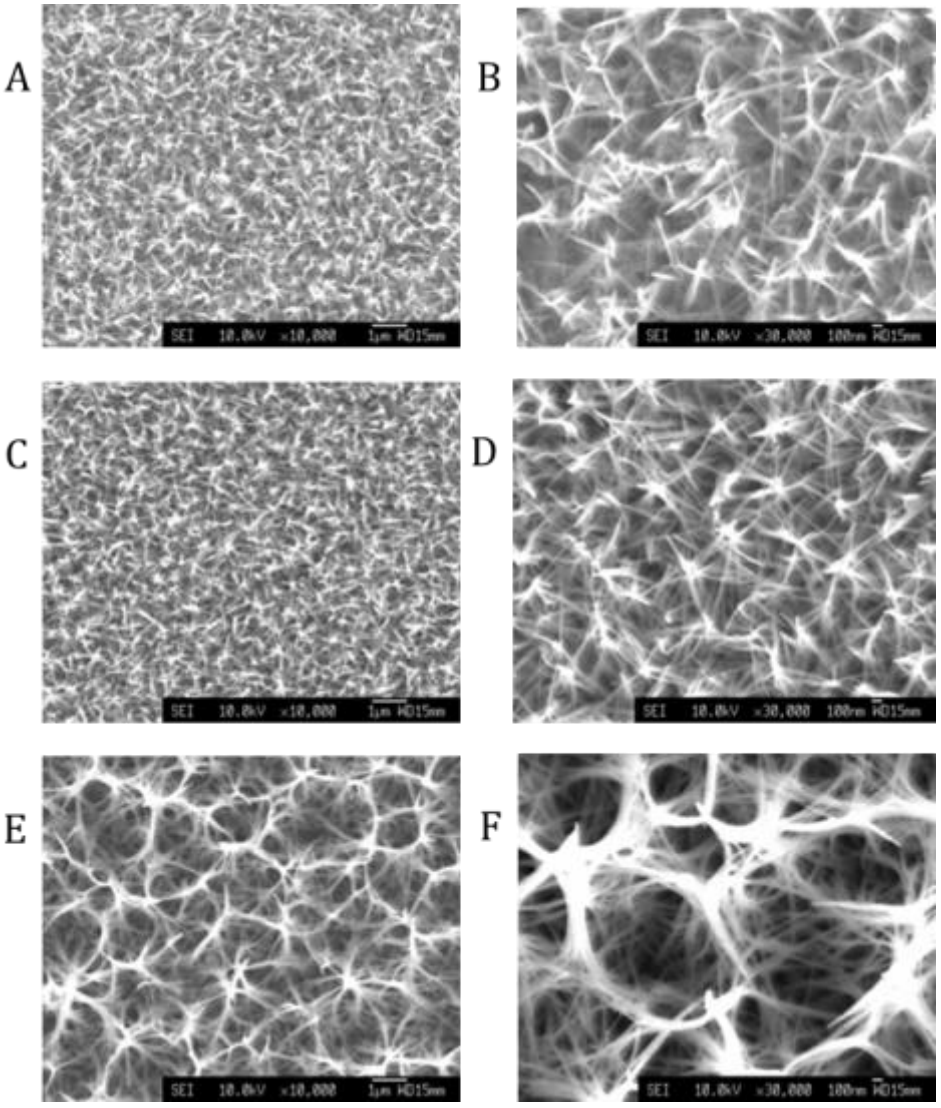

Figure 3-2 Imaging of nanowire structures

SEM images of 2 Hr treated titanium NW structure – x10000 magnification (A) and x30000 magnification (B). 2.5 Hr treated titanium NW structure - x10000 magnification (C) and x30000 magnification (D). 3 Hr treated titanium NW structure - x10000 magnification (E) and x30000 magnification (F) (Images provided by (Sjöström, Brydone et al. 2013)).

furnace, which was flushed with argon (Ar) at a flow rate of either 50 (NC) or 200 (NG) standard cubic centimetres per min (sccm) for 30 min. The tube was then heated to 850°C at a rate of 15°C/min. After reaching final temperature, acetone vapour was introduced into the tube by passing the Ar through a bottle containing acetone. The temperature was kept at 850°C with acetone vapour for 30 min, after which the tube was cooled to room temperature. The squares were then annealed at 600°C for 30 min in air to remove the carbon from the surfaces. Examples of the Ti NC and NG structures are shown in Figure 3-3 . Samples were stored in sterile containers until required.

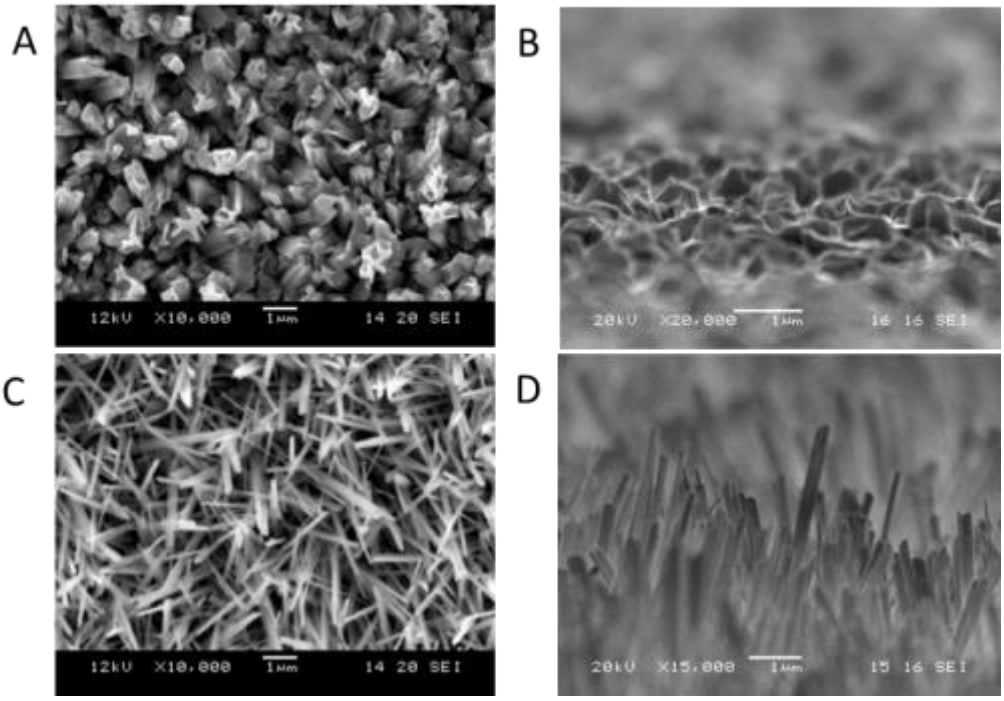

Figure 3-3 Imaging of NG and NC structures

SEM images of NC structure – x10000 magnification (A) and x20000 magnification (B). NG structure - x10000 magnification (C) and x20000 magnification (D) (Images provided by (Sjöström, Dalby et al. 2009)).

3.3.2.2 Sterilisation

Before bacterial work could commence all titanium samples were sterilised in a 24-well plate (Corning incorporated, NY, USA). Each well (containing 1 titanium sample) was filled with 500μL of 70% ethanol for 15mins. Following this period, the ethanol was removed and the samples were thoroughly washed with PBS twice. Samples were then placed under a hood (Microflow biological safety cabinet, Astec, Hampshire, UK) until air dried and subsequently sealed in a sterile container with Parafilm® until required.

3.3.2.3 Bacterial growth quantification

S. *aureus* Newman strain was cultured, grown overnight and standardised as described in (2.3.1). Following standardisation in DMEM + supplement media, 500μL of each sample was added to defined wells in a pre-sterilised, standard polystyrene 24-well plate containing titanium surfaces. The plate was incubated at 37ºC on a shaking platform for 1 hour. Following removal, supernatant liquid was removed and each sample was gently washed with PBS to remove any non-adherent bacteria. Each sample was then carefully removed and added to a

bijous containing 500µL of PBS and ultrasonnicated for 10 minutes at room temperature (Ultrasonic Heated bath, Fisherbrand®, Leicestershire, UK). It should be noted that it is impossible to remove all bacteria from the surfaces, however this method was the most successful and constant across all samples. Each sample was removed and the remaining liquid was transferred to a 1.5mL microfuge tube and centrifuged for 10 min at 5000rpm. All supernatant liquid was then discarded and 150µL of TE buffer was added to each tube in addition to 1µL of lysozyme, as per the DNA extraction protocol described (2.3.2.1) Following lysozyme incubation for 2 hours, DNA extraction and subsequent bacterial quantification using DNA qPCR was carried out (2.3.2.3). Previously obtained standard curves allowed bacterial concentrations to be calculated based on the Ct values obtained. All experiments were carried out in triplicate and repeated 3 times.

3.3.2.4 Imaging of bacteria

S. *aureus* Newman strain was cultured, grown overnight and standardised as described in (2.3.1). Following standardisation in DMEM + supplement media, 500µL of each sample was added to defined wells in a pre-sterilised, standard polystyrene 24-well plate containing sterile Ti nanosurfaces. The plate was incubated at 37^{o}C on a shaking platform for 1 hour. On removal, all supernatant was discarded and each sample was gently washed with PBS twice. SYTO®9 green fluorescent nucleic acid stain (Life Technologies, Paisley, UK) was used at a dilution of 2µL/ml in deionised water. 150µL of the nucleic acid stain was added to each sample and incubated in the dark at 37^{0}C for 20 minutes. Residual stain was then removed, and each sample was mounted on a microscope slide with a coverslip and imaged (Motic BA 400 microscope [Wetzlar, Germany] with CoolLED fluorescence excitation system [Andover, UK]) at 100x magnification. Image capture and analysis was carried out using Cell B imaging software (Olympus Soft Imaging solutions, version 2.5). These images were then further analysed using Cell Profiler® software (Carpenter, Jones et al. 2006), which provided a percentage bacterial coverage value for each surface. Percentage coverage values were then compared between surfaces. This experiment was carried out in triplicate, with 4 randomly selected images from each sample being used, giving a total of 12 images per surface.

3.3.2.5 Scanning electron microscopy (SEM)

S. *aureus* Newman strain was cultured, grown overnight and standardised as described in (2.3.1). Following standardisation in DMEM + supplement media, 500µL of each sample was added to defined wells in a pre-sterilised, standard polystyrene 24-well plate containing different titanium nanosurfaces. The plate was incubated at 37ºC on a shaking platform for 1 hour. Following incubation, samples were carefully washed with PBS and then fixed (2% para-formaldehyde, 2% gluteraldehyde, 0.15M sodium cacodylate and 0.15% w/v alcian blue (pH 7.4) for 18 hrs. The fixative was then removed and samples were washed with 0.15M sodium cacodylate buffer three times and then stored in 0.15M sodium cacodylate buffer at 4ºC until processing. Sample processing was carried out as described by Erlandsen *et al*, 2004 (Erlandsen, Kristich et al. 2004), allowing image acquisition using SEM. Randomly selected images were taken at x1000, x5000 and x10,000 magnifications for each surface.

3.3.2.6 Statistics

Graph production and statistical analysis were performed using GraphPad prism software (version 4; La Jolla, CA, USA). One-way analysis of variance (ANOVA) was used to investigate significant differences between independent pattern groups. If ANOVA revealed a statistical significance, a Dunnett's multiple comparison or Tukey's test was performed to determine statistical significance between groups, depending on individual experiments. If two pattern groups were compared, an unpaired student's T-test was employed. Statistical significance was achieved if $P<0.05$.

3.4 Results

3.4.1 Polystyrene nanosurfaces

3.4.1.1 Bacterial Concentrations

S. *aureus* Newman strain was cultured and grown under optimal conditions on different polystyrene nanopatterned surfaces in custom made 24-well plates. The results show a reduced bacterial concentration on the HEX and SQ nanosurfaces when compared to the control surface and other nanosurfaces (Figure 3-4). This trend was noted in all replicates; however, did not reach statistical significance. The highest bacterial concentrations were noted on the NEAR and DSQ 50 patterns when compared to control and remaining nanosurfaces. These observations were again, noted across all replicates but not found to be significant.

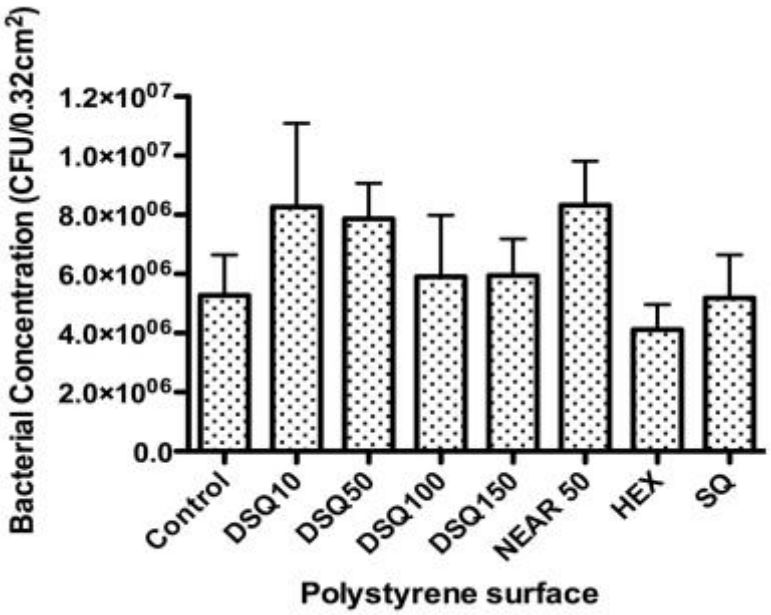

Figure 3-4 Average bacterial concentration on different polystyrene nanopatterned surfaces.

S. *aureus* Newman strain was standardised in DMEM + supplement media and grown on various nanopatterned polystyrene surfaces for a period 1 hour. Bacterial concentrations appeared to be lower on HEX and SQ patterns, when compared to Control, DSQ10, 50, 100, 150 and NEAR 50. This trend was not significant.

3.4.1.2 Imaging

Following culture and growth of S. *aureus* Newman strain on different polystyrene nanopit surfaces, each surface was imaged as described previously (3.3.1.4). Data analysis by Cell Profiler® software allowed the percentage bacterial coverage for each nanosurface to be calculated. It was assumed that the greater the percentage bacterial coverage; the higher bacterial adhesion to that particular surface. As illustrated below (Figure 3-5), percentage bacterial coverage is significantly lower on the HEX (P=0.05) and SQ (P=0.01) patterns when compared to the control surface, with an average coverage of 2% and 0.9% respectively. The highest bacterial percentage coverage was noted on Control, DSQ100 and NEAR50 with average percentage coverage of 4.2%, 3.7% and 3.6% respectively.

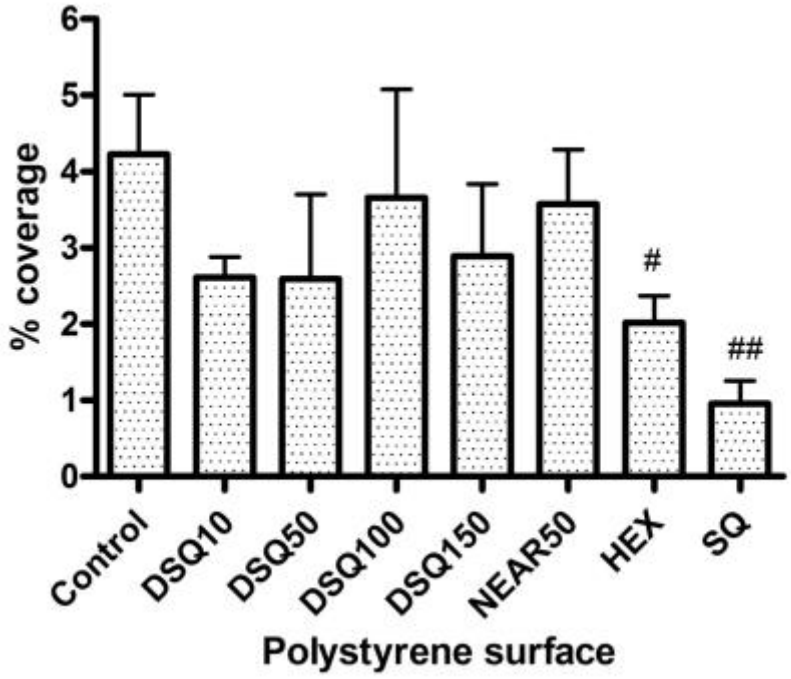

Figure 3-5 Average bacterial percentage coverage on different polystyrene nanopatterned surfaces.

S. *aureus* Newman strain was standardised in DMEM + supplement media and grown on various nanopatterned polystyrene surfaces for a period 1 hour. Bacterial percentage coverage was significantly lower on HEX and SQ patterns, when compared to Control ($^{\#}P=0.05$, $^{\#\#}P=0.01$ respectively). No significant difference was noted between all other surfaces.

3.4.2 Titanium nanowires

3.4.2.1 Bacterial concentrations

S. *aureus* Newman strain was cultured overnight and standardised in optimal media as previously described (2.3.1). S. *aureus* Newman strain was grown under optimal conditions on different Ti control (polished) and NW discs in 24-well plates. We found significantly higher bacterial concentrations on the 2.5Hr ($P<0.05$) and 3Hr ($P<0.01$) NW materials when compared to the control, polished Ti discs. Whilst the bacterial concentration was higher on the 2Hr discs, when compared to the polished control, this increase was not found to be significant. In addition, bacterial concentration was noted to increase incrementally as the duration of Ti disc treatment increased (i.e. surface nanoroughness). Although noted across all samples, no significant difference was noted between NW surface (Figure 3-6).

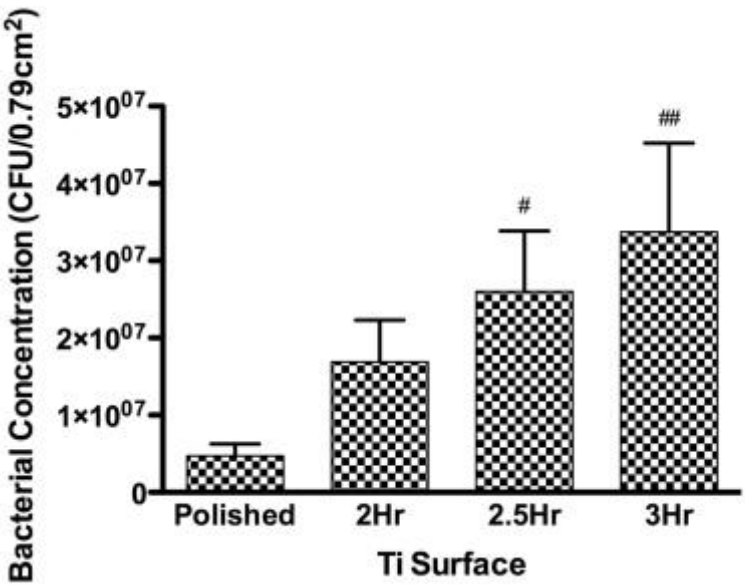

Figure 3-6 Average bacterial concentration on Ti NW surfaces

S. *aureus* Newman strain was standardised in DMEM + supplement media and grown on various NW Ti discs for a period 1 hour. Bacterial concentrations were significantly higher on the 2.5Hr ($^{\#}P<0.05$) and 3Hr ($^{\#\#}P<0.01$) discs when compared to the control Polished disc. No significant difference was noted between the 2Hr disc and the Polished, 2.5Hr and 3Hr discs.

3.4.2.2 Imaging

Following culture and growth of S. *aureus* Newman strain on different control (polished) and NW discs in 24-well plates, samples were stained and imaged as described previously (3.3.2.4). This provided a visual representation of the bacterial concentrations to support DNA extraction and qPCR data. As can be seen (Figure 3-7), the amount of nucleic acid stain appears least on the polished Ti control discs, with increasing fluorescence on the 2Hr, 2.5Hr and 3Hr NW Ti discs respectively.

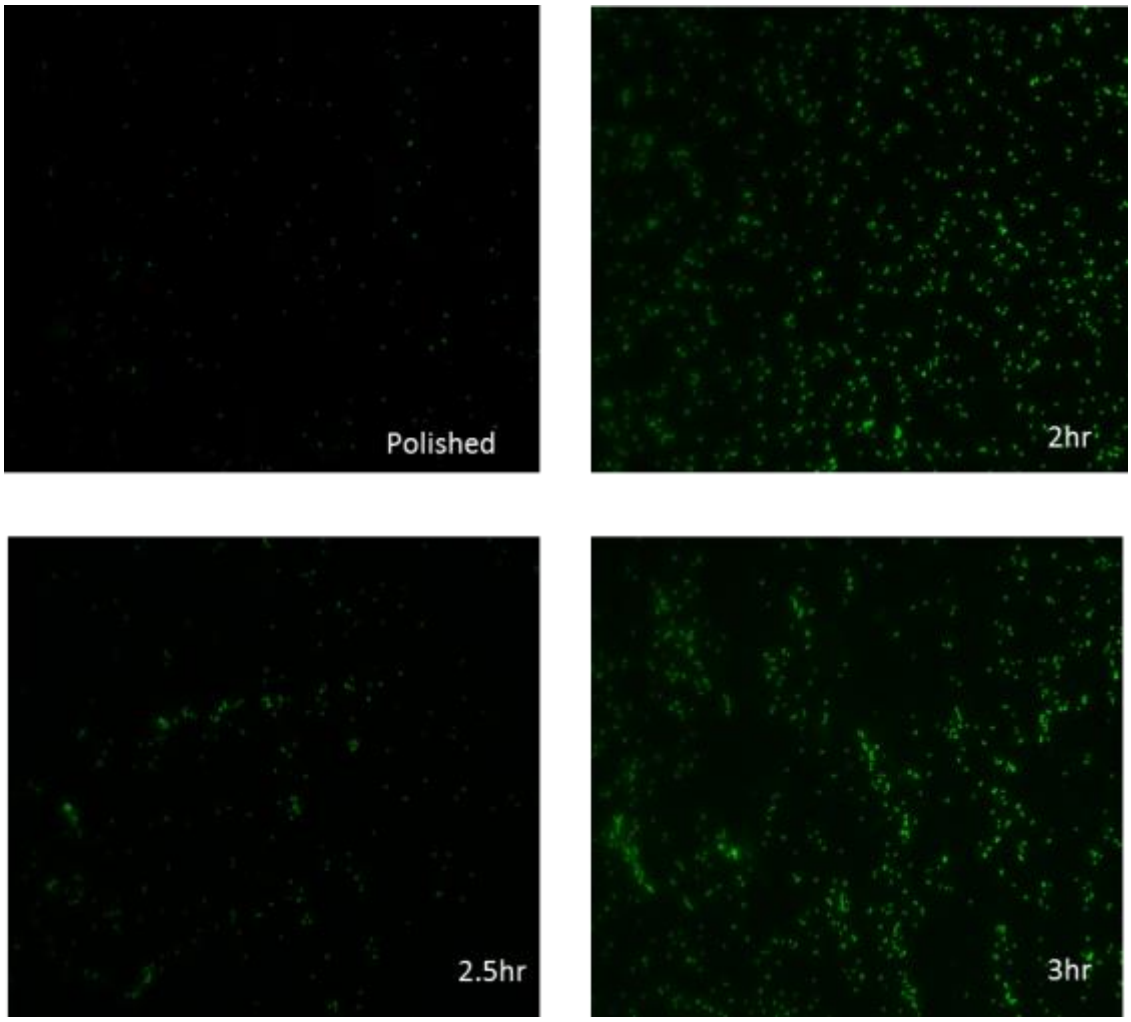

Figure 3-7 Fluorescent bacterial staining on different Ti NW surfaces

SA Newman strain was standardised in DMEM + supplement media and grown on various NW Ti discs for a period 1 hour. Following staining with SYTO®9 green fluorescent nucleic acid stain slides were imaged. 4 randomly selected images were taken from each slide (providing 12 images of each surface), the most representative of which are shown above. The least nucleic acid appears on the polished, control Ti disc, with increasing fluorescence on 2Hr, 2.5Hr and 3Hr Ti NW surfaces respectively.

These images were subsequently analysed using Cell Profiler® software, thus allowing the percentage bacterial coverage for each NW surface to be calculated. It was assumed that the greater the percentage bacterial coverage; the higher bacterial adhesion to that particular surface. As illustrated below (Figure 3-8), percentage bacterial coverage was significantly higher ($P<0.001$) on the 2Hr, 2.5Hr and 3Hr NW surfaces when compared to the control, polished surface (average percentage coverage values :10.7%, 10.9% and 12.8% respectively in comparison to 2.9% on the control surface). This supports the bacterial concentration data obtained from DNA extraction and qPCR (3.4.2.1).

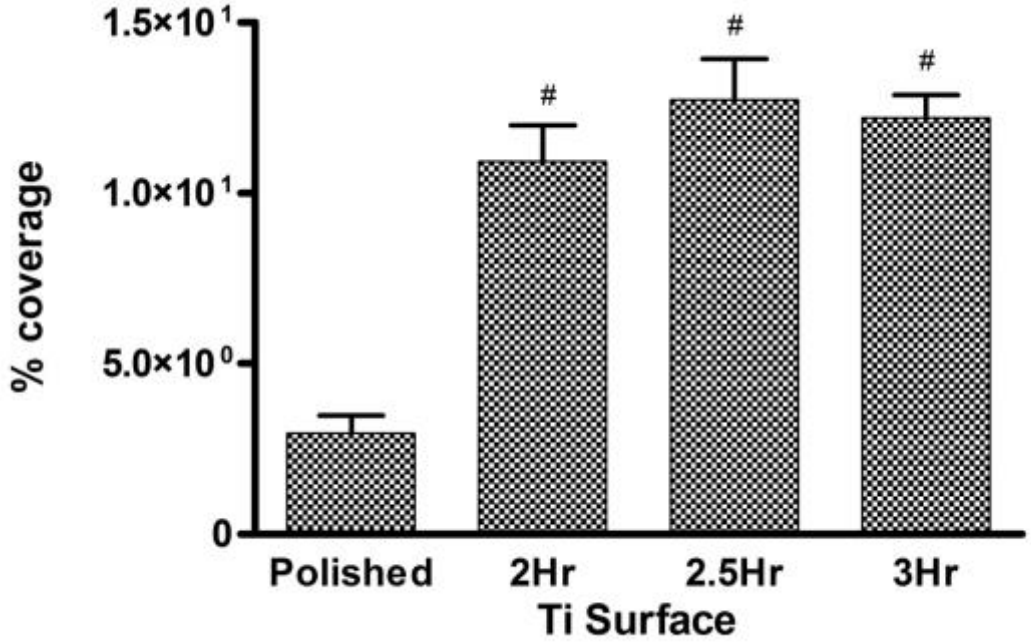

Figure 3-8 Average bacterial percentage coverage on different Ti NW pattern surfaces

S. *aureus* Newman strain was standardised in DMEM + supplement media and grown on various nanowire pattern Ti surfaces for a period 1 hour. Bacterial percentage coverage was significantly higher on 2Hr, 2.5Hr and 3Hr surfaces when compared to the polished control surface ($^{\#}P<0.001$). No significant difference was noted between nanowire patterns.

3.4.2.3 SEM imaging

In addition to the above, different nanowire surfaces were imaged using SEM to give a visual representation of bacterial/nanowire interactions (Figure 3-9 and Figure 3-10). These images appear to demonstrate increased bacterial concentrations on the 2Hr, 2.5Hr and 3Hr NW surfaces when compared to the control surface respectively. Increased bacterial 'clustering' is also evident on

the 2.5Hr and 3Hr Ti NW surfaces when compared to the control surface.

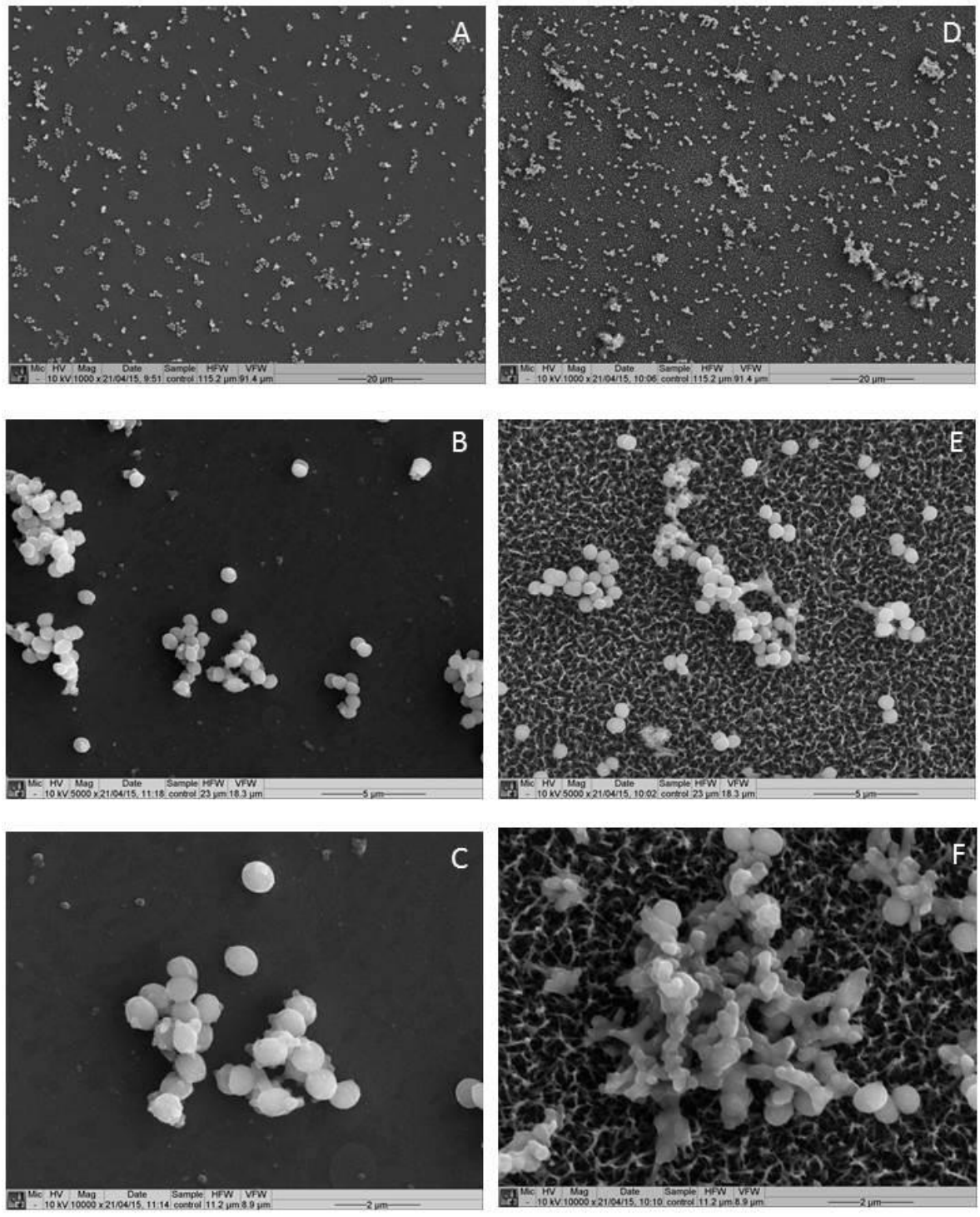

Figure 3-9 SEM images of Control and 2Hr Ti NW

S. *aureus* Newman strain was standardised in DMEM + supplement media and grown on control and 2Hr NW Ti surfaces for a period 1 hour. Following fixation and processing all slides were imaged using SEM. A=Control x1000 magnification, B=Control x5000 magnification, C=Control x10000 magnification, D=2hr x1000 magnification, E=2Hr x5000 magnification, F=2Hr x 10000 magnification.

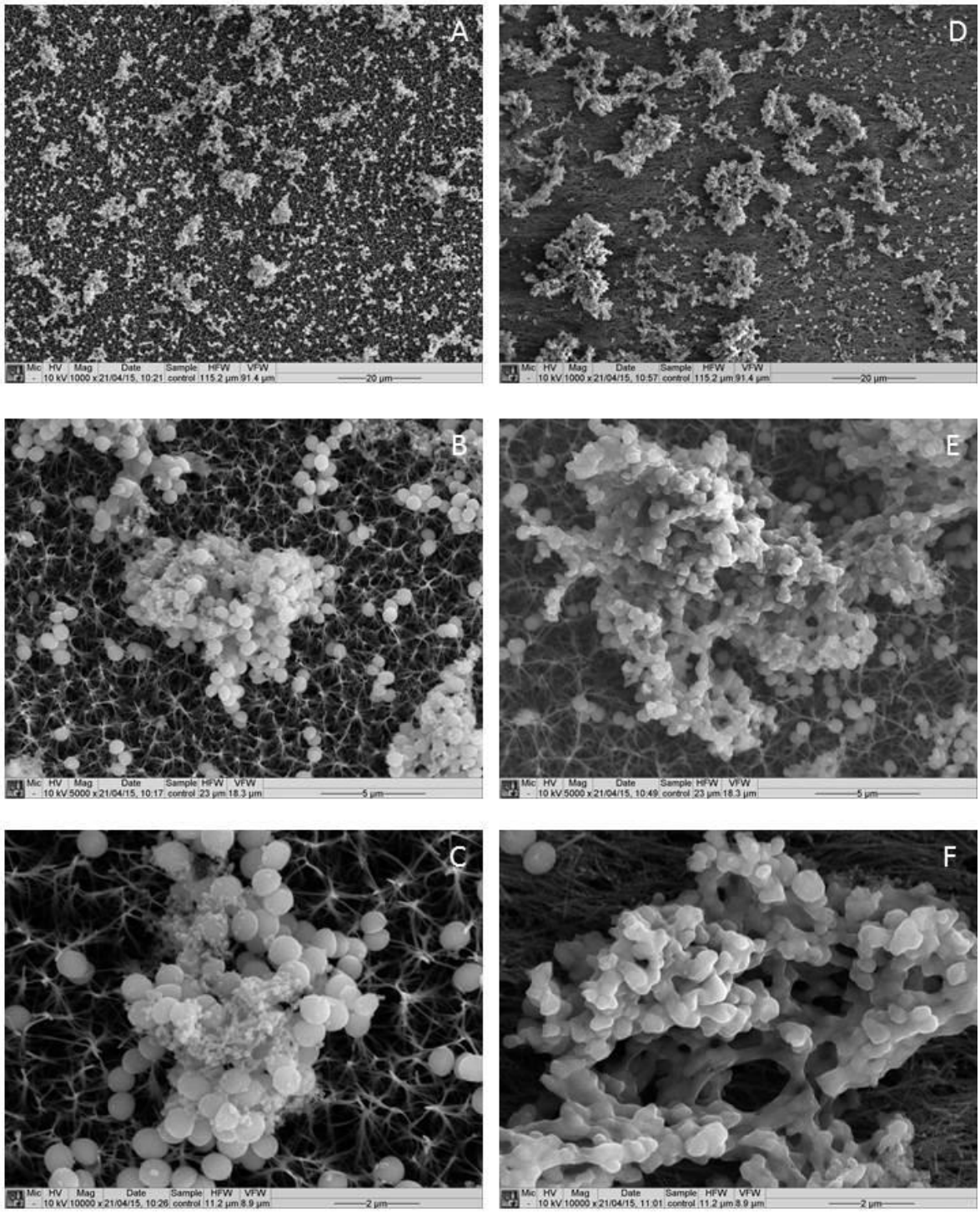

Figure 3-10 SEM images of 2.5Hr and 3Hr Ti NW

S. *aureus* Newman strain was standardised in DMEM + supplement media and grown on 2.5Hr and 3Hr NW Ti surfaces for a period 1 hour. Following fixation and processing all slides were imaged using SEM. A=2.5Hr x1000 mag, B=2.5Hr x5000 magnification, C=2.5Hr x10000 magnification, D=3hr x1000 magnification, E=3Hr x5000 magnification, F=3Hr x 10000 magnification.

3.4.3 Titanium NC and NG surfaces

3.4.3.1 Bacterial concentration

S. *aureus* Newman strain was cultured overnight and standardised in optimal media as previously described (2.3.1). S. *aureus* Newman strain was grown under optimal conditions on Ti control, NC and NG surfaces in 24-well plates. We found significantly lower bacterial concentrations on the NC surface when compared to the control Ti surface ($P<0.05$). In contrast similar bacterial concentrations were noted between the control and NG groups with no statistical difference (Figure 3-11).

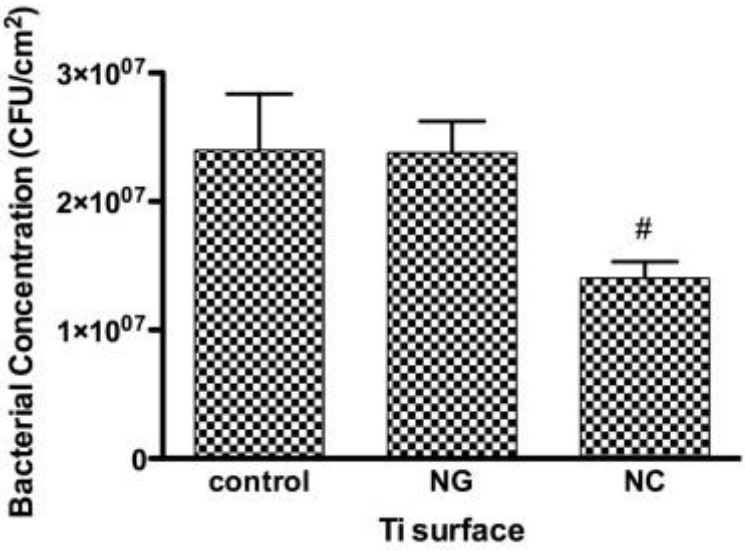

Figure 3-11 Average bacterial concentration on Ti NC, NG and control surfaces

S. *aureus* Newman strain was standardised in DMEM + supplement media and grown on NC, NG and control Ti surfaces for a period 1 hour. Bacterial concentrations were significantly lower on the NC Ti surface ($^{\#}P<0.05$). No significant difference was noted between the NG and control Ti surfaces.

3.4.3.2 Imaging

Following culture and growth of S. *aureus* Newman strain on control, NC and NG surfaces in 24-well plates, samples were stained and imaged as described previously (3.3.2.4). This provided a visual representation and comparison of the bacterial coverage on NC, NG and control surfaces. As can be seen (Figure 3-12),

the amount of nucleic acid stain appears least on the NC surfaces with increasing fluorescence on the NG and polished (control) surfaces.

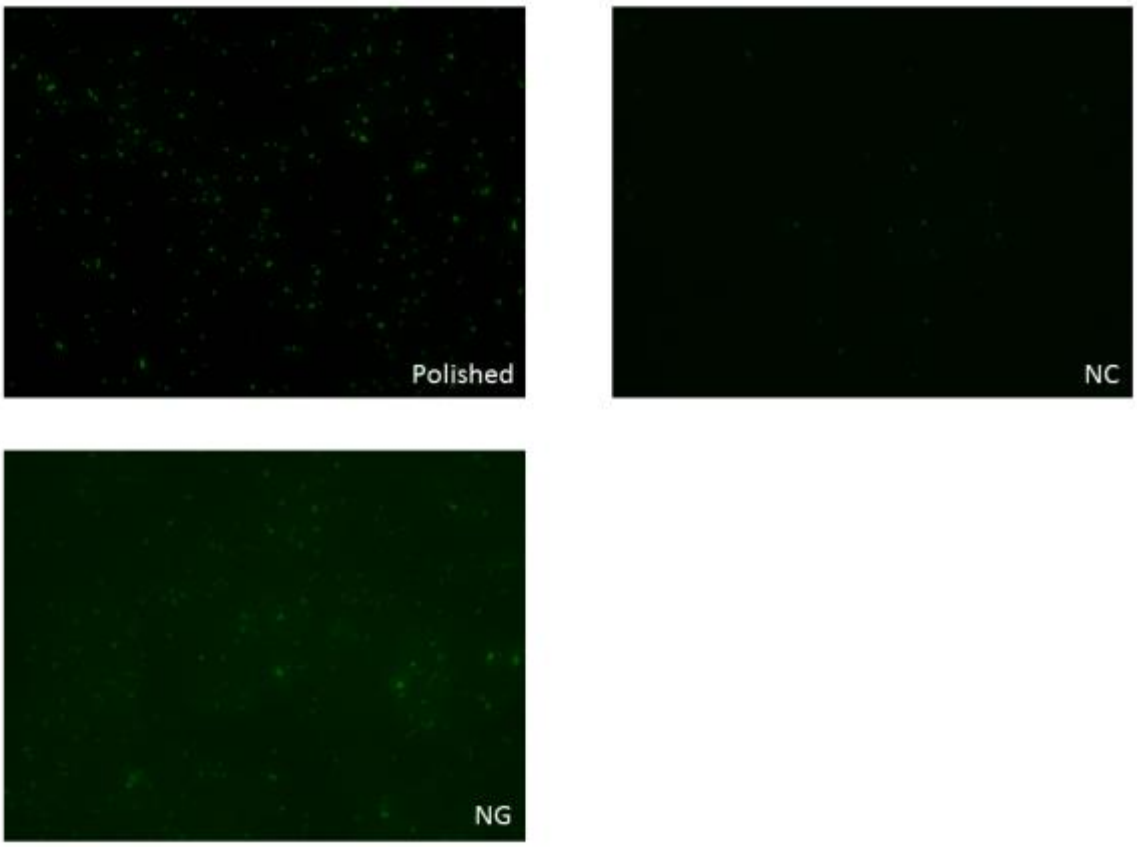

Figure 3-12 Fluorescent bacterial staining on Polished, NG and NC surfaces

SA Newman strain was standardised in DMEM + supplement media and grown on polished (control), NG and NC Ti surfaces for a period 1 hour. Following staining with SYTO®9 green fluorescent nucleic acid stain slides were imaged. 4 randomly selected images were taken from each slide (providing 12 images of each surface), the most representative of which are shown above. The least nucleic acid appears on the NC surface when compared to the NG and polished control surfaces.

These images were subsequently analysed using Cell Profiler® software, thus allowing the percentage bacterial coverage for each nanowire surface to be calculated. Again it was assumed that the greater the percentage bacterial coverage; the higher bacterial adhesion to that particular surface. As illustrated (Figure 3-13), percentage bacterial coverage was significantly lower ($P<0.001$) on the NC surface when compared to both the NG and the control, polished surface (average percentage coverage values: 0.19%, 2.21% and 2.29% respectively). This supports the bacterial concentration data obtained from DNA extraction and qPCR (3.4.3.1).

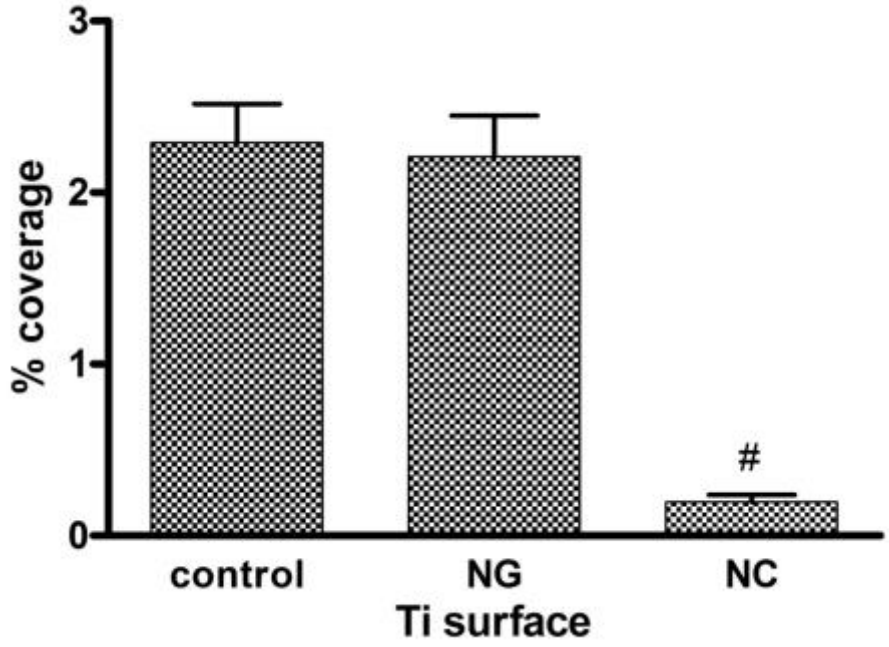

Figure 3-13 Average bacterial percentage coverage on NC, NG and polished Ti surfaces.

S. *aureus* Newman strain was standardised in DMEM + supplement media and grown on NC, NG and polished control Ti surfaces for a period 1 hour. Bacterial percentage coverage was significantly lower on the NC surface when compared to both the NG and polished control surface ($^{\#}P<0.001$). No significant difference was noted between NG and polished control surfaces.

3.4.3.3 SEM imaging

In addition to the above, the NC, NG and control surfaces were imaged using SEM to give a visual representation of the bacterial/nanosurface interactions (Figure 3-9 and Figure 3-10). These images demonstrate a similar bacterial coverage on both the NG and control Ti surfaces. There is also an increased bacterial 'clustering', particularly on the NG Ti surface under high magnification when compared to both the control and NC Ti surfaces. Bacterial coverage and 'clustering' appears reduced on the NC Ti surface across all magnifications when compared to the NG and control Ti surfaces.

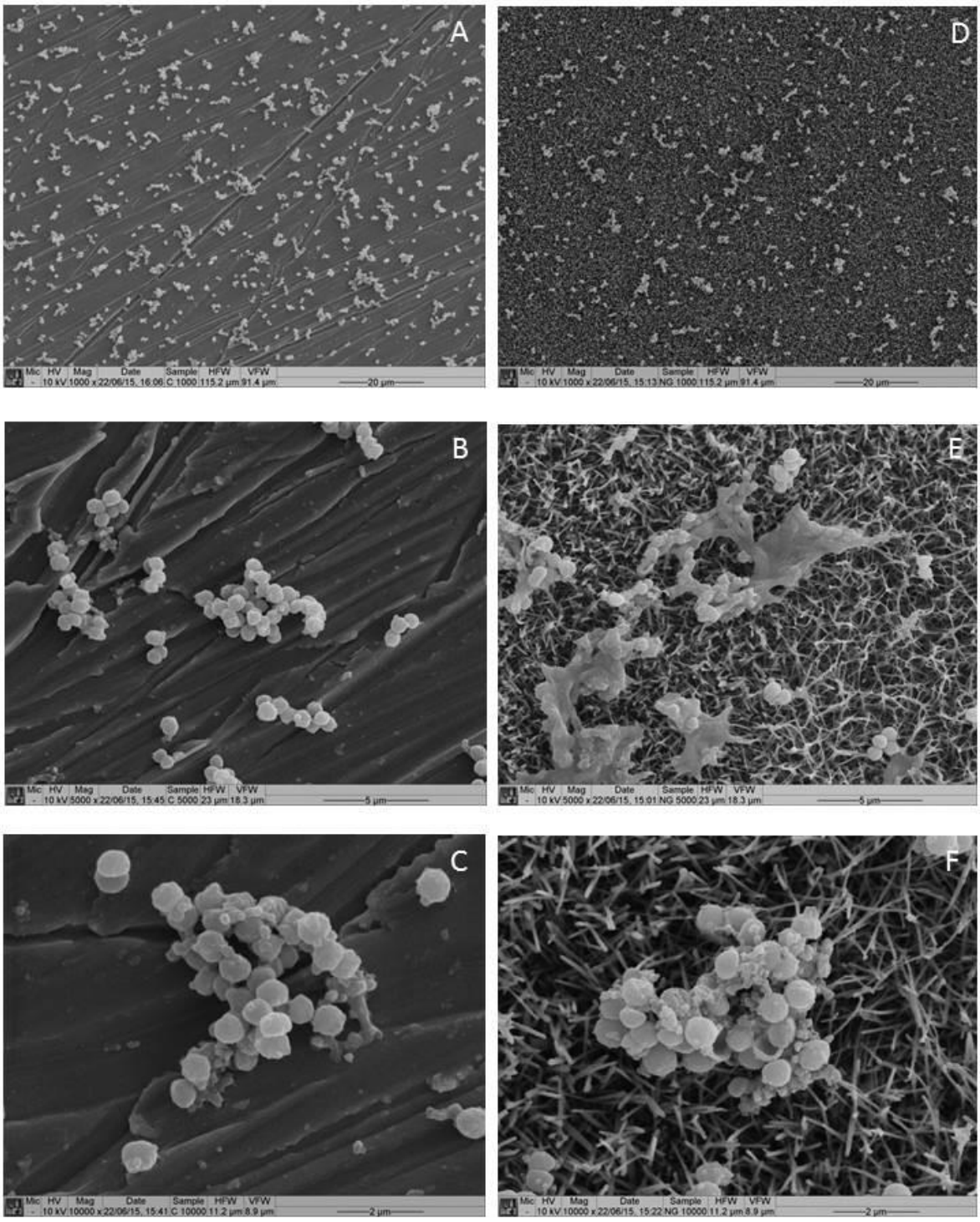

Figure 3-14 SEM images of control and NG Ti surfaces

S. *aureus* Newman strain was standardised in DMEM + supplement media and grown on control and NG Ti surfaces for a period 1 hour. Following fixation and processing all slides were imaged using SEM. A=control x1000 mag, B=control x5000 magnification, C=control x10000 magnification, D=NG x1000 magnification, E=NG x5000 magnification, F=NG x 10000 magnification.

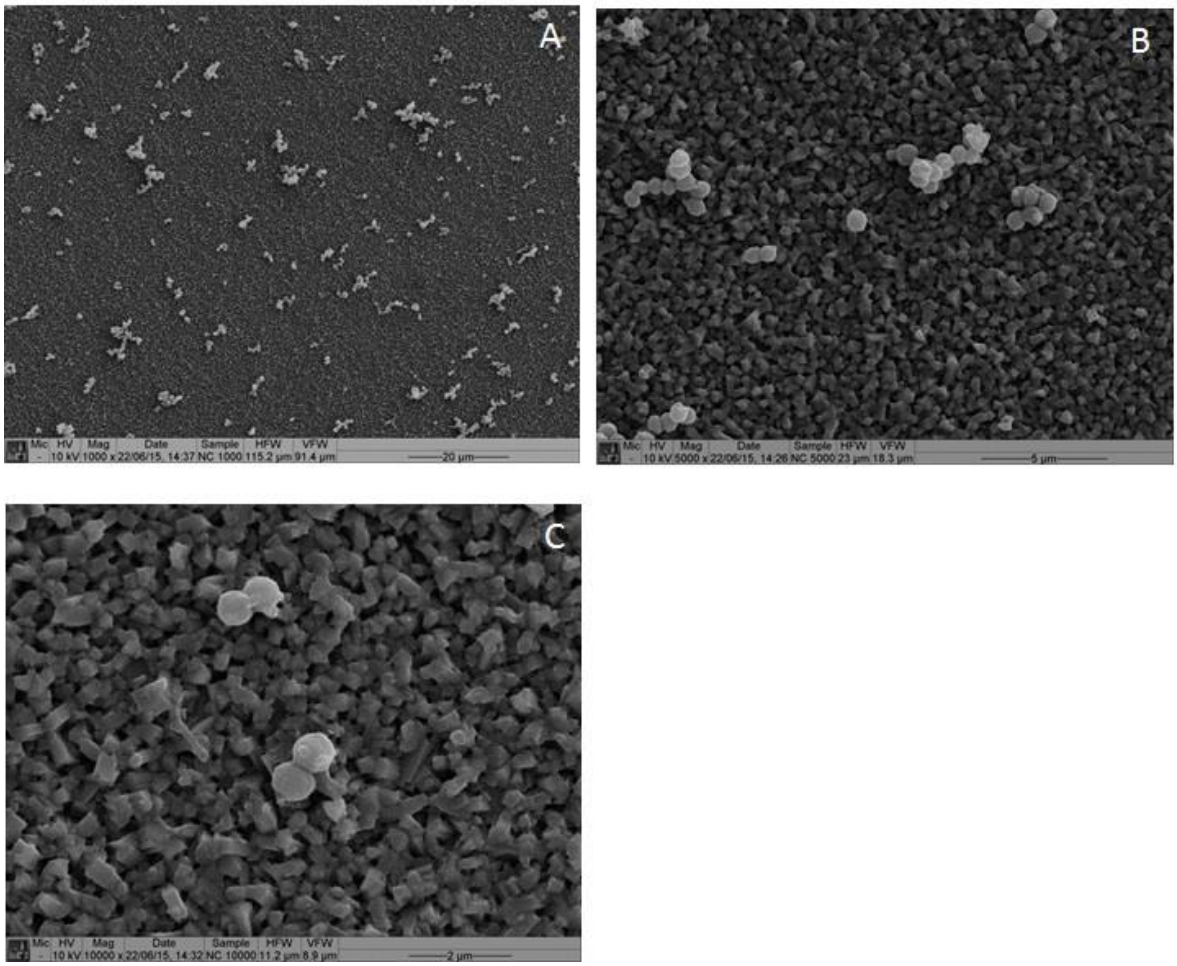

Figure 3-15 SEM images of NC Ti surfaces

S. *aureus* Newman strain was standardised in DMEM + supplement media and grown on NC Ti surfaces for a period 1 hour. Following fixation and processing all slides were imaged using SEM. A= NC x1000 mag, B=NC x5000 magnification, C=NC x10000 magnification.

3.5 Discussion

Bacteria are known to form biofilms in a multitude of environments, from hydrothermic pools (Reysenbach and Cady 2001) and acid mines (Edwards, Bond et al. 2000) to infected orthopaedics devices (Xu and Siedlecki 2012). The primary stage in bacterial colonisation and subsequent biofilm formation is bacterial adhesion (Mack, Nedelmann et al. 1994, Heilmann, Schweitzer et al. 1996, Sauer, Camper et al. 2002, Hall-Stoodley, Costerton et al. 2004). It has been suggested that by altering surface topography, cell behaviour (McMurray, Gadegaard et al. 2011), bacterial adhesion (Xu and Siedlecki 2012) and long term implant survival can be affected (Sjöström, Brydone et al. 2013). This is certainly the case in relation to dental implants, where increased osteoblastic cell adhesion, spreading and propagation was demonstrated when grown on specific titanium nanopatterns (Pelaez-Vargas, Gallego-Perez et al. 2011). Other studies have shown reduced bacterial adhesion on nanopatterned polyurethane, and suggests that the accessible contact surface area available for bacterial adhesion is important (Xu and Siedlecki 2012). By creating nanopillars, Xu *et al* (2002) reduced the contact surface area by up to 75% when compared to a flat control surface (Xu and Siedlecki 2012). Dalby *et al* found that highly ordered nanotopographies (namely the HEX and SQ pattern) produced low cellular adhesion and osteoblastic differentiation whilst cells on random nanotopographies exhibited a more osteoblastic morphology (Dalby, Gadegaard et al. 2007, Hart, Gadegaard et al. 2007). This suggests that the use of disorder may be an effective strategy in promoting influence over at least MSCs for regenerative medicine and tissue engineering. Similar to the Dalby group using MSC's, our study, using the same nanopit patterns, found reduced bacterial adhesion on the SQ and HEX patterns when compared to the control, un-patterned surface. Although this was not found to be significant when comparing bacterial concentrations, a clear trend was noted throughout all technical and biological replicates. This was supported by further imaging analysis, showing a significantly lower average percentage bacterial coverage on both the SQ and HEX patterns when compared to the control surface ($P=0.05$ and $P=0.01$ respectively). Highest bacterial concentrations were found on the DSQ10, 50 and NEAR 50 pattern's, suggesting that bacterial adhesion favours disordered nanotopographies. This was again supported by high average percentage

coverage values on DSQ100 and NEAR50 surfaces. This has also been observed in MSC's (Dalby, Gadegaard et al. 2007, Hart, Gadegaard et al. 2007), clearly showing that nanotopography has huge effects on stem cell differentiation (Dalby, McCloy et al. 2006). Mechanisms behind this are still being understood. It has been suggested that specific nanotopographical surfaces affect focal adhesion via altered protein adsorption to the surface (Oh, Brammer et al. 2009), and that gene expression in skeletal stem cells changes as a result of altered nanotopography (Dalby, Gadegaard et al. 2007, Dalby, Andar et al. 2008). Could it be that these mechanisms are also occurring in bacteria during adhesion? Several studies have also suggested that bacterial micro colony formation can be prevented by creating a physical barrier to spread at a nanometre level (Chung, Schumacher et al. 2007). It may be that the organised SQ and HEX nanopatterns are the optimal nanopit orientations to prevent bacteria microcolony formation, keeping the bacteria in small, isolated clusters and preventing communication.

Subsequently, we focused on a more clinically relevant material, Ti. The Ti alloy Ti-6A1-4V (Ramachandran 2006) is the most commonly used Ti alloy in orthopaedics, due to its reduced elastic modulus, good wear characteristics, excellent biocompatibility and fatigue resistance (Learmonth, Young et al.). Most research to date has focused on materials other than Ti, using production methods previously described (3.3.1.1). Although providing interesting results (Chung, Schumacher et al. 2007, Xu and Siedlecki 2012), the translation of these nanosurfaces to Ti is critically important, both to prosthetic development and to allow verification of findings on other materials (Sjöström, Brydone et al. 2013). Our collaborators have designed and developed a technique that allows production of highly defined nanopatterns on Ti (3.3.2.1). Unlike previous studies that have used Ti nanopillers (Sjöström, Dalby et al. 2009) and controlled oxidisation (de Oliveira, Zalzal et al. 2007) to alter the Ti surface, these new methods can produce novel surface topographies such as NW, NC and NG (Figure 3-2 and Figure 3-3). Our research showed a significant increase in bacterial concentrations on both the 2.5Hr ($P<0.05$) and 3Hr ($P<0.01$) treated Ti NW surfaces when compared to the polished Ti control surface after 1 hour bacterial incubation (3.4.2.1). This suggests that as nanoroughness increases, so does bacterial adhesion. This theory was further supported visually with fluorescent

nucleic acid staining that clearly showed increased fluorescence with increasing nanoroughness (3.4.2.2). Subsequent image analysis using Cell Profiler® software showed average percentage bacterial coverage was significantly higher ($P<0.001$) on the 2Hr, 2.5Hr and 3Hr NW surfaces when compared to the control surface, further supporting a bacterial preference for Ti nanoroughened surfaces. Indeed unpublished research by our collaborators has suggested that osteogenesis is increased on the 2hr treated NW surface, but interestingly is reduced on the 2.5hr and 3hr NW topographies with significantly lower mean cell numbers when compared to a control surfaces (unpublished results, PM Tsimbouri at Dalby group, Centre for Cell engineering, University of Glasgow). Whilst the explanation behind the osteogenic differences is out with the remit of this study, the stepwise increase in bacterial concentrations with nano-roughness remains interesting. S. *aureus* has been shown to prefer micro-roughened titanium, owing to an increased amount of contact guidance when compared to smooth surfaces (Ivanova, Truong et al. 2009). The adhesion differences noted on our nanowires may therefore be due to similar interactions, albeit at a nanoscale. It should also be noted that our nanowire surfaces are not regular or uniform. As such, depressed areas within the surface exist (Figure 3-2) which may encourage bacterial collection and subsequent adhesion. Whilst visible on the 2hr and 2.5hr treated samples, they are clearly more apparent on the 3hr surface. This increased roughness or 'pitting' may enhance bacterial adhesion and subsequent colonisation. Visual analysis of SEM images (Figure 3-9 and Figure 3-10) certainly appears to show increased bacterial 'clustering' as Ti nanoroughness increases. This may represent a quicker bacterial adhesion, thus allowing increased bacterial communication and perhaps quicker biofilm development.

In addition it has been suggested that surfaces with nanoprotrusions may affect bacterial attachment and growth (Ivanova, Truong et al. 2009, Ivanova, Hasan et al. 2012, Ivanova, Hasan et al. 2013). The wing nanostructure of a species of cicada, *Psaltoda claripennis,* have been shown to induce cellular death (Ivanova, Hasan et al. 2012). This bacteriocidal effect is based primarily on the physical surface structure, as significant alteration of the chemistry on the wing (through gold covering) failed to prevent cellular death (Ivanova, Hasan et al. 2012). Further development of this theory resulted in the production of hexagonal

arrays of spherically capped, conical nanopillars that were found to induce the same effect on gram-negative organisms such as *P. aeruginosa* (Ivanova, Hasan et al. 2012, Pogodin, Hasan et al. 2013). Subsequent studies have focussed on the nanostructure of the dragonfly wing, *Diplacodes bipunctata* (Ivanova, Hasan et al. 2013). Ivanova *et al* found that fabricated black silica nanopillar structures, possessing a disordered arrangement, have a bacteriocidal effect on both gram positive and gram negative bacteria, again through physical interaction forces that are dependent on the surface of a material (Ivanova, Hasan et al. 2013). It is postulated cell death occurs as a result of altered surface structure, associated stresses and forced cell deformation. Consequently, our research has incorporated similar disordered, hexagonal array nanopillars (NC and NG) surfaces onto Ti.

Our study shows that a disordered NC Ti nanopattern, hexagonal in nature, significantly reduced bacterial concentrations following a 1hr incubation period when compared to a polished, control surface ($P<0.05$). The bacterial percentage coverage was also noted to be significantly lower on the NC surfaces, with over a 10-fold reduction when compared to the control surface. It is postulated that this reduction is through similar mechanisms to those described by Ivanova *et al,* and primarily related to altered surface interactions. These NC arrangements were generally shorter and wider (200-300nm) than the NG surfaces and were noted to have sharp edges and pyramidal shaped tips (Figure 3-3). Such mechanical characteristics have been shown to cause sufficient damage to the bacterial cell membrane, resulting in bacterial cell lysis on silicon (Gorth, Puckett et al. 2012). It is therefore postulated that similar interactions are occurring on our Ti NC structures. Interestingly however, the NG surface had no significant difference on bacterial concentrations or percentage coverage when compared to the polished, control surface. These nanostructures have a significantly longer length and smaller diameter to the NC surfaces (10-100nm), making them less rigid and sharp. It may be therefore, that the NG surfaces are simply not strong enough to affect bacterial deformation and subsequent cellular death, and instead move to allow bacterial colonisation. Indeed on examination of our SEM images, coverage and bacterial clustering appears higher on the NG and control surfaces when compared to the NC Ti surfaces at all magnifications (Figure 3-14 and Figure 3-15). Clearly the surface structure on a material has

significant effects on bacterial adhesion, however from a bone implant perspective, finding a structure that is both bacteriocidal and osseoinductive may prove difficult. Given that the above surfaces are thought to work via cell deformation and altered internal osmotic turgor pressures (Arnoldi, Fritz et al. 2000, Jiang and Sun 2010), it would seem logical that other cell lineages, such as MSC's will also be affected. As a result, further research in this area is recommended.

In addition to mechano-responsive microbiology, it has been suggested that adhesion is mediated by surface proteins (Hussain, Herrmann et al. 1997), extracellular proteins (Heilmann, Schweitzer et al. 1996), adhesins (McKenney, Hübner et al. 1998) and autolysins (Heilmann and Götz 1998). The exact metabolic pathways involved in bacterial adhesion are poorly understood and may provide potential targets for anti-microbial treatments. This topic is therefore the focus of Chapter 4.

Chapter 4

Metabolomic Profiling of Bacterial Adhesion

4.1 Introduction

Metabolomics is defined as 'the quantitative measurement of the dynamic multiparametric metabolic response of living systems to pathophysiological stimuli or genetic modification' (Nicholson, Lindon et al. 1999). Metabolomics is the study of a complement of small molecules (known as metabolites) within a system, known as the metabolome. The metabolome was first described by Oliver *et al* (1998) whilst studying the yeast genome (Oliver, Winson et al. 1998), and resultant metabolomics development is often referred to as metabonomics (Nicholson, Lindon et al. 1999) or metabolic profiling (Niwa 1986) by some groups. The ability to provide a 'snap-shot' of cell metabolism is emerging as a useful tool across a multitude of disciplines, ranging from plant physiology to human disease, nutrition and drug discovery, but has only become possible as a result of recent technological breakthroughs in small molecule separation and identification (Wishart 2008).

The earliest application of a pre-cursor to metabolomics is considered to be the use of gas chromatography-mass spectrometry for metabolite profiling of clinical urine in the 1970's (Politzer, Dowty et al. 1976, Jellum 1977, Gates and Sweeley 1978). Further development of nuclear magnetic resonance (NMR) spectroscopy by Nicholson *et al* in the 1980's (Bales, Bell et al. 1988) and later mass spectrometry (MS), liquid chromatography (LC) and capillary electrophoresis (CE) in combination with appropriate software programs has allowed analysis (Dunn, Bailey et al. 2005) and rapid development of such analytical techniques. Presently, the two main methods used in metabolomics are NMR and MS (Either LC or CE) (Goodacre, Vaidyanathan et al. 2004, Dunn, Bailey et al. 2005, Glinski and Weckwerth 2006, Dettmer, Aronov et al. 2007). While NMR is recognised to require little sample preparation and can offer structural and quantitative details about compounds (Giavalisco, Hummel et al. 2008), it has a low sensitivity when analysing complex biological samples (Dunn, Bailey et al. 2005, Dettmer, Aronov et al. 2007, Eisenreich and Bacher 2007). In comparison, MS-based methods have better compound separation and are ultimately more sensitive. MS methods therefore dominate metabolomic literature (Giavalisco, Hummel et al. 2008), and will be the method used in this study. In addition, the

information gained from a metabolomics experiment can be further improved by the introduction of techniques such as flux analysis (Sauer, Lasko et al. 1999, Wiechert 2001, Fischer and Sauer 2003). Essentially this allows the targeting of specific compounds that are predicted to be involved in specific metabolomics pathways, and relies on the incorporation of labelled isotopes (such as ^{13}C) into metabolite pools (Birkemeyer, Luedemann et al. 2005). These compounds can subsequently be traced 'downstream', highlighting any specific pathways demonstrating increased metabolic activity. Another equally important aspect of metabolomics is a compiled database containing descriptive and spectral information of all constituent chemicals found in different metabolomes (Smith, O'Maille et al. 2005, Cotter, Maer et al. 2006, Moco, Bino et al. 2006, Wishart, Tzur et al. 2007). The relatively recent production and widespread availability of such databases has allowed the detection and characterisation of multiple metabolomes in a matter of minutes (Dunn, Bailey et al. 2005, Moco, Bino et al. 2006, Wishart 2008).

In general, metabolomics analyses can be classified as either targeted or untargeted. Targeted analyses focuses on particular groups of metabolites, usually within one or more related pathways of interest (Dudley, Yousef et al. 2010), allowing identification and quantification of as many metabolites within the group as possible (Ramautar, Demirci et al. 2006). This method aims to quantify these selected metabolites, usually up to a few hundred compounds and requires the ability to differentiate the targeted metabolites from other compounds (Lu, Bennett et al. 2008). This method is highly sensitive and robust and can be used to isolate potential metabolic signatures for disease. For example, targeted metabolomics has recently been used to identify citric acid metabolites and a group of essential amino acids as metabolic signatures for myocardial ischaemia and diabetes respectively (Sabatine, Liu et al. 2005, Wang, Larson et al. 2011). In comparison, untargeted metabolomics aims to detect as many groups of metabolites as possible allowing the identification of patterns (Monton and Soga 2007) and comparison without bias (Patti, Yanes et al. 2012). By using techniques such as LCMS, large numbers of metabolites may be identified using relatively small sample volumes (Patti, Yanes et al. 2012). Metabolomic software in conjunction with previously described metabolomics databases can then be used to identify specific metabolites based on the

accurate mass of the compound. This type of metabolomics is useful in identification of any altered metabolomic pathways in disease, that may represent new drug targets; an application referred to as 'therapeutic metabolomics'(Rabinowitz, Purdy et al. 2011). This method, applied by Dang *et al* (2009), discovered increased levels of 2-hydroxyglutarate in specific mutated cancer cells, known to be a common feature in some primary brain cancers (Dang, White et al. 2009).

Currently bacterial metabolomics has focused mainly on the classification (Hettick, Green et al. 2008) and understanding of normal bacterial metabolism. Schaub *et al* (2008) found altered glycolysis dynamics under differing growth rates and glucose availability in *E. coli* (Schaub and Reuss 2008), whilst Koek *et al* (2006) found a time-related progression of metabolites with bacterial growth (Koek, Muilwijk et al. 2006). While interactions between surface topography and bacterial adhesion are documented, the effects of targeting bacterial metabolism therapeutically are not, and as such remain a novel area of research and is therefore the focus of this chapter.

Recently developed metabolomic methods, specific to the S. *aureus* biofilm, highlighted the metabolic differences between planktonic and biofilm bacterial states and the need to study microbes in their different growth states (Stipetic, Dalby et al. 2016). By combining this technique and a novel glucose 'heavy' labelling method, developed by the author, bacterial metabolic pathways involved in bacterial adhesion will be identified and therapeutically targeted. It should be noted that while the bacterial metabolome has been widely researched (Kanehisa and Goto 2000), the specific pathways involved in adhesion have not, therefore therapeutic agent selection for targeting will be conducted after metabolic pathway identification.

4.2 Chapter Aims

This study hypothesises that bacterial adhesion is reliant on specific metabolites and metabolic pathways. The regulation of which may be affected by altered surface nanotopography. The aim of this chapter was to analyse the S. *aureus*

metabolome using LCMS and ascertain any changes in specific metabolites and metabolomic pathways. If identified, possible targeted therapeutic agents will be analysed to ascertain their effect of bacterial adhesion and subsequent biofilm formation.

Work from this chapter has been published in:

Hansom D et al *THE EFFECTS OF NANOPATTERN SURFACE TECHNOLOGY ON ORTHOPAEDIC JOINT REPLACEMENT INFECTION*. Bone & Joint Journal Orthopaedic Proceedings Supplement, 2015. **97-B**(SUPP 3): p. 2.

Work from this chapter has been presented at the following conferences:

Hansom D, Tsimbouri M, Ramage G, Burgess K, Dalby M, Meek D and Clarke J. 'Nano-topographical modulation of cells and bacteria for next generation orthopaedic implants.' Centre of Cell Engineering – Glasgow Orthopaedic Research Initiative, December 2014.

Hansom D, Burgess K, Meek D, Clarke J, Ramage G. 'The effects of nanopattern surface technology on orthopaedic joint replacement.' Glasgow Meeting of Orthopaedic research, March 2015.

Hansom D, Burgess K, Meek D, Clarke J, Ramage G 'Nano-topographical modulation of cells and bacteria for next generation orthopaedic implants.' El-Minia University Hospital Scientific Day, Egypt, February 2015.

Hansom D, Burgess K, Gadengaard N, Millar N, Clarke J & Ramage G. 'The effects of nanopattern surface technology on orthopaedic joint replacement.' European Federation of National Associations of Orthopaedics and Traumatology, June 2016.

Hansom D, Burgess K, Gadengaard N, Millar N, Clarke J & Ramage G. 'The effects of nanopattern surface technology on orthopaedic joint replacement.' British Orthopaedic Research Society, September 2016.

4.3 Materials and Methods

S. *aureus* Newman strain was used for these experiments. Bacteria were collected, cultured and standardised under optimal growth conditions as per chapter 2. All metabolomics experiments were carried out on Ti control and nanowire discs only (3.3.2).

4.3.1 Metabolomic sample preparation

In order to highlight any metabolomic differences, heavy labelled glucose (D-Glucose-$^{13}C_6$, Sigma-Aldrich, Dorset, UK) was substituted for standard glucose in DMEM + supplement media. Following bacterial standardisation in heavy labelled DMEM + supplement media, 500µL of each sample was added to defined wells in a pre-sterilised, standard polystyrene 24-well plate (Corning Incorporated, New York, USA) containing nanowire and control titanium discs. The plate was incubated at 37ºC on a shaking platform for 1 hour. On removal, all supernatant was discarded and each disc was gently washed in sterile ammonium bicarbonate (10mM). Each Ti disc was transferred to a bijou, and kept on ice. A 1ml: 1g mixture of a chloroform, ethanol and ddH_20 (CEW, ratio 1:3:1) and acid washed glass beads (Sigma-Aldrich, Dorset, UK) was produced and 500µL was added to each bijou. Samples were placed on a cell disrupter (Disrupter Genie bead beater, Scientific industries Inc., New York, USA) operating at a speed of 3000 rpm, at 4°C. On removal all the liquid/bead mixture was transferred to an microcentrifuge and centrifuged at 10,000 rpm for 10 minutes to remove the beads. The supernatant was subsequently transferred to a fresh microcentrifuge. A pool sample was produced by adding 10µL of each sample to a separate glass vial. Each metabolomic sample vial contained a minimum of 20µL from the corresponding microcentrifuge. Samples were then stored at -80ºC until metabolomic analysis could be performed. This was carried out in triplicate and repeated on three separate occasions.

4.3.2 Metabolomic analysis

Metabolomic data acquisition was carried out using a Thermo Scientific Ultimate 3000 RSLC system (Thermo Scientific, CA, USA) coupled with a Thermo Scientific Exactive Orbitrap system equipped with a HESI II interface (Thermo Scientific,

Hemel Hempstead, UK), as per Haggarty *et al*, 2015 (Haggarty, Oppermann et al. 2015). Subsequent data analysis was carried out as per Appendix 1.

Metabolomic data was analysed to highlight any peaks resulting from incorporation of heavy labelled carbon (ranging from C1-C6). This data was then collated and normalised in relation to the intensity of unlabelled carbon in each sample. By swapping unlabelled glucose for D-Glucose-$^{13}C_6$ directly before nanosurface exposure to bacteria, any unlabelled metabolite peaks were due to metabolism that preceded any bacteria/surface interaction. Thus these values can be presumed to be constant across all samples and thus used to standardise our labelled metabolite results. This allows changes in labelled metabolites to be expressed as fold increases and attributed to an increased flux through metabolic pathways and not merely due to increased bacterial concentrations.

4.3.3 Targeted therapeutic metabolomics

Based on the metabolomics data generated, a targeted approach to investigate specific metabolites was performed. Standardised bacteria (2.3.1) in DMEM + Supplements were added to pre-defined wells of a 24 well plate (500µL). Different concentrations of Β-chloro-L-alanine (β-CLA [250µg/ml, 500µg/ml and 1000µg/ml]) and cycloserine (CS [12.5µg/ml, 25µg/ml and 50µg/ml]) were added to pre-defined wells. In addition, no β-CLA/CS and blank control wells were also incorporated. The plates were incubated in an incubator at 37^0C for 24 hours. Following incubation, supernatant was removed and the biofilms were washed with PBS. They were then left to air dry under a hood (Microflow biological safety cabinet, Astec, Hampshire, UK), and subsequently stained with 500µL of 0.05% crystal violet (CV [diluted in ddH_2O]) for 20 min. Wells contents were then discarded and excess CV washed away using tap water. Plates were tapped to ensure all excess CV was removed. Ethanol (1ml of 100%) was added to each well and thoroughly mixed to release CV dye. 200µL of each sample was then transferred to a clean 24 well flat bottomed plate and OD's were measured at 570nm (FLUOstar Omega, BMG labtech). Negative controls containing no organisms were included for each β-CLA/CS concentration, and all testing was carried out in triplicate on three separate occasions.

4.3.4 Minimum inhibitory concentration (MIC) and growth kinetics

The inhibitory potential of ß-CLA and CS on planktonic growth was assessed by conducting an inhibitory experiment. Separate stock solutions of ß-CLA and CS in Mueller Hinton broth (MHB) (Sigma-Aldrich, Dorset, UK) were prepared (4mg/ml). 200µl was then added to 5 rows (A-E) in column 1 of a 96-well, round bottom, polystyrene microtitre plate (Corning Incorporated, New York, USA). Using a multichannel pipette 100µl of MHB was added to 5 wells in columns 2-11 of the microtitre plate. 100µl was then taken from lane 1, and serially double diluted across sequential columns. Standardised inoculum in MHB (1 X 10^5 CFU/mL) was then added to columns 1-11 (100µl). Lane 12 was loaded with 200µl of standardised inoculum (acting as a positive control), while row H (columns 1-5) was loaded with 200µl of sterile MHB (acting as a negative control). The plates were then incubated at 37^0C for 24hrs, after which they were visually analysed for growth. Subsequently the serial ß-CLA and CS concentration dilutions were used to analyse the growth kinetics. To achieve this, the OD was measured every hour, for 24hrs, allowing identification of any effect on bacterial growth kinetics.

4.3.5 Statistical analysis

Graph production and statistical analysis were performed using GraphPad prism software (version 4; La Jolla, CA, USA). One-way analysis of variance (ANOVA) was used to investigate significant differences between groups. If ANOVA revealed a statistical significance, a Dunnett's multiple comparison or Tukey's test was performed to determine statistical significance between groups, depending on individual experiments. If two pattern groups were compared, an unpaired student's T-test was employed. Statistical significance was achieved if $P<0.05$.

4.4 Results

Following metabolomic data processing, compounds with increased abundances of labelled carbon were identified. The retention times of these peaks were then compared to standards from the same run, allowing robust compound identification. Each experimental run was carried out on different days due to the lengthy sample preparation and processing. Therefore, whilst similar trends are noted across all replicates, these cannot be directly compared to one another as retention times and comparable standards differ with each experimental run. All graphs illustrating retention times and intensities are taken from the first experimental run but are representative of three experimental runs. Additionally, as all non-labelled carbon was substituted for labelled carbon at the start of each experimental run, unlabelled carbon peaks were expected to remain static throughout all experiments. These unlabelled peaks therefore acted as controls, and subsequent fold changes could be calculated for each labelled compound the demonstrated an increased intensity. All measured metabolites data can be found on the supplementary CD at the back of this thesis.

4.4.1 Pyruvate intensity

Pyruvate showed an increased intensity across all surfaces (Figure 4-1).

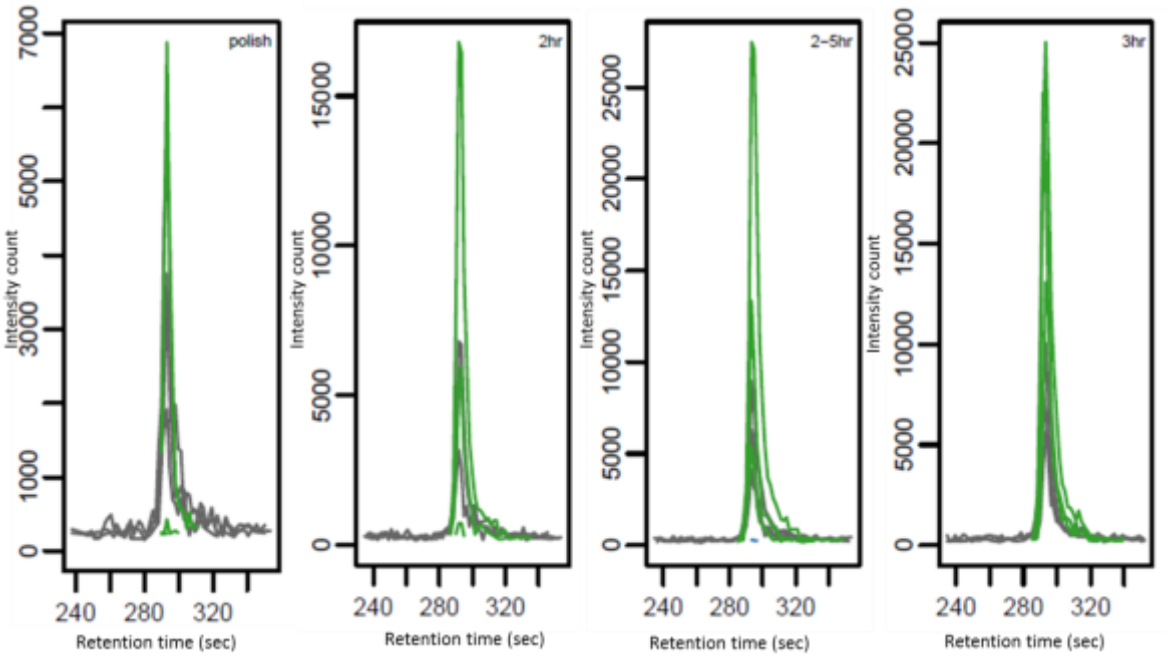

Figure 4-1 Labelled pyruvate following metabolomics extraction from S. *aureus* (run 1 data)

S. *aureus* Newman strain was standardised in DMEM + supplement media and grown on Ti surfaces for a period 1 hour. Pyruvate abundance is represented by the blue (1C labelled), green (3C labelled), brown (4C labelled) and grey (unlabelled) line on each graph.

The fold change in intensity was noted to increase with escalating nanoroughness, with the highest intensity fold change being noted on the 3Hr treated Ti surface (Figure 4-2). This trend was not found to be significant.

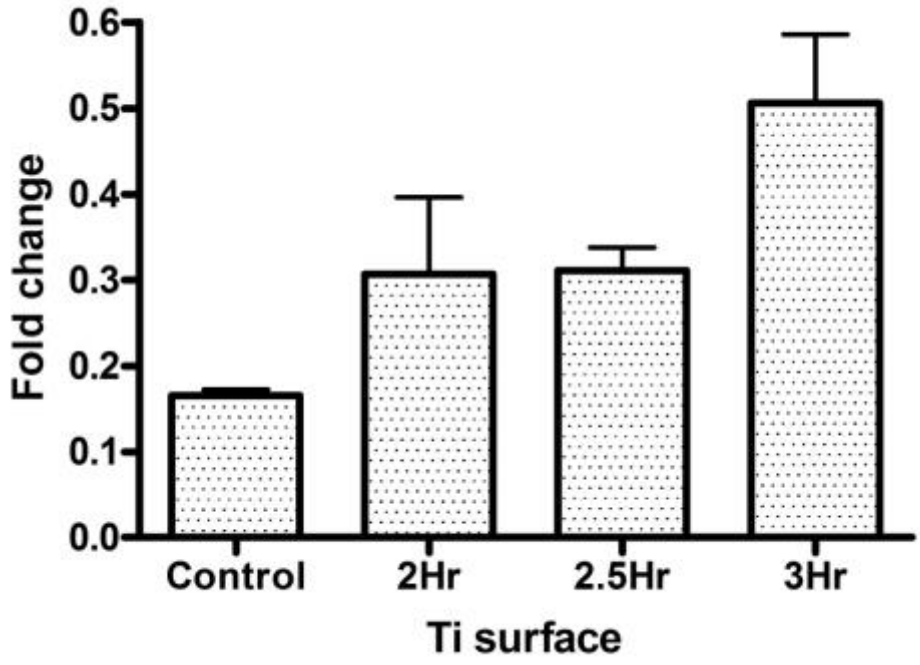

Figure 4-2 Fold changes in intensity of labelled pyruvate on different Ti surfaces

Following metabolomic extraction and processing as described, labelled pyruvate was noted in all samples, with the highest fold change being present on the 3Hr Ti discs.

4.4.2 Alanine intensity

Alanine showed increased intensity across all surfaces (Figure 4-3).

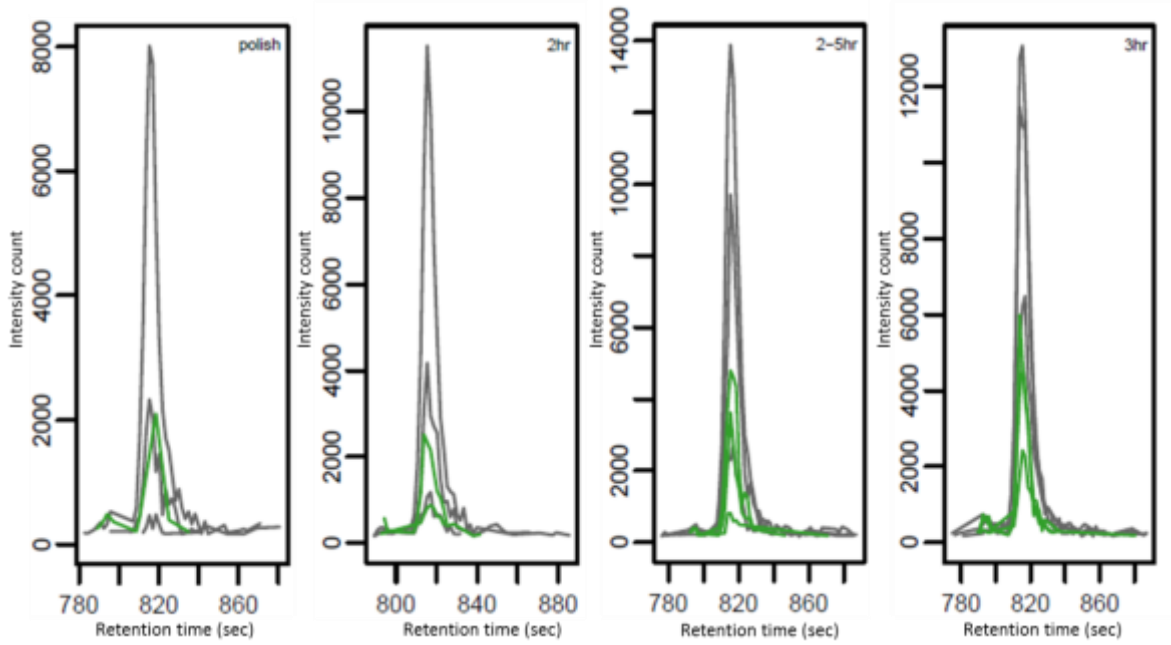

Figure 4-3 Labelled alanine following metabolomics extraction from S. *aureus* (run 1 data)

S. *aureus* Newman strain was standardised in DMEM + supplement media and grown on Ti surfaces for a period 1 hour. Alanine intensity count is represented by the green (3C labelled) and grey (unlabelled) line on each graph.

The fold change in intensity was noted to increase with nanoroughness, with the highest intensity fold change being significantly higher on the 2.5Hr and the 3Hr ($P<0.05$) treated Ti surfaces when compared to the control Ti surface (Figure 4-4). No significant difference was noted between the control and 2Hr treated Ti surfaces.

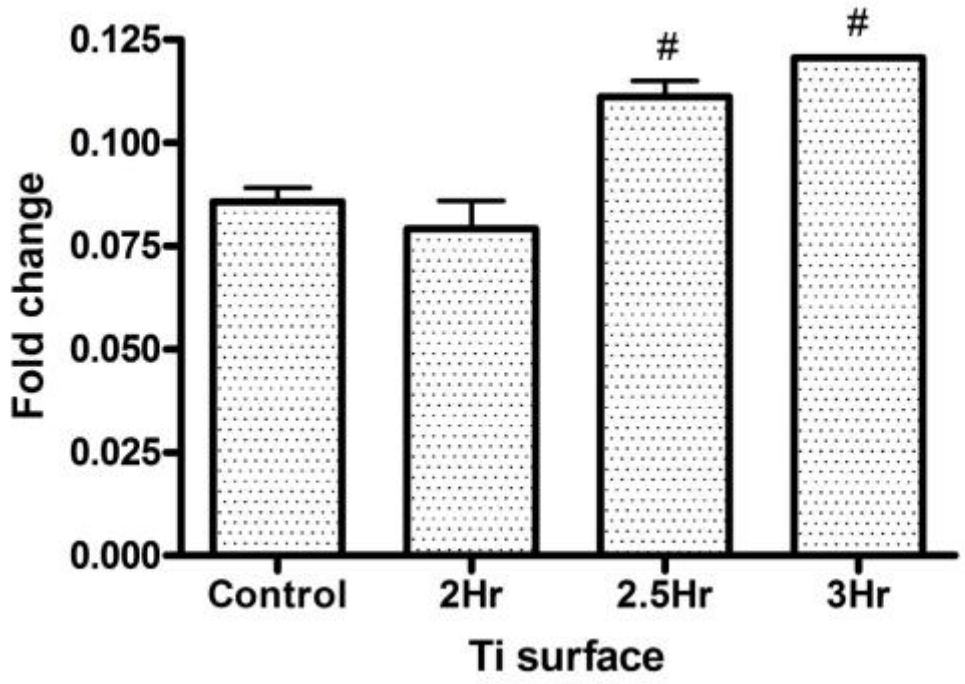

Figure 4-4 Fold changes in intensity of labelled alanine on different Ti surfaces

Following metabolomic extraction and processing as described, labelled alanine was noted in all samples, with the highest fold changes being present on the 2.5Hr and 3Hr Ti discs ($^{\#}P<0.05$, 1-way ANOVA).

4.4.3 Aspartate intensity

Aspartate intensity was noted to be increased across all surfaces (Figure 4-5).

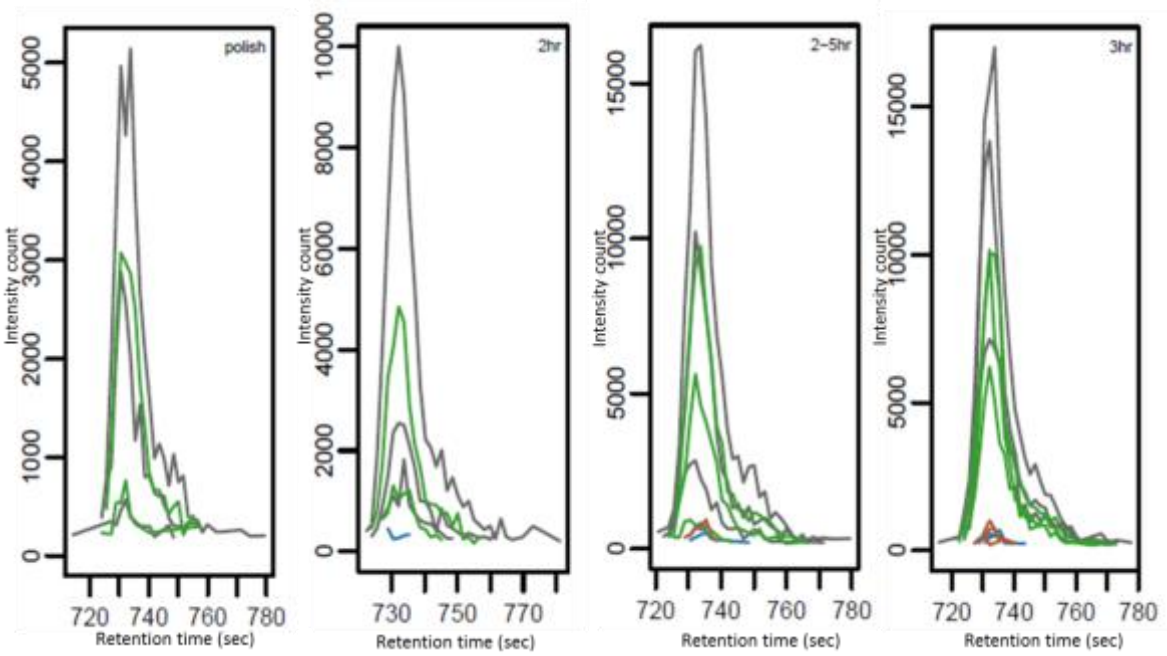

Figure 4-5 Labelled aspartate following metabolomics extraction from S. *aureus* (run 1 data)

S. *aureus* Newman strain was standardised in DMEM + supplement media and grown on Ti surfaces for a period 1 hour. Aspartate intensity is represented by the blue (1C labelled), green (3C labelled), brown (4C labelled) and grey (unlabelled) line on each graph.

Fold change in intensity was noted to increase with nanoroughness, with the highest intensity fold change being highest on the 3Hr treated Ti surface when compared to all other Ti surfaces (Figure 4-6). This trend was not found to be significant.

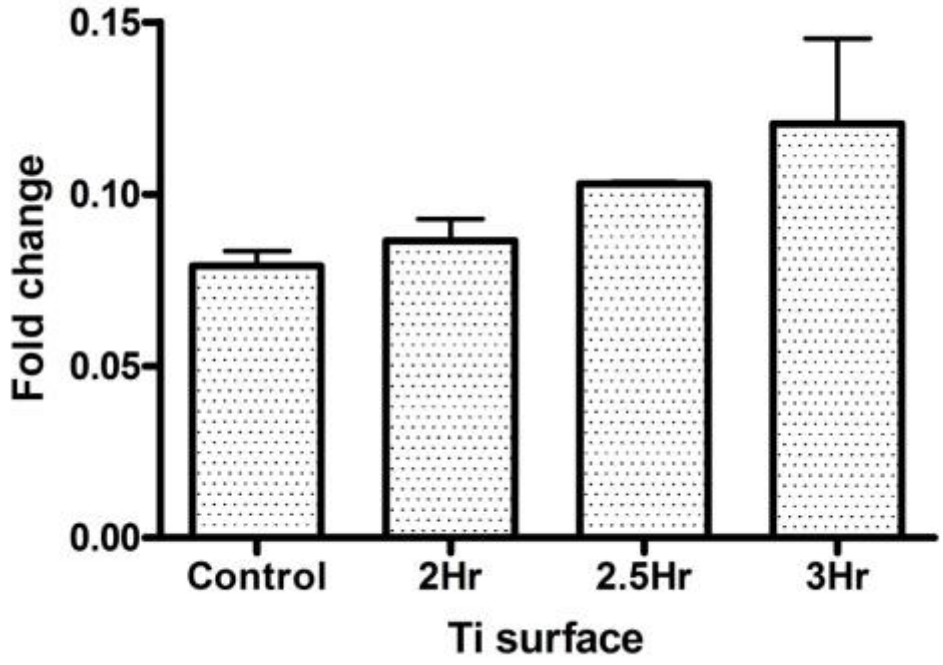

Figure 4-6 Fold changes in intensity of labelled aspartate on different Ti surfaces

Following metabolomic extraction and processing as described, labelled aspartate was noted in all samples, with the highest fold change being present on the 3Hr Ti discs.

4.4.4 Carbamoyl-aspartate intensity

Carbamoyl-aspartate (CA) intensity counts were noted to be increased across all surfaces (Figure 4-7).

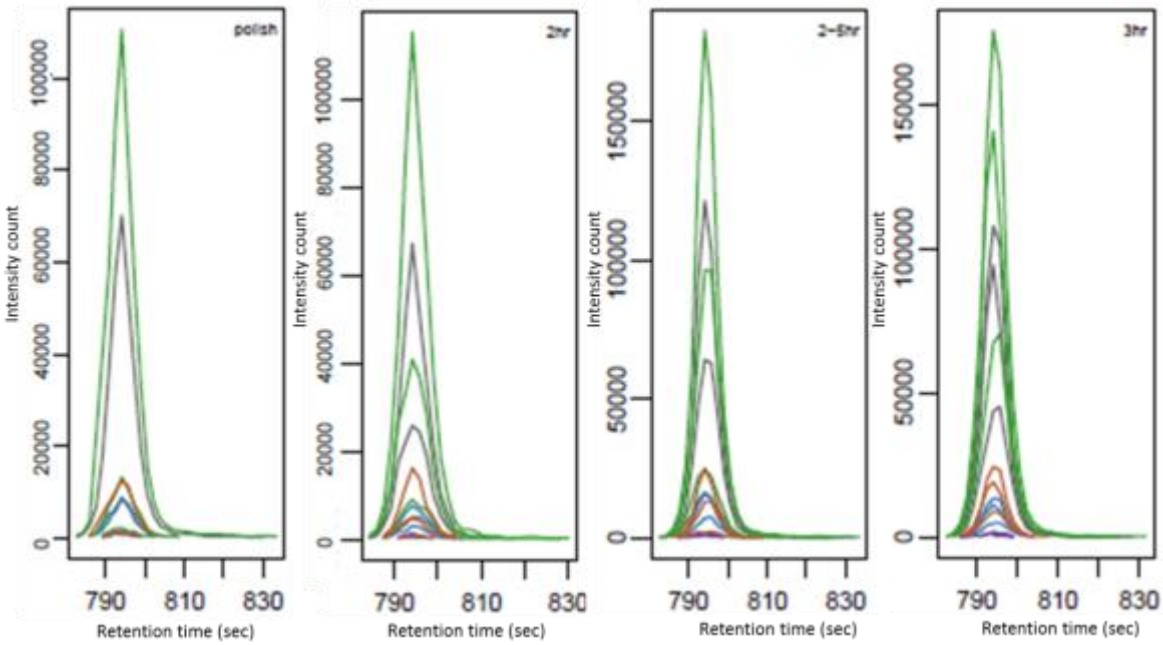

Figure 4-7 Labelled CA following metabolomics extraction from S. *aureus*

S. *aureus* Newman strain was standardised in DMEM + supplement media and grown on Ti for a period 1 hour. CA intensity count is represented by the green (3C labelled), blue (1C labelled), purple (2C labelled), brown (4C labelled) and grey (unlabelled) line on each graph.

The highest fold change appeared to be on the control surface with a gradual decline in intensity fold change as nanoroughness increased (Figure 4-8). This trend was not significant.

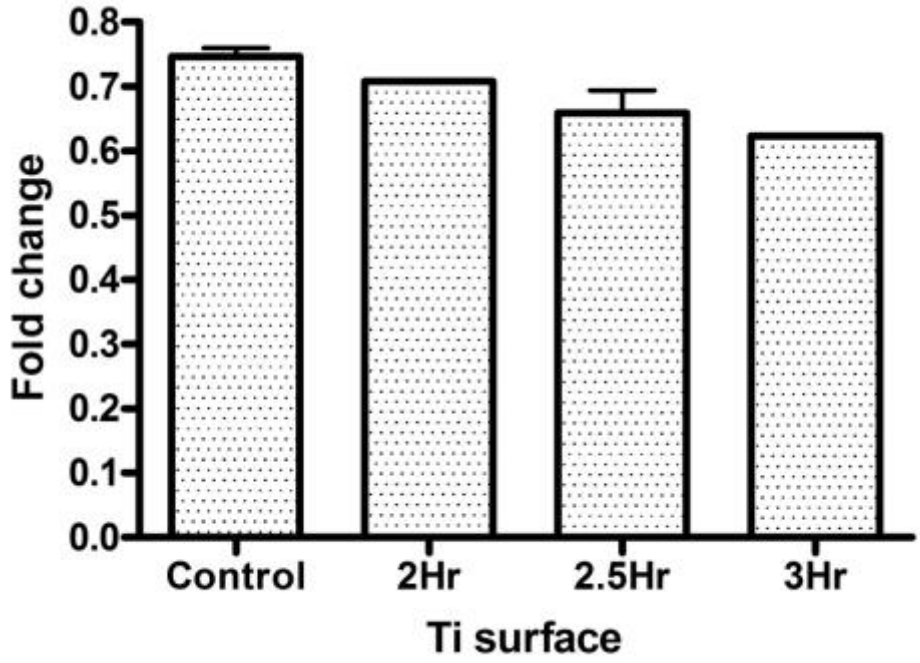

Figure 4-8 Fold changes in intensity of labelled aspartate on different Ti surfaces

Following metabolomic extraction and processing as described, labelled CA was noted in all samples, with the highest fold change being present on the control Ti discs.

4.4.5 Summary of upregulated metabolites

The above data is summarised is the table below:

METABOLITE	INTENSITY COUNT (WITH INCREASING NANOROUGHNES)	SIGNIFICANT
PYRUVATE	⇑	No
ALANINE	⇑	Yes
ASPARTATE	⇑	No
CA	⇓	No

4.4.6 Unlabelled metabolites

Whilst the above compounds showed clear increases in labelled intensity counts, other compounds that were perhaps expected to be metabolised showed no labelling. For example, key metabolites in the citric acid cycle such as acetyl-

CoA, citrate and oxaloacetate showed no heavy labelling whatsoever. Raw data is available on the DVD at the back of this thesis.

4.4.7 Targeted therapeutic metabolomics

Metabolite recognition highlighted the movement of labelled compounds, thus allowing the identification of upregulated metabolic pathways involved in bacterial adhesion. Subsequently, compounds known to inhibit these pathways and associated enzymes could be identified and utilised. The exact mechanism of action of these compounds and why they were selected is explained in the discussion.

Introduction of beta-chloro-L-alanine (ß-CLA), resulted in a reduction in biofilm density when stained with CV. As the concentration of ß-CLA was increased, the biofilm density decreased significantly ($P<0.05$ for 250µg/ml and 500µg/ml, $P<0.01$ for 1000µg/ml) as shown in Figure 4-9.

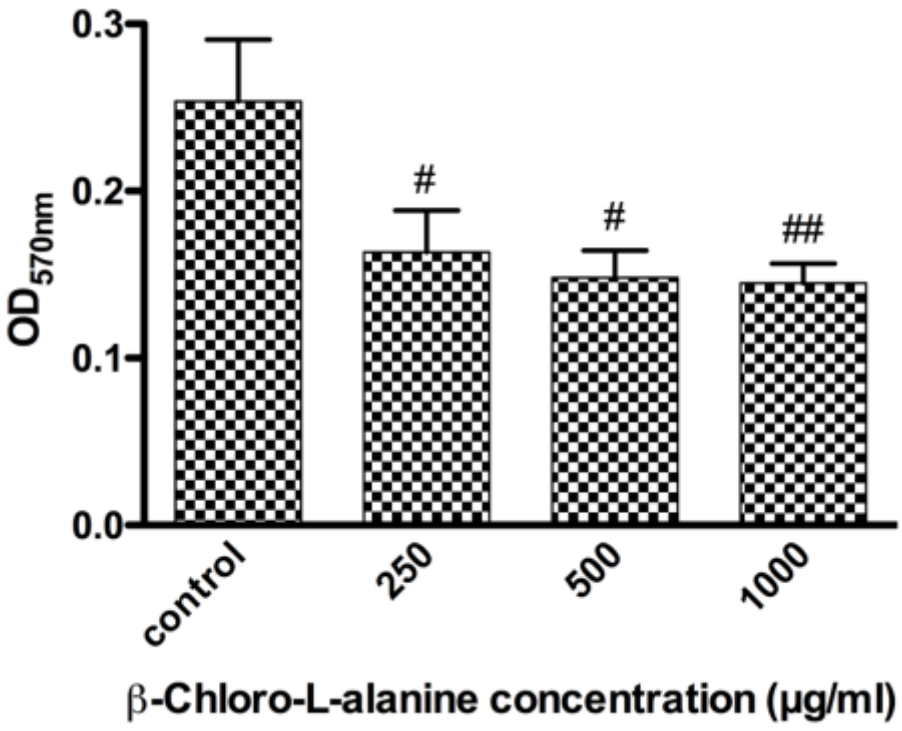

Figure 4-9 OD measurements of biofilm growth with different ß-CLA concentrations

S. *aureus* Newman strain was standardised in DMEM + supplement media and grown, with the addition of different ß-CLA concentrations, for a period 24 hours. Biofilm density was significantly reduced with 250µg/ml and 500µg/ml ($^{\#}P<0.05$) and 1000µg/ml ($^{\#\#}P<0.01$) concentrations, when compared to the no-ß-CLA control (1-way ANOVA).

Introduction of cycloserine (CS) resulted in a reduction in biofilm density when stained with CV. As the concentration of CS was increased, the biofilm density decreased significantly ($P<0.001$ for 12.5µg/ml, 25µg/ml and 50µg/ml) as shown in Figure 4-10.

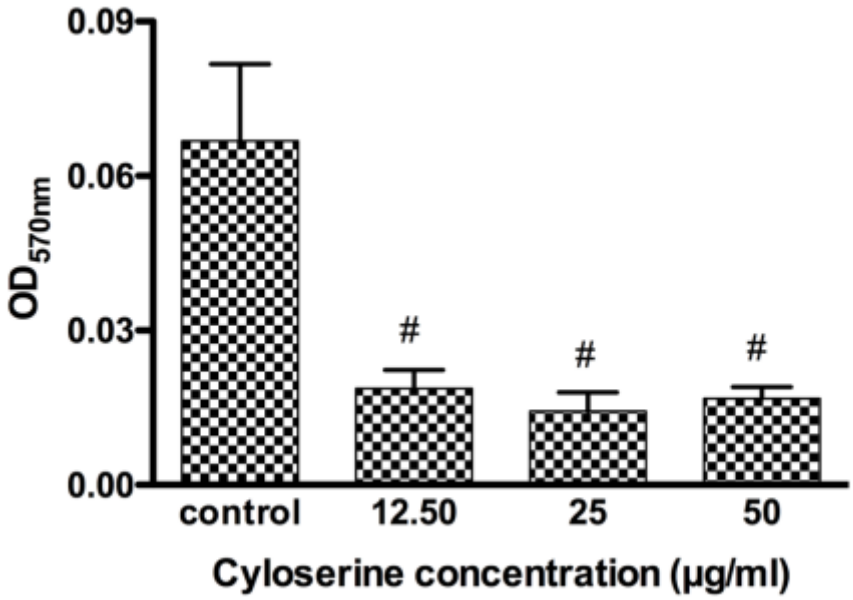

Figure 4-10 OD measurements of biofilm growth with different CS concentrations

S. *aureus* Newman strain was standardised in DMEM + supplement media and grown, with the addition of different CS concentrations, for a period 24 hours. Biofilm density was significantly reduced with12.5µg/ml, 25µg/ml and 50µg/ml ($^{\#}P<0.001$) concentrations, when compared to the no-CS control (1-way ANOVA).

4.4.8 MIC and growth kinetics

Visualisation of the ß-CLA plates revealed and MIC of 1000µg/ml. Bacterial growth was visually apparent at concentrations lower than this in the form of a pellet at the bottom of the well. In contrast, the CS plates revealed a dose dependant reduction in bacterial growth with increasing CS concentrations. Subsequent 24hr growth kinetics however revealed a dose dependant response for both inhibitory compounds over the concentrations range shown in Figure 4-11 and Figure 4-12. With ß-CLA, all concentrations were found to have significantly lower OD measurements, when compared to the control ($P<0.05$, 1-way ANOVA) with no significant difference between concentrations. CS, however, showed a significant difference ($P<0.05$, 1-way ANOVA) in OD when higher concentrations (100,50 and 25 µg/ml) of CS were compared with lower concentrations and control (12.5 µg/ml).

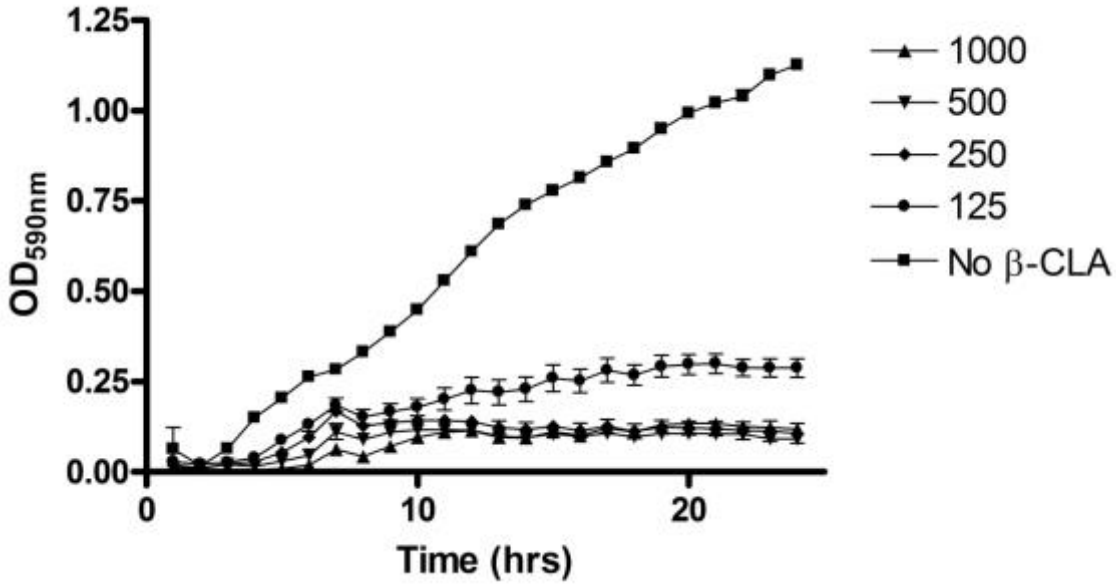

Figure 4-11 Growth kinetics for S. *aureus* with different β-CLA concentrations

S. *aureus* Newman strain was standardised in DMEM + supplement media and grown, with the addition of different β-CLA concentrations, for a period 24 hours. OD was measured every hour for 24hrs, allowing the growth kinetics to be identified (1-way ANOVA).

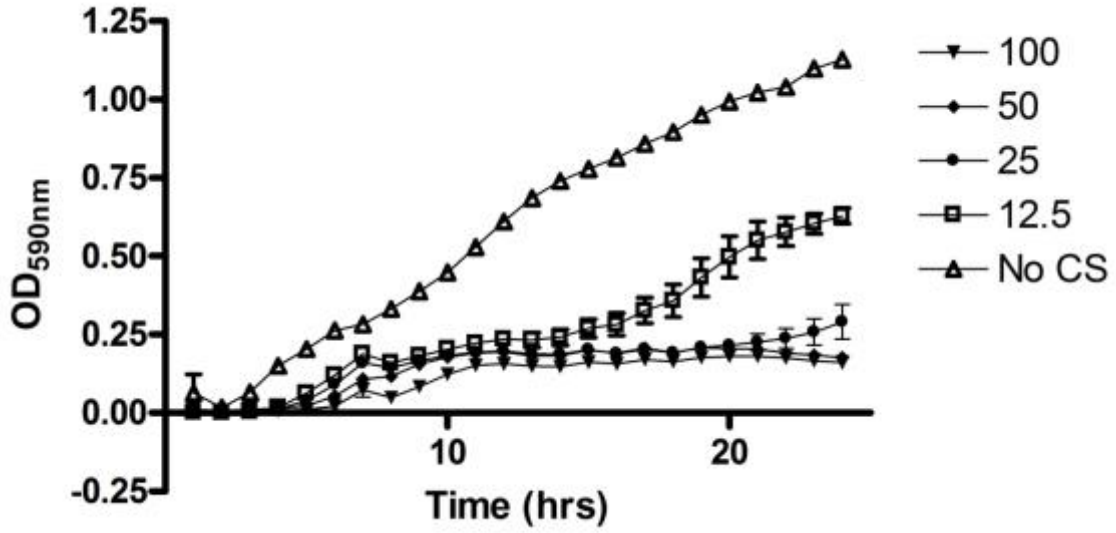

Figure 4-12 Growth kinetics for S. *aureus* with different CS concentrations

S. *aureus* Newman strain was standardised in DMEM + supplement media and grown, with the addition of different CS concentrations, for a period 24 hours. OD was measured every hour for 24hrs, allowing the growth kinetics to be identified (1-way ANOVA).

4.5 Discussion

Since the emergence of metabolomics in the late 1990's, this field has rapidly advanced and developed (Jellum 1977, Gates and Sweeley 1978, Niwa 1986, Bales, Bell et al. 1988, Oliver, Winson et al. 1998, Goodacre, Vaidyanathan et al. 2004, Dunn, Bailey et al. 2005, Glinski and Weckwerth 2006, Wishart 2008). Despite these innovations, bacterial metabolomics (specifically bacterial adhesion and subsequent biofilm development) remains an exciting and under researched area. As previously suggested surface nanotopography affects bacterial adhesion and subsequent biofilm development (Chung, Schumacher et al. 2007, Díaz, Schilardi et al. 2008, Ivanova, Truong et al. 2009, McMurray, Gadegaard et al. 2011, Xu and Siedlecki 2012). This chapter aims to offer a link between bacterial metabolomics and bacterial adhesion.

Bacterial metabolism refers to a collection of reactions in which molecules are broken down primarily to generate energy. In addition, it includes the study of uptake and consumption of compounds required for bacterial growth and maintenance of a steady state, known as assimilation reactions (Jurtshuk 1996). These reactions are catalysed within the bacterial cell via enzymatic systems, with the primary end point of bacterial self-replication. Bacterial metabolism therefore encompasses the chemical changes that occur to allow microbial cells to live, function and replicate.

Bacteria primarily obtain energy from oxidation of organic compounds; often carbohydrate (glucose), lipids and proteins, and are therefore chemoorganoheterotrophic (Gottschalk 1986). These carbon and nitrogen containing substrates can be used either aerobically or anaerobically to produce energy, usually via glycolysis, resulting in the production of pyruvate and energy (2xATP per cycle) (Strasters and Winkler 1963). The fate of pyruvate depends on the particular environmental conditions and metabolic pathways present within the organism, and in the case of bacteria are numerous. By incorporating heavy labelled glucose into our growth media, we were able to identify which metabolic pathways are utilised by S. *aureus* during surface adhesion.

Pyruvate was noted to be heavily labelled (Figure 4-1), in all samples, suggesting that glycolysis is occurring, providing the bacteria with an energy source. It also

appears that flux through this glycolytic pathway is increased with escalating nanoroughened Ti surfaces (Figure 4-2). Whilst not found to be significant, this trend suggests that these NW Ti surfaces are somehow causing an up-regulation of bacterial glycolysis, and ensuing pyruvate production. The subsequent fate of pyruvate is, however, more interesting. High levels of labelled alanine were found across all samples (Figure 4-3), suggesting conversion of pyruvate to alanine via alanine transaminase (EC:2.6.1.21) (Baba, Bae et al. 2008). The absence of labelled compounds such as Acetyl-CoA and oxaloacetate in our results suggests that pyruvate does not enter the citric acid cycle but is instead almost completely converted to alanine. Alanine is known to be involved in peptidoglycan (murein) production (Walsh 1989). In addition, to producing an inflammatory response in humans (Timmerman, Mattsson et al. 1993, Card, Jasuja et al. 1994), peptidoglycans play a key role within the bacterial cell wall (Walsh 1989) and are found on the outside of the cytoplasmic membrane of most bacteria (Rogers, Fey et al. 2009). Alanine, in conjunction with other amino acids (such as lysine), allows cross-linking between two alternating amino sugar chains, forming a mesh-like 3-dimensional peptidoglycan layer (Rogers, Perkins et al. 1980), a component of the EPS. This layer has unique properties; it is able to withstand changes in osmotic pressure yet is not rigid and remains flexible. Wide pores are also noted, thus allowing diffusion of large molecules such as proteins (Vollmer, Blanot et al. 2008). Peptidoglycans also act to keep cells together after cell division, therefore increasing adherence capacity and subsequent biofilm formation (Mercier, Durrieu et al. 2002). These results suggest that bacterial aggregation and subsequent biofilm formation is a result of increased alanine metabolism, causing up-regulation of peptidoglycan production. Alanine, and consequently peptidoglycan production appears to be further enhanced by increasing the nanoroughness of the surface to which the bacteria is adhering. It is not clear exactly how this up-regulatory mechanism works, however it would seem logical for the bacteria to exude all its energy into peptidoglycan production, aggregation and biofilm production on a nanoroughened surface to which it can easily stick, rather than a polished, smooth surface to which it cannot. Could it be that some kind of ‘surface identification’ mechanism exists, allowing the bacteria to decide whether it is efficient use of energy to attempt surface adhesion? Bacteria are known to express and control mechanosensitive potassium channels, allowing a cellular

response to membrane tension forces (Vogel and Sheetz 2006, Kobayashi and Sokabe 2010). While this response only occurs at high tensions (Kung 2005), thus suggesting a cellular lysis-prevention role, it is postulated that a similar mechanism exists that allows for surface identification and adhesion modulation. Further research in this area, perhaps looking at the bacterial proteomics of adhesion, is recommended.

In addition, labelled aspartate was also noted to be increased across all samples (Figure 4-5), again with a step-wise increase in intensity fold change noted with escalating nanoroughness (Figure 4-6). Aspartate, or aspartic acid, is an non-essential amino acid and is recognised as being important in protein metabolism as well as being connected to the citric acid cycle component, oxaloacetate (Michal and Schomburg 1999). It is also known to be the precursor for lysine, methionine, threonine, purines and pyrimidine bases in microorganisms (Oikawa 2007). As mentioned previously, no labelled compounds involved in the citric acid cycle were observed, again suggesting that this cycle is not involved in this stage of bacterial growth. While it is recognised that aspartate can be converted to alanine, via L-aspartate 4-decarboxylase (Oikawa 2007), our results suggest that this may be a reversible reaction and that alanine can also be converted to aspartate. Whilst the source of aspartate appears unclear, its subsequent role is similar to that of alanine. As mentioned, lysine production is dependent on aspartate, which is another amino acid involved in the production of peptidoglycans (Royet and Dziarski 2007). This suggests a further increase in this metabolic pathway, with the end goal of producing bacterial aggregation and peptidoglycan layer formation. In addition to its role in peptidoglycan metabolism, aspartate and to some extent lysine, are also recognised to be involved in signal transduction in bacteria (Stock, Stock et al. 1990). In *E. coli,* aspartate is thought to be involved in chemotaxis, and when substituted, affects chemotaxis via signal transduction (Lukat, Lee et al. 1991). While *S. aureus* is not motile, it is hypothesised that aspartate has some influence on signal transduction.

Aspartate is also a key factor in purine and pyrimidine metabolism (Allison and Eugui 1996, Baba, Bae et al. 2008). Both purines and pyrimidines contain aromatic rings in their structure, the nucleotides of which function as precursors for DNA and RNA synthesis (Hammond and Gutteridge 1984). It is therefore

likely that the increased labelling of aspartate metabolism signifies increased production of bacterial DNA, and subsequent bacterial replication. Again a trend of increased fold change with nanoroughness was noted, suggesting that aspartate production, much the same as alanine production, is up-regulated with increased nanoroughness (Figure 4-6). In contrast to alanine however, aspartate's involvement in purine/pyrimidine metabolism (Allison and Eugui 1996, Baba, Bae et al. 2008) and subsequent bacterial replication (Hammond and Gutteridge 1984) suggests that higher aspartate levels should result in increased bacterial DNA.

Further analysis of our metabolomic data has shown high abundance of labelled CA (Figure 4-8), a metabolic product of aspartate via carbamoyl-aspartate transferase (EC 2.1.3.2). CA is also involved in pyrimidine metabolism (Hammond and Gutteridge 1984, Baba, Bae et al. 2008), again implicating the importance of this pathway during the adhesion of S. *aureus* to surfaces. Interestingly however, the highest CA fold change was noted on our control surface, with a gradual fold change reduction as NW roughness increases. While not significant, this result suggests that, on smoother surfaces bacteria channel energy into pyrimidine metabolism via CA, rather than purine and peptidoglycan metabolism via alanine and aspartate. The relevance of this is unclear, however is may be that given that the bacteria appear to be less adherent to smoother surfaces, the pathways associated with adherence remain relatively static, whilst planktonic bacterial replication remains unaffected.

Subsequent metabolic cross-referencing with the Kyoto Encyclopedia of Genes and Genomes (KEGG) database (Kanehisa and Goto 2000), allowed specific metabolic pathways to be identified (Figure 4-13). By 'heavy' labelling glucose we are able to see how S. *aureus* uses the glucose provided by the media, and into which subsequent pathways this energy is then directed. Following conversion to pyruvate, via glycolysis, the two main end points appear to be proteoglycan, purine and pyrimidine metabolism. It is logical to assume that this is advantageous to the bacteria as it provides bacterial protection, via aggregation and biofilm development, as well as bacterial replication through nucleotide production and subsequent DNA synthesis. Looking back at the stages of biofilm development (Jahoda 2009), adhesion is critical and once achieved a cascade of biofilm development ensues. Prevention of this biofilm forming

process, by inhibiting the metabolic pathways associated with adhesion, may provide a novel target for anti-bacterial therapies.

Through analysis of the pathways identified (Figure 4-13), a key step in peptidoglycan, purine and pyrimidine metabolism is the conversion of pyruvate to D-Alanine via D-alanine transaminase (EC 2.6.1.2). This is a reversible transamination reaction (Dumitru, Iordachescu et al. 1970), and can thus be inhibited by compounds such as ß-CLA, explaining its involvement in this study. ß-CLA is an amino acid analogue that inhibits a number of enzymes, including alanine transaminase (Whalen, Wang et al. 1985). The use of B-CLA has been shown to effectively impair cell growth both in cancer (Beuster, Zarse et al. 2011) and bacteria (Manning, Merrifield et al. 1974) by preventing the production of D-alanine. Alanine is known to be involved in peptidoglycan production (Walsh 1989) and plays a key role within the bacterial cell wall (Walsh 1989) and is involved in forming the biofilm (Rogers, Perkins et al. 1980).

Additionally, once formed D-alanine can then be either converted to L-alanine (via alanine racemase [EC 5.1.1.1]) or enter peptidoglycan metabolism (via D-alanine-D-alanine ligase EC 6.3.2.4]). The anti-tuberculosis drug CS is known to inhibit both these enzymes (Curtiss, Charamella et al. 1965), thus ensuring its use in this study also. CS is a second-line anti-tuberculosis drug and is known to inhibit a number of enzymes including alanine racemase and D-alanine-D-alanine ligase (Curtiss, Charamella et al. 1965). It is known to have an inhibitory effect on hepatocytes (Cornell, Zuurendonk et al. 1984) and cancer cell growth (Beuster, Zarse et al. 2011) and is involved in alanine production. It has been suggested that CS is a structural analogue of D-alanine and may prevent the normal incorporation of alanine in the bacterial cell wall and protein production (Neuhaus and Lynch 1964).

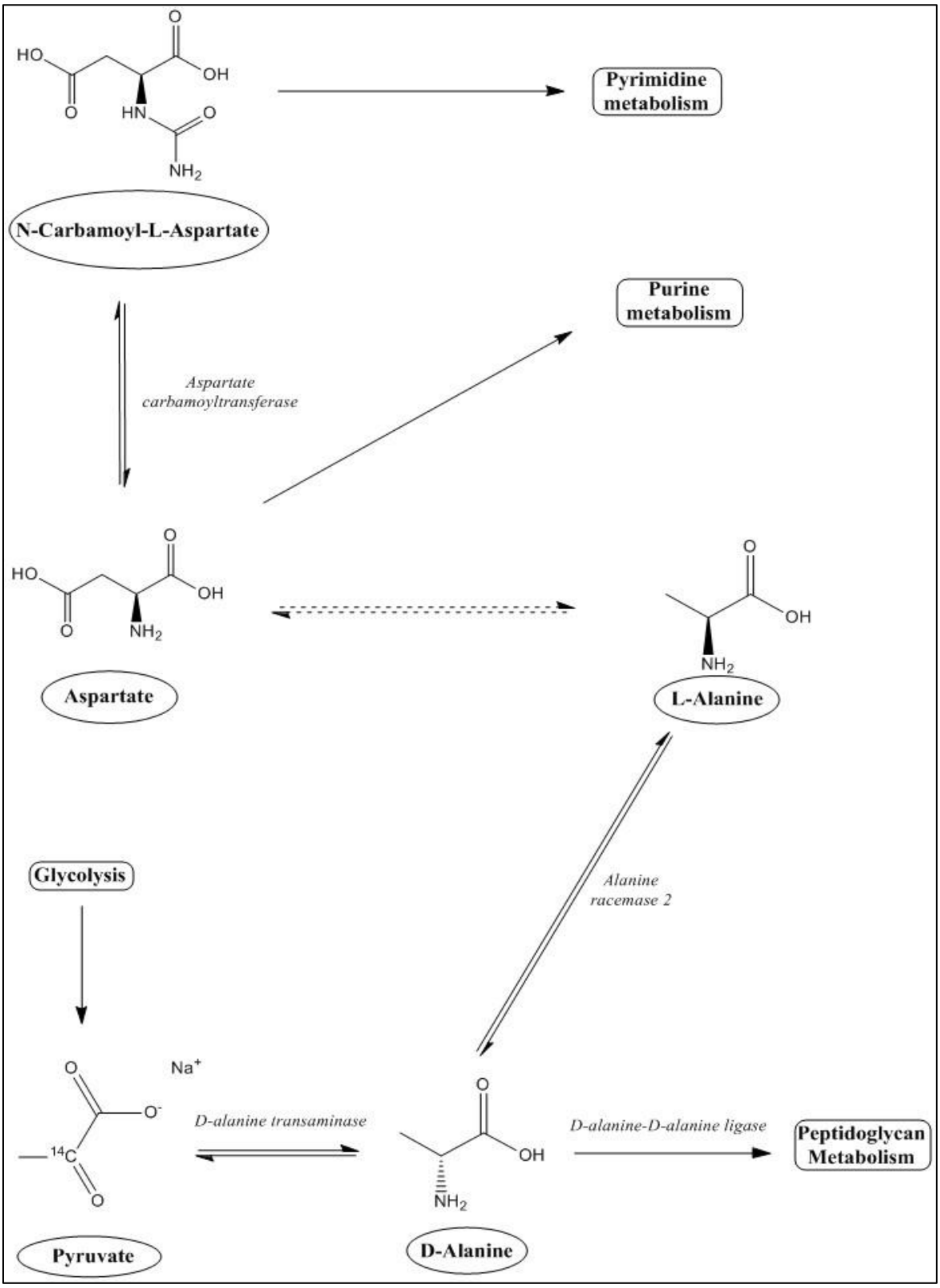

Figure 4-13 Metabolic pathways linking identified metabolites, adapted from (Kanehisa and Goto 2000).

Following metabolite identification, KEGG referencing shows how these metabolites fit into known metabolic pathways in Newman strain of S.*aureus*.

ß-CLA was found to have a planktonic MIC of 1000 µg/ml, however biofilm mass was found to be significantly reduced at much lower concentrations than this (250µg/ml and 500µg/ml ($^{\#}P<0.05$)). Initially it appeared that whilst the planktonic bacterial concentrations were not being affected by these ß-CLA concentrations, the ability of S. *aureus* to form biofilms was. However, subsequent 24hr growth kinetic analysis (Figure 4-11) shows a dose dependant type response to increasing ß-CLA concentrations, suggesting that inhibition of planktonic bacterial growth is also occurring. This implies that ß-CLA interferes with two key metabolic pathways; firstly by inhibiting D-alanine transaminase and subsequent conversion of pyruvate to D-alanine (Beuster, Zarse et al. 2011), thus reducing peptidoglycan, purine and pyrimidine metabolism . This impairs the ability of S. *aureus* to adhere, aggregate and form biofilms. Secondly, bacterial DNA replication (reliant of purine and pyrimidine metabolism) will also likely be affected which will affect planktonic bacteria and biofilm formation alike. While ß-CLA is not clinically used as an anti-microbial, its effects on S. *aureus* are clear, thus its use perhaps as an implant coating of for local treatment should be considered. Further research relating to ß-CLA's effect on other cell lineages is merited.

Similar results were also noted with the addition of CS (4.3.4), and growth kinetic analysis again showed a dose dependent type response in relation to differing CS concentrations. In addition, no clear MIC was noted, suggesting that CS perhaps has a more bacteriocidal effect on planktonic cells. As previously mentioned, CS is used in the treatment of tuberculosis and acts by inhibiting alanine racemase and D-alanine-D-alanine ligase (Curtiss, Charamella et al. 1965), resulting in inhibition of peptidoglycan, purine and pyrimidine metabolism (Figure 4-13). Again while this will clearly affect biofilm formation, it also influences bacterial replication and thus has implications on both planktonic cells and biofilm formation. In addition, CS is known to penetrate the central nervous system, and thus can have several neurological side effects such as headaches, depression, dizziness, confusion, dysarthria and psychosis to name a few (Nitsche, Jaussi et al. 2004). Further research into its clinical use is therefore recommended.

In conclusion, it is evident that surface adhesion of *S. aureus* is reliant on specific metabolites and pathways. Our novel labelling techniques combined

with LC-MS has allowed identification of these metabolites and pathways, thus opening the door to targeting therapeutic treatments. Our pilot study suggests that compounds such as β-CLA and CS inhibit key bacterial adhesion pathways, with the later also potentially having a bacteriocidal affect. It must be stressed, however, that these agents do have known side effects and that their influence on other cell lineages is largely unknown. Further research is therefore recommended.

Chapter 5

Final Discussion

5.1 Introduction

Implantable medical devices or biomaterials are used extensively in orthopaedic joint replacements (Scottish-Arthoplasty-Project 2014, ScottishArthoplastyProject 2014). Successful arthroplasty relies primarily on good osseointegration (Willert and Buchhorn 1998) and prevention of post-operative complications (1.2). *Staphylococcus* species are frequently isolated from orthopaedic infections, namely *S. aureus* and *S. epidermidis* (Garvin, Hinrichs et al. 1999, Nickinson, Board et al. 2010), which constitutes just over a third of all confirmed prosthetic joint infections (Trampuz and Widmer 2006). Arthroplasty failure due to infection is largely due to biofilm production, a 3D matrix produced and secreted by the bacteria that involves a series of co-ordinated molecular events (Fux, Stoodley et al. 2003). Additionally it provides a protective coating, thus allowing the bacteria to withstand high doses of particular antibiotics that would kill planktonic cells outright (Bjarnsholt 2013). The initial adhesion phase of complex biofilm formation is critical (Mack, Nedelmann et al. 1994, Heilmann and Götz 1998, Jahoda 2009), and is affected both by material surface topography (Ivanova, Truong et al. 2009, McMurray, Gadegaard et al. 2011, Ivanova, Hasan et al. 2012, Xu and Siedlecki 2012, Sjöström, Brydone et al. 2013) and metabolic pathway activation (Kanehisa and Goto 2000, Stipetic, Dalby et al. 2016). In addition, bacterial metabolomic profiling has focused primarily on normal growth (Schwab, Watson et al. 1955, Koek, Muilwijk et al. 2006, Hettick, Green et al. 2008, Schaub and Reuss 2008), without focus on biofilm formation or production. It is postulated that advances in nanopattern fabrication techniques (Sjöström, Dalby et al. 2009, Sjöström, Brydone et al. 2013) and metabolomic analysis (Wishart 2008, Dudley, Yousef et al. 2010, Wang, Larson et al. 2011, Patti, Yanes et al. 2012) will improve our understanding and subsequent clinical management of these infections, benefiting the patient, the NHS and society.

5.2 Optimising biofilm growth in S. *aureus*

Multiple methods of standardising, optimising and quantifying staphylococcal biofilm growth exist (Bergamini, Bandyk et al. 1989, Atanassova, Meindl et al. 2001, Alarcon, Vicedo et al. 2006, Stepanović, Vuković et al. 2007), however, a generic method, used by the majority is not readily recognised. Historically, a multitude of different growth media have been used for staphylococcal culture (May, Houghton et al. 1964, Christensen, Simpson et al. 1982, Safdar, Narans et al. 2003). However, it was felt that none could be incorporated into future MSC co-culture studies. Osseointegration is essential for long-term survival of TJR; thus our culture medium had to be optimal for culture of MSCs as well as bacteria. DMEM + supplements media has been used extensively in cell culture laboratories (Webber, Harris et al. 1985, Palmer, Schwartz et al. 2001, Dalby, Cates et al. 2004). Our results show that DMEM + supplements caused predictable bacterial growth when compared to other growth media (2.3.1.3). In addition, it would allow subsequent co-culture experimentation with MSCs to be carried out if necessitated, thus increasing its clinical relevance.

Bacterial biofilm growth is a time dependant phenomenon, with adhesion being the critical stage. This is essentially a battle between tissue cell integration and bacterial adhesion to the same surface (Gristina, Hobgood et al. 1987). If adhesion can be prevented, subsequent developmental stages can be averted, thus reducing THR infection rates. Adhesion is recognised as being a two-phase process consisting of an initial, reversible and instantaneous phase (phase one or docking phase) and a second time-dependant, irreversible molecular and cellular phase (phase two or locking phase) (Dunne 2002, Katsikogianni and Missirlis 2004, Barbu, Mackenzie et al. 2014). Whilst significant literature exists defining and characterising these stages (Costerton, Cheng et al. 1987, Costerton, Stewart et al. 1999, Donlan and Costerton 2002, Dunne 2002, Hall-Stoodley, Costerton et al. 2004), little exists in relation to the time periods of the specific biofilm development phases. Phase two adhesion of bacterial to plant root systems is suggested to occur within 5 min of exposure (James, Suslow et al. 1985), however, research with respect to clinically relevant bacteria and biomaterial adhesion is scarce. Given that adhesion is recognised as a ‘race to

the surface', being able to accurately establish a time course for this event is essential. Our growth curve data provided a rough adhesion time frame of 0 to 2 hours after bacteria/surface exposure (2.3.1.3). A more exact quantification method was subsequently employed to allow precise time frame detection. Multiple bacterial quantification methods exist, each with specific advantages and drawbacks (2.3.2.3). Quantitative PCR is used extensively in dental (Williams, Trope et al. 2006) and medical (Larsen, Vogensen et al. 2010) fields, and was utilised in this study to provide a real time quantification of bacterial DNA. This allowed identification of a pre-exponential growth period, felt to represent the adhesion/aggregation phase of bacterial growth, directly before the next stage of development, maturation (exponential bacterial growth). Recognition of this optimal bacterial incubation period (60 min), allowed us to accurately analyse bacterial adhesion in subsequent experiments. When combined with an optimised qPCR technique (2.3.3.2), precise bacterial quantification at the adhesion phase of biofilm development was achieved. Whilst the qPCR technique is highly sensitive and specific (Yang, Habib et al. 2007, Smith and Osborn 2009), it is limited by its inability to discriminate between live and dead cells (Àlvarez, González et al. 2013). The importance of this in our study however is negligible, as it was assumed that only live bacteria could adhere to a surface. Future studies and techniques that focus on live/dead qPCR, such as those described by Alvarez *et al* (2013) and Sherry *et al* (2016) may be on benefit in this regard (Sherry, Lappin et al. 2016).

5.3 Biofilms and nanotopographies

Whilst adhesion is dependent on cell-surface interactions (3.1), alterations to the surface topography at a nanoscale have also been shown to have major effects on cell behaviour (McMurray, Gadegaard et al. 2011), bacterial adhesion (Xu and Siedlecki 2012) and ultimately long term implant survival (Sjöström, Brydone et al. 2013). The exact effects of surface topography are somewhat confusing. While some studies suggest increased surface roughness reduces bacterial adhesion and subsequently biofilm formation (Ivanova, Truong et al. 2009, Ivanova, Hasan et al. 2012, Xu and Siedlecki 2012, Ivanova, Hasan et al. 2013), others imply that bacteria show no preference to surface topography and

disregard surface roughness as factor in adhesion (Scheuerman, Camper et al. 1998, Taylor, Verran et al. 1998, Bos, van der Mei et al. 1999). The sheer existence of these studies, in conjunction with MSC research on nanosurfaces (Dalby, Gadegaard et al. 2007, Hart, Gadegaard et al. 2007, Dalby, Andar et al. 2008) provides a strong case for surface nanotopography affecting cellular attachment, regardless of whether it enhances or inhibits adhesion.

The large variation between different nanosurfaces and materials is highlighted in this study. While no significant difference was shown between differing polystyrene nanopit arrays (3.4.1), a trend towards reduced adhesion on ordered nanopit structures and increased adhesion on disordered arrays was demonstrated. Similar observations have been noted in MSC studies, suggesting adhesion promotion by disorder and adhesion inhibition by ordered nanopit arrays (Dalby, Andar et al. 2008). Further MSCs studies suggest gene expression is affected by nanotopography (Dalby, Gadegaard et al. 2007, Dalby, Andar et al. 2008), therefore it may be that these mechanisms are also occurring in bacteria during adhesion. This theory would benefit from further genomic or proteomic studies and may provide novel antibacterial nanopit surfaces. It has also been suggested that bacterial micro-colony formation can be prevented by creating a physical barrier to spread at a nanometre level (Chung, Schumacher et al. 2007). It may be that the organised SQ and HEX nanopatterns in our study are the optimal nanopit orientations to prevent bacteria microcolony formation, keeping the bacteria in small, isolated clusters and preventing communication. A study by Diaz *et al* (2009) focusing on *Pseudomonas fluorescens* found reduced adhesion to parallel nanometre channels and concluded that sub-micropatterns are influential on bacterial colonisation strategies. It was felt that these ordered arrays posed a physical barrier to the bacteria, requiring a higher energy expenditure to ‘overcome’ the channel walls (Díaz, Schilardi et al. 2008). It is postulated that similar interactions may be occurring between bacteria and our polystyrene nanopit ordered arrays, namely SQ and HEX, however further studies are required to confirm this theory.

This hypothesis was further supported moving onto more clinically relevant materials such as Ti. We found fabricated NW Ti to significantly affect bacterial adhesion, with and exponential rise in bacterial concentration with increasing nanoroughness (3.3.2). These NW surfaces are noted to be highly disordered, and

therefore inducive to increased bacterial adhesion as previously theorised. Additionally it has been suggested that such surfaces provide increased contact guidance (Díaz, Schilardi et al. 2008), perhaps allowing quicker attachment and biofilm production. This was demonstrated by our SEM imaging of bacterial surface interactions, where increased bacterial aggregation and clumping on rougher nanosurfaces was illustrated (3.4.2.3) . Finally, it should be noted that while these disordered NW surfaces contained surface depressions that may invoke bacterial collection and adhesion, they did not exhibit any nanoprotrusions that have also been shown to affect bacterial growth (Ivanova, Truong et al. 2009, Ivanova, Hasan et al. 2012, Ivanova, Hasan et al. 2013).

While nanoprotrusions have been studied on materials such as black silicon (Ivanova, Hasan et al. 2013) and polyurethane (Xu and Siedlecki 2012), the incorporation of such nanoprotrusions onto clinically relevant materials (Ti) was innovative and unique. Our NC pattern, hexagonal in nature, showed a 10-fold reduction in bacterial adhesion when compared to a control, polished Ti surface (3.4.2.1). Similar nanopillar structures found on dragonfly wings (Ivanova, Hasan et al. 2012) and black silica (Ivanova, Hasan et al. 2013) have shown bacteriocidal properties. It is postulated that cell death occurs as a result of altered surface structure and stresses resulting in a forced cell deformation (Ivanova, Hasan et al. 2013). Additionally, our NC patterns were noted to have sharp edges with a pyramidal tip, characteristics that have been shown to cause significant cell membrane damage, resulting in cell lysis (Gorth, Puckett et al. 2012). The ability to kill bacteria that attach to a clinically relevant material based purely on surface structure is a novel area of research. While the effects of these surfaces on MSCs and osseointegration negates further research, the potential for application in implant development and as an alternative to chemical based treatments is vast.

5.4 Biofilm metabolomics

While multiple mechanical theories as to the mechanism behind bacterial adhesion exist (Fletcher and Loeb 1979, Paul and Loeb 1983, Fletcher 1996, Dunne 2002), it has been suggested that adhesion is mediated by surface

proteins (Hussain, Herrmann et al. 1997), extracellular proteins (Heilmann, Schweitzer et al. 1996), adhesins (McKenney, Hübner et al. 1998) and autolysins (Heilmann and Götz 1998). The metabolomic pathways underlying these mechanisms remain an under investigated research area. Despite the rapid advancement and development of metabolomic techniques (Jellum 1977, Gates and Sweeley 1978, Niwa 1986, Bales, Bell et al. 1988, Oliver, Winson et al. 1998, Goodacre, Vaidyanathan et al. 2004, Dunn, Bailey et al. 2005, Glinski and Weckwerth 2006, Wishart 2008) bacterial metabolomics studies (specifically bacterial adhesion and subsequent biofilm development) remain scarce. The novel incorporation of labelled glucose into our media allowed the identification of metabolic pathways utilised by S. *aureus* during adhesion. Our results indicate up-regulation of glycolysis, peptidoglycan, purine and pyrimidine metabolism characterised by fold increases in pyruvate, alanine, aspartate and CA (4.4). The importance of these pathways is well documented, playing key roles in the bacterial cell wall (Rogers, Perkins et al. 1980, Walsh 1989), EPS production (Rogers, Perkins et al. 1980), adherence (Mercier, Durrieu et al. 2002), aggregation and DNA/RNA synthesis (Hammond and Gutteridge 1984). Furthermore, the absence of labelled compounds such as Acetyl-CoA and oxaloacetate in our results suggests that pyruvate does not enter the citric acid cycle but is instead almost completely converted to alanine. This unexpected result suggests that in the initial phase of bacterial exposure to a surface, energy is preferentially directed into pathways providing bacterial protection (via EPS and thus biofilm production) and replication (via increased RNA/DNA synthesis). What's more, this response is amplified as Ti nanoroughness increases, with higher fold changes in pyruvate, alanine and aspartate being noted on 3Hr NW Ti in comparison to smooth control Ti surface (0). This, in conjunction with lower fold changes in CA on 3Hr NW Ti, suggests that on roughened surfaces, energy is directed to peptidoglycan and purine metabolism, whilst on smoother surfaces pyrimidine metabolism is favoured. The theory behind this is not clear; however one explanation may be in relation to contact guidance. Increasing nanoroughness is known to provide increased contact guidance (Díaz, Schilardi et al. 2008). It may be that metabolic pathway activation in bacteria is dependent on the degree of contact guidance available; i.e. low contact guidance results in increased bacterial replication as adhesion is not possible, while high contact guidance results in increased purine and

peptidoglycan production thus inducing adhesion. Certainly in MSCs studies, increasing contact guidance has positive effects on epithelial cell growth (Teixeira, Abrams et al. 2003). Bacterial research in this field however, remains scarce and may prove beneficial in future studies.

Subsequent identification and use of therapeutic agents that target these pathways provided a clinical angle to our metabolomic analysis. While multiple antibiotics are used to try and treat infection, few are aimed directly at preventing bacterial adhesion to implants. Both therapeutic agents in our study were chosen based on their ability to inhibit the identified bacterial adhesion pathways. While both our inhibitory compounds (β-CLA and CS) were found to reduce biofilm growth (4.3.3), this was a dose dependant phenomenon, suggesting that inhibition of planktonic bacterial growth was also occurring. More specifically, our results suggest that β-CLA works on two key metabolic pathways; firstly by inhibiting D-alanine transaminase and subsequent conversion of pyruvate to D-alanine (Beuster, Zarse et al. 2011), thus reducing peptidoglycan, purine and pyrimidine metabolism. This impairs the ability of S. *aureus* to adhere, aggregate and form biofilms. Secondly, bacterial DNA replication (reliant of purine and pyrimidine metabolism) will also likely be affected which will affect planktonic bacteria and biofilm formation alike. Differentiation between these two potential modes of action would be an interesting focus of future research. A similar dose dependant type response was noted with the addition of CS to our bacterial cultures. Interestingly, however, no clear MIC was noted, suggesting that CS perhaps has a more bacteriocidal effect on planktonic cells. As previously mentioned, CS is used in the treatment of tuberculosis and acts by inhibiting alanine racemase and D-alanine-D-alanine ligase (Curtiss, Charamella et al. 1965), resulting in inhibition of peptidoglycan, purine and pyrimidine metabolism. Again, while this will clearly affect biofilm formation, it also influences bacterial replication and thus has implications on both planktonic cells and biofilm formation. In addition, CS is known to penetrate the central nervous system, and thus can have several neurological side effects such as headaches, depression, dizziness, confusion, dysarthria and psychosis to name a few (Nitsche, Jaussi et al. 2004). Further research into its clinical use is therefore recommended.

It is evident that by targeting metabolic pathways with therapeutic treatments such as β-CLA and CS, bacterial adhesion and thus biofilm development can be influenced. While the potential benefits of such treatments is clear, these agents do have known side effects and their influence on other cell lineages is largely unknown. Further research is therefore recommended.

5.5 Future work, study limitations and clinical relevance.

This body of work has optimised the surface adhesion phase of biofilm production in S. *aureus*, allowing the effects of different materials and nanotopographies on this growth period to be evaluated. Further labelled metabolomic analysis has highlighted the specific metabolites and pathways involved in this process. Whilst a specific time frame for the initial adhesion phase of bacterial growth was documented, subsequent S. *aureus* biofilm studies would benefit from further analysis using similar techniques used in this study. In addition, incorporation of a co-culture model involving both S. *aureus* and MSCs may elicit changes in the growth kinetics of both cell lineages and subsequently may affect cellular adhesion and metabolism. If successful, such co-cultures could also be translated to our nanopattern materials, thus providing a more accurate representation of the implant in situ. A further aspect that was not addressed in the present study was surface hydrophobicity. While several studies suggest that hydrophobic surfaces delay adhesion and hydrophilic surfaces promote attachment (Quirynen, Van Der Mei et al. 1994, Tang, Cao et al. 2009, Loo, Young et al. 2012), opposing studies also exist (Sousa, Teixeira et al. 2009). While the cicada wing (on which our NC and NG surfaces are based) has an antibacterial effect that is not influenced by hydrophobicity (Ivanova, Hasan et al. 2012), our polystyrene nanopits and Ti NW surfaces would benefit from future hydrophobicity studies. A further limitation of our study was the isolated use of staphylococcus species, and later solely S. *aureus* Newman strain. Although the results in this thesis are compelling for this strain, the effects of such nanotopographies on other bacterial strains may be entirely different. With thousands of bacterial pathogens in existence, future investigation combining techniques developed in this study and different bacterial species would be interesting and warranted.

The use of metabolomic labelling analysis in bacteria has highlighted some important metabolites and pathways used in the adhesion of S. *aureus* to different surfaces. Though interesting in its own right, metabolic pathway identification also opens the door to targeted therapeutic treatments. Two such agents were subsequently analysed in this study based on their ability to inhibit identified adhesion pathways. Although these agents both reduced biofilm production, dose dependant responses were noted suggesting the inhibition of planktonic bacterial growth with or without biofilm growth inhibition. Further research perhaps analysing the mature biofilms response to such agents may provide more information. In addition, future research may focus on the effects of such agents on other cell lineages, addressing known side effects and exploring the possibility of local coverage of implants, rather than systemic applications. Given the current concerns regarding antimicrobial resistance (Appelbaum 1992, Cohen 1992, Organization 2001, Livermore 2002), the further development of targeted metabolomics may deliver therapeutic agents that can provide antibacterial treatments for medical implants in the future.

5.6 Conclusions

Our study shows that by altering nanotopography, bacterial adhesion and therefore biofilm formation can be affected. Specific nanopatterned surfaces may reduce implant infection associated morbidity and mortality. The identification of metabolic pathways involved in adhesion allows for a targeted approach to biofilm eradication in S. *aureus*. This is of significant benefit to the patient, the surgeon and the NHS, and may well extend far beyond the realms of orthopaedics.

Appendix 1 - C13 Analytical Method and Processing

The column was maintained at 30°C and samples were eluted with a linear gradient (20 mM ammonium carbonate in water (A) and acetonitrile (B) over 26 min at a flow rate of 0.3 ml/min as follows:

Time (minutes)	% water	% acetonitrile
0	20	80
15	80	20
15	95	5
17	95	5
17	20	80
24	20	80

The injection volume was 10 µl and samples were maintained at 4°C prior to injection. For the MS analysis, a Thermo Orbitrap Exactive (Thermo Fisher Scientific) was operated in polarity switching mode and the MS settings were as follows:

- Resolution 50,000
- AGC 106
- m/z range 70–1400
- Sheath gas 40
- Auxiliary gas 5
- Sweep gas 1
- Probe temperature 150°C
- Capillary temperature 275°C

For positive mode ionisation: source voltage +4.5 kV, capillary voltage +50 V, tube voltage +70 kV, skimmer voltage +20 V.
For negative mode ionisation: source voltage-3.5 kV, capillary voltage-50 V, tube voltage-70 V, skimmer voltage-20 V.

Mass calibration was performed for each polarity immediately prior to each analysis batch. The calibration mass range was extended to cover small metabolites by inclusion of low-mass contaminants with the standard Thermo calmix masses (below m/z 1400), C2H6NO2 for positive ion electrospray ionisation (PIESI) mode (m/z 76.0393) and C3H5O3 for negative ion electospray ionisation (NIESI) mode (m/z 89.0244). To enhance calibration stability, lock-mass correction was also applied to each analytical run using these ubiquitous low-mass contaminants.

Thermo Scientific .raw LC-MS flies were converted to mzXML format using proteowizard (Kessner, Chambers et al. 2008). The resultant mzXML files were processed using XCMS to pick peaks (Tautenhahn, Böttcher et al. 2008) with mzMatch to filter, match and annotate the peaks. mzMatch-ISO was used to select and group labelled peaks for statistical analysis (Chokkathukalam, Jankevics et al. 2013).

List of references

Abdulkarim, A., P. Ellanti, N. Motterlini, T. Fahey and J. M. O'Byrne (2013). "Cemented versus uncemented fixation in total hip replacement: a systematic review and meta-analysis of randomized controlled trials." Orthopedic reviews **5**(1).

Ahnfelt, L., P. Herberts, H. Malchau and G. Andersson (1990). "Prognosis of total hip replacement: a Swedish multicenter study of 4,664 revisions." Acta Orthopaedica **61**(S238): 2-26.

Ainscow, D. and R. Denham (1984). "The risk of haematogenous infection in total joint replacements." Journal of Bone & Joint Surgery, British Volume **66**(4): 580-582.

Alarcon, B., B. Vicedo and R. Aznar (2006). "PCR-based procedures for detection and quantification of *Staphylococcus aureus* and their application in food." Journal of applied microbiology **100**(2): 352-364.

Albrektsson, T., P.-I. Brånemark, H.-A. Hansson and J. Lindström (1981). "Osseointegrated titanium implants: requirements for ensuring a long-lasting, direct bone-to-implant anchorage in man." Acta Orthopaedica **52**(2): 155-170.

Albrektsson, T., A. Eriksson, B. Friberg, U. Lekholm, L. Lindahl, M. Nevins, V. Oikarinen, J. Roos, L. Sennerby and P. Astrand (1993). "Histologic investigations on 33 retrieved Nobelpharma implants." Clinical materials **12**(1): 1-9.

Albrektsson, T. and C. Johansson (2001). "Osteoinduction, osteoconduction and osseointegration." European Spine Journal **10**(2): S96-S101.

Allan, I., H. Newman and M. Wilson (2001). "Antibacterial activity of particulate Bioglass® against supra-and subgingival bacteria." Biomaterials **22**(12): 1683-1687.

Allison, A. and E. Eugui (1996). "Purine metabolism and immunosuppressive effects of mycophenolate mofetil (MMF)." Clinical transplantation **10**(1 Pt 2): 77-84.

Alt, V., A. Bitschnau, J. Osterling, A. Sewing, C. Meyer, R. Kraus, S. A. Meissner, S. Wenisch, E. Domann and R. Schnettler (2006). "The effects of combined gentamicin-hydroxyapatite coating for cementless joint prostheses on the reduction of infection rates in a rabbit infection prophylaxis model." Biomaterials **27**(26): 4627-4634.

Àlvarez, G., M. González, S. Isabal, V. Blanc and R. León (2013). "Method to quantify live and dead cells in multi-species oral biofilm by real-time PCR with propidium monoazide." AMB Express **3**(1): 1-8.

An, Y. H., R. B. Dickinson and R. J. Doyle (2000). Mechanisms of bacterial adhesion and pathogenesis of implant and tissue infections. Handbook of Bacterial Adhesion, Springer**:** 1-27.

Antoci, V., Jr., C. S. Adams, N. J. Hickok, I. M. Shapiro and J. Parvizi (2007). "Antibiotics for local delivery systems cause skeletal cell toxicity in vitro." Clin Orthop Relat Res **462**: 200-206.

Antti-Poika, I., G. Josefsson, Y. Konttinen, L. Lidgren, S. Santavirta and L. Sanzén (1990). "Hip arthroplasty infection: current concepts." Acta Orthopaedica **61**(2): 163-169.

Appelbaum, P. C. (1992). "Antimicrobial resistance in *Streptococcus pneumoniae*: an overview." Clinical Infectious Diseases **15**(1): 77-83.

Arko, R., J. Rasheed, C. Broome, F. Chandler and A. Paris (1984). "A rabbit model of toxic shock syndrome: clinicopathological features." Journal of Infection **8**(3): 205-211.

Arnoldi, M., M. Fritz, E. Bäuerlein, M. Radmacher, E. Sackmann and A. Boulbitch (2000). "Bacterial turgor pressure can be measured by atomic force microscopy." Physical Review E **62**(1): 1034.

Atanassova, V., A. Meindl and C. Ring (2001). "Prevalence of *Staphylococcus aureus* and staphylococcal enterotoxins in raw pork and uncooked smoked ham—a comparison of classical culturing detection and RFLP-PCR." International Journal of Food Microbiology **68**(1): 105-113.

Athanasou, N., R. Pandey, R. De Steiger, D. Crook and P. Smith (1995). "Diagnosis of infection by frozen section during revision arthroplasty." Journal of Bone & Joint Surgery, British Volume **77**(1): 28-33.

Atkins, B. L., N. Athanasou, J. J. Deeks, D. W. Crook, H. Simpson, T. E. Peto, P. McLardy-Smith, A. R. Berendt and O. C. S. Group (1998). "Prospective evaluation of criteria for microbiological diagnosis of prosthetic-joint infection at revision arthroplasty." Journal of clinical microbiology **36**(10): 2932-2939.

Auernheimer, J., D. Zukowski, C. Dahmen, M. Kantlehner, A. Enderle, S. L. Goodman and H. Kessler (2005). "Titanium implant materials with improved biocompatibility through coating with phosphonate-anchored cyclic RGD peptides." Chembiochem **6**(11): 2034-2040.

Baba, T., T. Bae, O. Schneewind, F. Takeuchi and K. Hiramatsu (2008). "Genome sequence of *Staphylococcus aureus* strain Newman and comparative analysis of staphylococcal genomes: polymorphism and evolution of two major pathogenicity islands." Journal of bacteriology **190**(1): 300-310.

Babb, J., P. Lynam and G. Ayliffe (1995). "Risk of airborne transmission in an operating theatre containing four ultraclean air units." Journal of Hospital Infection **31**(3): 159-168.

Bales, J. R., J. D. Bell, J. K. Nicholson, P. J. Sadler, J. Timbrell, R. D. Hughes, P. Bennett and R. Williams (1988). "Metabolic profiling of body fluids by proton

NMR: Self-poisoning episodes with paracetamol (acetaminophen)." Magnetic resonance in medicine **6**(3): 300-306.

Barbu, E. M., C. Mackenzie, T. J. Foster and M. Höök (2014). "SdrC induces staphylococcal biofilm formation through a homophilic interaction." Molecular microbiology **94**(1): 172-185.

Baty, A. M., C. C. Eastburn, S. Techkarnjanaruk, A. E. Goodman and G. G. Geesey (2000). "Spatial and temporal variations in chitinolytic gene expression and bacterial biomass production during chitin degradation." Applied and environmental microbiology **66**(8): 3574-3585.

Belt, H. v. d., D. Neut, W. Schenk, J. R. v. Horn, H. C. v. d. Mei and H. J. Busscher (2001). "Infection of orthopedic implants and the use of antibiotic-loaded bone cements: a review." Acta Orthopaedica **72**(6): 557-571.

Bender, J. and W. Hughes (1980). "Fatal *Staphylococcus epidermidis* sepsis following bone marrow transplantation." The Johns Hopkins Medical Journal **146**(1): 13-15.

Bergamini, T. M., D. F. Bandyk, D. Govostis, R. Vetsch and J. B. Towne (1989). "Identification of *Staphylococcus epidermidis* vascular graft infections: A comparison of culture techniques." Journal of vascular surgery **9**(5): 665-670.

Bernheimer, A. W. and R. F. Bey (1986). "Copurification of Leptospira interrogans serovar pomona hemolysin and sphingomyelinase C." Infection and immunity **54**(1): 262-264.

Beuster, G., K. Zarse, C. Kaleta, R. Thierbach, M. Kiehntopf, P. Steinberg, S. Schuster and M. Ristow (2011). "Inhibition of alanine aminotransferase in silico and in vivo promotes mitochondrial metabolism to impair malignant growth." Journal of Biological Chemistry **286**(25): 22323-22330.

Bhakdi, S., H. Bayley, A. Valeva, I. Walev, B. Walker, U. Weller, M. Kehoe and M. Palmer (1996). "Staphylococcal alpha-toxin, streptolysin-O, and *Escherichia coli* hemolysin: prototypes of pore-forming bacterial cytolysins." Archives of microbiology **165**(2): 73-79.

Biggs, M. J. P., R. G. Richards and M. J. Dalby (2010). "Nanotopographical modification: a regulator of cellular function through focal adhesions." Nanomedicine: Nanotechnology, Biology and Medicine **6**(5): 619-633.

Biosystems, A. (2010) "Applied Biosystems StepOne™ and StepOnePlus™ Real-Time PCR Systems - Reagent guide."

Birkemeyer, C., A. Luedemann, C. Wagner, A. Erban and J. Kopka (2005). "Metabolome analysis: the potential of in vivo labeling with stable isotopes for metabolite profiling." Trends in biotechnology **23**(1): 28-33.

Bjarnsholt, T. (2013). "The role of bacterial biofilms in chronic infections." APMIS **121**(s136): 1-58.

Blouse, L., G. Lathrop, L. Kolonel and R. Brockett (1978). "Epidemiologic features and phage types associated with nosocomial infections caused by

Staphylococcus epidermidis." Zentralblatt fur Bakteriologie, Parasitenkunde, Infektionskrankheiten und Hygiene. Erste Abteilung Originale. Reihe A: Medizinische Mikrobiologie und Parasitologie **241**(1): 119-135.

Boettcher, W. G. (1992). "Total hip arthroplasties in the elderly: morbidity, mortality, and cost effectiveness." Clinical orthopaedics and related research **274**: 30-34.

Bos, R., H. C. van der Mei and H. J. Busscher (1999). "Physico-chemistry of initial microbial adhesive interactions--its mechanisms and methods for study." FEMS Microbiol Rev **23**(2): 179-230.

Boulos, L., M. Prevost, B. Barbeau, J. Coallier and R. Desjardins (1999). "LIVE/DEAD< sup>®</sup>< i> Bac</i> Light™: application of a new rapid staining method for direct enumeration of viable and total bacteria in drinking water." Journal of Microbiological Methods **37**(1): 77-86.

Bowersox, J. (1999). "Experimental staph vaccine broadly protective in animal studies." NIH **27**: 55-58.

Branemark, P. I., B. O. Hansson, R. Adell, U. Breine, J. Lindstrom, O. Hallen and A. Ohman (1977). "Osseointegrated implants in the treatment of the edentulous jaw. Experience from a 10-year period." Scand J Plast Reconstr Surg Suppl **16**: 1-132.

Busscher, H., M. Cowan and H. Van der Mei (1992). "On the relative importance of specific and non-specific approaches to oral microbial adhesion." FEMS microbiology reviews **8**(3-4): 199-209.

Buttaro, M., R. Pusso and F. Piccaluga (2005). "Vancomycin-supplemented impacted bone allografts in infected hip arthroplasty TWO-STAGE REVISION RESULTS." Journal of Bone & Joint Surgery, British Volume **87**(3): 314-319.

Callaghan, J. J., R. P. Katz and R. C. Johnston (1999). "One-stage revision surgery of the infected hip: a minimum 10-year followup study." Clinical orthopaedics and related research **369**: 139-143.

Campoccia, D., L. Montanaro and C. R. Arciola (2006). "The significance of infection related to orthopedic devices and issues of antibiotic resistance." Biomaterials **27**(11): 2331-2339.

Card, G. L., R. R. Jasuja and G. L. Gustafson (1994). "Activation of arachidonic acid metabolism in mouse macrophages by bacterial amphiphiles." Journal of leukocyte biology **56**(6): 723-728.

Carpenter, A. E., T. R. Jones, M. R. Lamprecht, C. Clarke, I. H. Kang, O. Friman, D. A. Guertin, J. H. Chang, R. A. Lindquist and J. Moffat (2006). "CellProfiler: image analysis software for identifying and quantifying cell phenotypes." Genome biology **7**(10): R100.

Carpentier, B. and O. Cerf (1993). "Biofilms and their consequences, with particular reference to hygiene in the food industry." Journal of Applied Bacteriology **75**(6): 499-511.

Cash, D. and V. Khanduja (2014). "The case for ceramic-on-polyethylene as the preferred bearing for a young adult hip replacement." Hip International **24**(5 (September-October 2014)): 421-427.

Chan, F. W., J. D. Bobyn, J. B. Medley, J. J. Krygier and M. Tanzer (1999). "Wear and lubrication of metal-on-metal hip implants." Clinical orthopaedics and related research **369**: 10-24.

Charnley, J. (1960). "ANCHORAGE OF THE FEMORAL HEAD PROSTHESIS."

Cheung, A. L., J. M. Koomey, C. A. Butler, S. J. Projan and V. A. Fischetti (1992). "Regulation of exoprotein expression in *Staphylococcus aureus* by a locus (sar) distinct from agr." Proceedings of the National Academy of Sciences **89**(14): 6462-6466.

Choi, S. and W. L. Murphy (2010). "Sustained plasmid DNA release from dissolving mineral coatings." Acta Biomater **6**(9): 3426-3435.

Chokkathukalam, A., A. Jankevics, D. J. Creek, F. Achcar, M. P. Barrett and R. Breitling (2013). "mzMatch–ISO: an R tool for the annotation and relative quantification of isotope-labelled mass spectrometry data." Bioinformatics **29**(2): 281-283.

Chow, T. and X. Yang (2004). "Ventilation performance in operating theatres against airborne infection: review of research activities and practical guidance." Journal of Hospital Infection **56**(2): 85-92.

Christensen, G. D., W. Simpson, J. Younger, L. Baddour, F. Barrett, D. Melton and E. Beachey (1985). "Adherence of coagulase-negative staphylococci to plastic tissue culture plates: a quantitative model for the adherence of staphylococci to medical devices." Journal of clinical microbiology **22**(6): 996-1006.

Christensen, G. D., W. A. Simpson, A. L. Bisno and E. H. Beachey (1982). "Adherence of slime-producing strains of *Staphylococcus epidermidis* to smooth surfaces." Infection and Immunity **37**(1): 318-326.

Chung, K. K., J. F. Schumacher, E. M. Sampson, R. A. Burne, P. J. Antonelli and A. B. Brennan (2007). "Impact of engineered surface microtopography on biofilm formation of *Staphylococcus aureus*." Biointerphases **2**(2): 89-94.

Coelho, M., A. T. Cabral and M. Fernandes (2000). "Human bone cell cultures in biocompatibility testing. Part I: osteoblastic differentiation of serially passaged human bone marrow cells cultured in α-MEM and in DMEM." Biomaterials **21**(11): 1087-1094.

Cohen, M. L. (1992). "Epidemiology of drug resistance: implications for a post—antimicrobial era." Science **257**(5073): 1050-1055.

Colin, D., I. Mazurier, S. Sire and V. Finck-Barbancon (1994). "Interaction of the two components of leukocidin from *Staphylococcus aureus* with human polymorphonuclear leukocyte membranes: sequential binding and subsequent activation." Infection and immunity **62**(8): 3184-3188.

Cornell, N., P. Zuurendonk, M. Kerich and C. Straight (1984). "Selective inhibition of alanine aminotransferase and aspartate aminotransferase in rat hepatocytes." Biochem. J **220**: 707-716.

Costerton, J., P. S. Stewart and E. Greenberg (1999). "Bacterial biofilms: a common cause of persistent infections." Science **284**(5418): 1318-1322.

Costerton, J. W., K. Cheng, G. G. Geesey, T. I. Ladd, J. C. Nickel, M. Dasgupta and T. J. Marrie (1987). "Bacterial biofilms in nature and disease." Annual Reviews in Microbiology **41**(1): 435-464.

Cotter, D., A. Maer, C. Guda, B. Saunders and S. Subramaniam (2006). "Lmpd: Lipid Maps Proteome Database." Nucleic acids research **34**(suppl 1): D507-D510.

Coventry, M. (1975). "Treatment of infections occurring in total hip surgery." The Orthopedic clinics of North America **6**(4): 991-1003.

Curtiss, R., L. J. Charamella, C. M. Berg and P. E. Harris (1965). "Kinetic and genetic analyses of D-cycloserine inhibition and resistance in *Escherichia coli*." Journal of bacteriology **90**(5): 1238-1250.

Dalby, B., S. Cates, A. Harris, E. C. Ohki, M. L. Tilkins, P. J. Price and V. C. Ciccarone (2004). "Advanced transfection with Lipofectamine 2000 reagent: primary neurons, siRNA, and high-throughput applications." Methods **33**(2): 95-103.

Dalby, M. J., A. Andar, A. Nag, S. Affrossman, R. Tare, S. McFarlane and R. O. Oreffo (2008). "Genomic expression of mesenchymal stem cells to altered nanoscale topographies." Journal of The Royal Society Interface **5**(26): 1055-1065.

Dalby, M. J., N. Gadegaard, R. Tare, A. Andar, M. O. Riehle, P. Herzyk, C. D. Wilkinson and R. O. Oreffo (2007). "The control of human mesenchymal cell differentiation using nanoscale symmetry and disorder." Nature materials **6**(12): 997-1003.

Dalby, M. J., D. McCloy, M. Robertson, H. Agheli, D. Sutherland, S. Affrossman and R. O. Oreffo (2006). "Osteoprogenitor response to semi-ordered and random nanotopographies." Biomaterials **27**(15): 2980-2987.

Dang, L., D. W. White, S. Gross, B. D. Bennett, M. A. Bittinger, E. M. Driggers, V. R. Fantin, H. G. Jang, S. Jin and M. C. Keenan (2009). "Cancer-associated IDH1 mutations produce 2-hydroxyglutarate." Nature **462**(7274): 739-744.

Davies, D. and G. Geesey (1995). "Regulation of the alginate biosynthesis gene algC in Pseudomonas aeruginosa during biofilm development in continuous culture." Applied and environmental microbiology **61**(3): 860-867.

Davis, C. C., M. J. Kremer, P. M. Schlievert and C. A. Squier (2003). "Penetration of toxic shock syndrome toxin-1 across porcine vaginal mucosa ex vivo: permeability characteristics, toxin distribution, and tissue damage." American journal of obstetrics and gynecology **189**(6): 1785-1791.

Davis, J. P., P. J. Chesney, P. J. Wand and M. LaVenture (1980). "Toxic-shock syndrome: epidemiologic features, recurrence, risk factors, and prevention." New England Journal of Medicine **303**(25): 1429-1435.

Davis, N., A. Curry, A. Gambhir, H. Panigrahi, C. Walker, E. Wilkins, M. Worsley and P. Kay (1999). "Intraoperative bacterial contamination in operations for joint replacement." Journal of Bone & Joint Surgery, British Volume **81**(5): 886-889.

De Beer, D., P. Stoodley, F. Roe and Z. Lewandowski (1994). "Effects of biofilm structures on oxygen distribution and mass transport." Biotechnology and bioengineering **43**(11): 1131-1138.

de Groot, K., R. Geesink, C. P. Klein and P. Serekian (1987). "Plasma sprayed coatings of hydroxylapatite." J Biomed Mater Res **21**(12): 1375-1381.

de Oliveira, P. T., S. F. Zalzal, M. M. Beloti, A. L. Rosa and A. Nanci (2007). "Enhancement of in vitro osteogenesis on titanium by chemically produced nanotopography." Journal of biomedical materials research Part A **80**(3): 554-564.

Del Curto, B., M. F. Brunella, C. Giordano, M. P. Pedeferri, V. Valtulina, L. Visai and A. Cigada (2005). "Decreased bacterial adhesion to surface-treated titanium." Int J Artif Organs **28**(7): 718-730.

Deora, R., T. Tseng and T. K. Misra (1997). "Alternative transcription factor sigmaSB of *Staphylococcus aureus*: characterization and role in transcription of the global regulatory locus sar." Journal of bacteriology **179**(20): 6355-6359.

Dettmer, K., P. A. Aronov and B. D. Hammock (2007). "Mass spectrometry-based metabolomics." Mass spectrometry reviews **26**(1): 51-78.

Díaz, C., P. Schilardi, D. Mele and M. F. Lorenzo (2008). "Influence of Surface Sub-micropattern on the Adhesion of Pioneer Bacteria on Metals." Artificial organs **32**(4): 292-298.

Dinges, M. M., P. M. Orwin and P. M. Schlievert (2000). "Exotoxins of *Staphylococcus aureus*." Clinical microbiology reviews **13**(1): 16-34.

Donelli, G., I. Francolini, D. Romoli, E. Guaglianone, A. Piozzi, C. Ragunath and J. Kaplan (2007). "Synergistic activity of dispersin B and cefamandole nafate in inhibition of staphylococcal biofilm growth on polyurethanes." Antimicrobial agents and chemotherapy **51**(8): 2733-2740.

Dong, Y.-H. and L.-H. Zhang (2005). "Quorum sensing and quorum-quenching enzymes." J. Microbiol **43**(5): 101-109.

Dongari-Bagtzoglou, A. (2008). "Pathogenesis of mucosal biofilm infections: challenges and progress." Expert review of anti-infective therapy **6**(2): 201-208.

Donlan, R. M. (2002). "Biofilms: microbial life on surfaces." Emerg Infect Dis **8**(9).

Donlan, R. M. and J. W. Costerton (2002). "Biofilms: survival mechanisms of clinically relevant microorganisms." Clin Microbiol Rev **15**(2): 167-193.

Dudley, E., M. Yousef, Y. Wang and W. Griffiths (2010). "Targeted metabolomics and mass spectrometry." Adv Protein Chem Struct Biol **80**: 45-83.

Dumitru, I. F., D. Iordachescu and S. Niculescu (1970). "Chromatographic purification, crystallization and study of vegetable L-alanine: 2-oxoglutarate-aminotransferase properties." Experientia **26**(8): 837-838.

Dunn, W. B., N. J. C. Bailey and H. E. Johnson (2005). "Measuring the metabolome: current analytical technologies." Analyst **130**(5): 606-625.

Dunne, W. M. (2002). "Bacterial adhesion: seen any good biofilms lately?" Clinical microbiology reviews **15**(2): 155-166.

Dupont, J. A. (1986). "Significance of operative cultures in total hip arthroplasty." Clinical orthopaedics and related research **211**: 122-127.

Duthie, E. and L. L. Lorenz (1952). "Staphylococcal coagulase: mode of action and antigenicity." Journal of general microbiology **6**(1-2): 95-107.

Edwards, K. J., P. L. Bond, T. M. Gihring and J. F. Banfield (2000). "An archaeal iron-oxidizing extreme acidophile important in acid mine drainage." Science **287**(5459): 1796-1799.

Eisenreich, W. and A. Bacher (2007). "Advances of high-resolution NMR techniques in the structural and metabolic analysis of plant biochemistry." Phytochemistry **68**(22): 2799-2815.

Engesaeter, L. B., S. A. Lie, B. Espehaug, O. Furnes, S. E. Vollset and L. I. Havelin (2003). "Antibiotic prophylaxis in total hip arthroplasty: effects of antibiotic prophylaxis systemically and in bone cement on the revision rate of 22,170 primary hip replacements followed 0-14 years in the Norwegian Arthroplasty Register." Acta Orthop Scand **74**(6): 644-651.

Epicentre (2014) "Ready-Lyse™ Lysozyme Solution."

Erlandsen, S. L., C. J. Kristich, G. M. Dunny and C. L. Wells (2004). "High-resolution visualization of the microbial glycocalyx with low-voltage scanning electron microscopy: dependence on cationic dyes." Journal of Histochemistry & Cytochemistry **52**(11): 1427-1435.

Eskelinen, A., V. Remes, I. Helenius, P. Pulkkinen, J. Nevalainen and P. Paavolainen (2006). "Uncemented total hip arthroplasty for primary osteoarthritis in young patients: a mid-to long-term follow-up study from the Finnish Arthroplasty Register." Acta orthopaedica **77**(1): 57-70.

Fischer, E. and U. Sauer (2003). "Metabolic flux profiling of Escherichia coli mutants in central carbon metabolism using GC-MS." European Journal of Biochemistry **270**(5): 880-891.

Fletcher, M. (1976). "The effects of proteins on bacterial attachment to polystyrene." Journal of general microbiology **94**(2): 400-404.

Fletcher, M. (1996). "Bacterial attachment in aquatic environments: a diversity of surfaces and adhesion strategies." Bacterial adhesion: molecular and ecological diversity: 1-24.

Fletcher, M. and G. Loeb (1979). "Influence of substratum characteristics on the attachment of a marine pseudomonad to solid surfaces." Applied and Environmental Microbiology **37**(1): 67-72.

Foster, C. S., L. P. Fong and G. Singh (1989). "Cataract Surgery and Intraocular Lens Implantation in Patients with Uveitis." Ophthalmology **96**(3): 281-288.

Fred, E. B. and S. A. Waksman (1928). "Laboratory manual of general microbiology-with special reference to the microorganisms of the soil."

Freer, J. and J. Arbuthnoti (1982). "Toxins of *Staphylococcus aureus*." Pharmacology & therapeutics **19**(1): 55-106.

Fuchs, S., T. Haritopoulou and M. Wilhelmi (1996). "Biofilms in freshwater ecosystems and their use as a pollutant monitor." Water Science and Technology **34**(7): 137-140.

Fux, C. A., P. Stoodley, L. Hall-Stoodley and J. W. Costerton (2003). "Bacterial biofilms: a diagnostic and therapeutic challenge."

Gallardo-Moreno, A. M., M. A. Pacha-Olivenza, L. Saldana, C. Perez-Giraldo, J. M. Bruque, N. Vilaboa and M. L. Gonzalez-Martin (2009). "In vitro biocompatibility and bacterial adhesion of physico-chemically modified Ti6Al4V surface by means of UV irradiation." Acta Biomater **5**(1): 181-192.

Garvin, K. L., S. H. Hinrichs and J. A. Urban (1999). "Emerging antibiotic-resistant bacteria: their treatment in total joint arthroplasty." Clinical orthopaedics and related research **369**: 110-123.

Gates, S. C. and C. C. Sweeley (1978). "Quantitative metabolic profiling based on gas chromatography." Clinical chemistry **24**(10): 1663-1673.

Geesink, R. G., K. de Groot and C. P. Klein (1987). "Chemical implant fixation using hydroxyl-apatite coatings. The development of a human total hip prosthesis for chemical fixation to bone using hydroxyl-apatite coatings on titanium substrates." Clin Orthop Relat Res(225): 147-170.

George I, L. and N. Rex A (1975). Marine Conditioning Films. Applied Chemistry at Protein Interfaces, AMERICAN CHEMICAL SOCIETY. **145:** 319-335.

Giavalisco, P., J. Hummel, J. Lisec, A. C. Inostroza, G. Catchpole and L. Willmitzer (2008). "High-resolution direct infusion-based mass spectrometry in combination with whole 13C metabolome isotope labeling allows unambiguous assignment of chemical sum formulas." Analytical chemistry **80**(24): 9417-9425.

Gibson, U., C. A. Heid and P. M. Williams (1996). "A novel method for real time quantitative RT-PCR." Genome research **6**(10): 995-1001.

Gill, S. R., D. E. Fouts, G. L. Archer, E. F. Mongodin, R. T. DeBoy, J. Ravel, I. T. Paulsen, J. F. Kolonay, L. Brinkac and M. Beanan (2005). "Insights on evolution of virulence and resistance from the complete genome analysis of an early methicillin-resistant *Staphylococcus aureus* strain and a biofilm-producing methicillin-resistant *Staphylococcus epidermidis* strain." Journal of bacteriology **187**(7): 2426-2438.

Glinski, M. and W. Weckwerth (2006). "The role of mass spectrometry in plant systems biology." Mass spectrometry reviews **25**(2): 173-214.

Goldman, E. and L. H. Green (2008). Practical handbook of microbiology, CRC Press.

Gomez, P. F. and J. A. Morcuende (2005). "A Historical and Economic Perspective on Sir John Charnley, Chas F. Thackray Limited, and the Early Arthroplasty Industry." The Iowa orthopaedic journal **25**: 30.

Goodacre, R., S. Vaidyanathan, W. B. Dunn, G. G. Harrigan and D. B. Kell (2004). "Metabolomics by numbers: acquiring and understanding global metabolite data." Trends in biotechnology **22**(5): 245-252.

Goodman, S. B., Z. Yao, M. Keeney and F. Yang (2013). "The Future of Biologic Coatings for Orthopaedic Implants." Biomaterials **34**(13): 3174-3183.

Górecki, A. and I. Babiak (2009). Infection of joint prosthesis and local drug delivery. The infected implant, Springer**:** 19-26.

Gorth, D. J., S. Puckett, B. Ercan, T. J. Webster, M. Rahaman and B. S. Bal (2012). "Decreased bacteria activity on Si3N4 surfaces compared with PEEK or titanium." International journal of nanomedicine **7**: 4829.

Gottschalk, G. (1986). Bacterial metabolism, Springer Science & Business Media.

Gristina, A. G., C. D. Hobgood, L. X. Webb and Q. N. Myrvik (1987). "Adhesive colonization of biomaterials and antibiotic resistance." Biomaterials **8**(6): 423-426.

Haggarty, J., M. Oppermann, M. J. Dalby, R. J. Burchmore, K. Cook, S. Weidt and K. E. Burgess (2015). "Serially coupling hydrophilic interaction and reversed-phase chromatography with simultaneous gradients provides greater coverage of the metabolome." Metabolomics: 1-6.

Hailer, N. P., G. Garellick and J. Kärrholm (2010). "Uncemented and cemented primary total hip arthroplasty in the Swedish Hip Arthroplasty Register: evaluation of 170,413 operations." Acta orthopaedica **81**(1): 34-41.

Hall-Stoodley, L., J. W. Costerton and P. Stoodley (2004). "Bacterial biofilms: from the natural environment to infectious diseases." Nature Reviews Microbiology **2**(2): 95-108.

Hammond, D. J. and W. E. Gutteridge (1984). "Purine and pyrimidine metabolism in the Trypanosomatidae." Molecular and biochemical parasitology **13**(3): 243-261.

Hammond, G. and H. Stiver (1978). "Combination antibiotic therapy in an outbreak of prosthetic endocarditis caused by *Staphylococcus epidermidis*." Canadian Medical Association Journal **118**(5): 524.

Harris, L. G., S. Tosatti, M. Wieland, M. Textor and R. G. Richards (2004). "*Staphylococcus aureus* adhesion to titanium oxide surfaces coated with non-functionalized and peptide-functionalized poly(l-lysine)-grafted-poly(ethylene glycol) copolymers." Biomaterials **25**(18): 4135-4148.

Hart, A., N. Gadegaard, C. D. Wilkinson, R. O. Oreffo and M. J. Dalby (2007). "Osteoprogenitor response to low-adhesion nanotopographies originally fabricated by electron beam lithography." Journal of Materials Science: Materials in Medicine **18**(6): 1211-1218.

Hay, I. D., K. Gatland, A. Campisano, J. Z. Jordens and B. H. Rehm (2009). "Impact of alginate overproduction on attachment and biofilm architecture of a supermucoid *Pseudomonas aeruginosa* strain." Applied and environmental microbiology **75**(18): 6022-6025.

He, J., T. Huang, L. Gan, Z. Zhou, B. Jiang, Y. Wu, F. Wu and Z. Gu (2012). "Collagen-infiltrated porous hydroxyapatite coating and its osteogenic properties: in vitro and in vivo study." J Biomed Mater Res A **100**(7): 1706-1715.

Heid, C. A., J. Stevens, K. J. Livak and P. M. Williams (1996). "Real time quantitative PCR." Genome research **6**(10): 986-994.

Heilmann, C., C. Gerke, F. Perdreau-Remington and F. Götz (1996). "Characterization of Tn917 insertion mutants of *Staphylococcus epidermidis* affected in biofilm formation." Infection and Immunity **64**(1): 277-282.

Heilmann, C. and F. Götz (1998). "Further characterization of Staphylococcus epidermidis transposon mutants deficient in primary attachment or intercellular adhesion." Zentralblatt für Bakteriologie **287**(1): 69-83.

Heilmann, C., O. Schweitzer, C. Gerke, N. Vanittanakom, D. Mack and F. Götz (1996). "Molecular basis of intercellular adhesion in the biofilm-forming Staphylococcus epidermidis." Molecular microbiology **20**(5): 1083-1091.

Hernigou, P., C.-H. Flouzat-Lachianette, R. Jalil, S. U. Batista, I. Guissou and A. Poignard (2010). "Treatment of infected hip arthroplasty." The open orthopaedics journal **4**: 126.

Herrmann, M., P. E. Vaudaux, D. Pittet, R. Auckenthaler, P. D. Lew, F. S. Perdreau, G. Peters and F. A. Waldvogel (1988). "Fibronectin, fibrinogen, and laminin act as mediators of adherence of clinical staphylococcal isolates to foreign material." Journal of Infectious Diseases **158**(4): 693-701.

Hettick, J. M., B. J. Green, A. D. Buskirk, M. L. Kashon, J. E. Slaven, E. Janotka, F. M. Blachere, D. Schmechel and D. H. Beezhold (2008). "Discrimination of Aspergillus isolates at the species and strain level by matrix-assisted laser desorption/ionization time-of-flight mass spectrometry fingerprinting." Analytical biochemistry **380**(2): 276-281.

Heukelekian, H. and A. Heller (1940). "Relation between food concentration and surface for bacterial growth." Journal of bacteriology **40**(4): 547.

Higuchi, R., C. Fockler, G. Dollinger and R. Watson (1993). "Kinetic PCR analysis: real-time monitoring of DNA amplification reactions." Biotechnology **11**: 1026-1030.

Hoeffel, D. P., S. H. Hinrichs and K. L. Garvin (1999). "Molecular diagnostics for the detection of musculoskeletal infection." Clinical orthopaedics and related research **360**: 37-46.

Høiby, N., T. Bjarnsholt, M. Givskov, S. Molin and O. Ciofu (2010). "Antibiotic resistance of bacterial biofilms." International journal of antimicrobial agents **35**(4): 322-332.

Høiby, N., T. Bjarnsholt, C. Moser, G. Bassi, T. Coenye, G. Donelli, L. Hall-Stoodley, V. Holá, C. Imbert and K. Kirketerp-Møller (2015). "ESCMID guideline for the diagnosis and treatment of biofilm infections 2014." Clinical Microbiology and Infection **21**: S1-S25.

Hoiby, N., O. Ciofu and T. Bjarnsholt (2010). "*Pseudomonas aeruginosa* biofilms in cystic fibrosis." Future Microbiol **5**(11): 1663-1674.

Honraet, K., E. Goetghebeur and H. J. Nelis (2005). "Comparison of three assays for the quantification of *Candida* biomass in suspension and CDC reactor grown biofilms." Journal of microbiological methods **63**(3): 287-295.

Honraet, K. and H. Nelis (2006). "Use of the modified robbins device and fluorescent staining to screen plant extracts for the inhibition of *S. mutans* biofilm formation." Journal of microbiological methods **64**(2): 217-224.

Hooper, G., A. Rothwell, M. Stringer and C. Frampton (2009). "Revision following cemented and uncemented primary total hip replacement a seven-year analysis from the New Zealand Joint Registry." Journal of Bone & Joint Surgery, British Volume **91**(4): 451-458.

Hussain, M., M. Herrmann, C. von Eiff, F. Perdreau-Remington and G. Peters (1997). "A 140-kilodalton extracellular protein is essential for the accumulation of *Staphylococcus epidermidis* strains on surfaces." Infection and immunity **65**(2): 519-524.

Ivanova, E. P., J. Hasan, H. K. Webb, G. Gervinskas, S. Juodkazis, V. K. Truong, A. H. Wu, R. N. Lamb, V. A. Baulin and G. S. Watson (2013). "Bactericidal activity of black silicon." Nature communications **4**.

Ivanova, E. P., J. Hasan, H. K. Webb, V. K. Truong, G. S. Watson, J. A. Watson, V. A. Baulin, S. Pogodin, J. Y. Wang and M. J. Tobin (2012). "Natural bactericidal surfaces: mechanical rupture of *Pseudomonas aeruginosa* cells by cicada wings." Small **8**(16): 2489-2494.

Ivanova, E. P., V. K. Truong, J. Y. Wang, C. C. Berndt, R. T. Jones, I. I. Yusuf, I. Peake, H. W. Schmidt, C. Fluke and D. Barnes (2009). "Impact of nanoscale roughness of titanium thin film surfaces on bacterial retention." Langmuir **26**(3): 1973-1982.

Jacobson, M. D., M. Weil and M. C. Raff (1997). "Programmed cell death in animal development." Cell **88**(3): 347-354.

Jahoda, D. (2009). Clinical strategy for the treatment of deep infection of hip arthroplasty. The Infected Implant, Springer**:** 27-42.

James, D. W., T. V. Suslow and K. E. Steinback (1985). "Relationship between rapid, firm adhesion and long-term colonization of roots by bacteria." Applied and environmental microbiology **50**(2): 392-397.

Jellum, E. (1977). "Profiling of human body fluids in healthy and diseased states using gas chromatography and mass spectrometry, with special reference to organic acids." Journal of Chromatography B: Biomedical Sciences and Applications **143**(5): 427-462.

Jett, M., R. Neill, C. Welch, T. Boyle, E. Bernton, D. Hoover, G. Lowell, R. E. Hunt, S. Chatterjee and P. Gemski (1994). "Identification of staphylococcal enterotoxin B sequences important for induction of lymphocyte proliferation by using synthetic peptide fragments of the toxin." Infection and immunity **62**(8): 3408-3415.

Jiang, H. and S. X. Sun (2010). "Morphology, growth, and size limit of bacterial cells." Physical review letters **105**(2): 028101.

Josefsson, G., G. Gudmundsson, L. Kolmert and S. Wijkström (1990). "Prophylaxis with systemic antibiotics versus gentamicin bone cement in total hip arthroplasty: a five-year survey of 1688 hips." Clinical orthopaedics and related research **253**: 173-178.

Jurtshuk, P. (1996). Bacterial Metabolism. Medical Microbiology. S. Baron. Galveston (TX), University of Texas Medical Branch at Galveston. The University of Texas Medical Branch at Galveston.

Kanehisa, M. and S. Goto (2000). "KEGG: kyoto encyclopedia of genes and genomes." Nucleic acids research **28**(1): 27-30.

Kasemo, B. (1998). "Biological surface science." Current Opinion in Solid State and Materials Science **3**(5): 451-459.

Katsikogianni, M. and Y. Missirlis (2004). "Concise review of mechanisms of bacterial adhesion to biomaterials and of techniques used in estimating bacteria-material interactions." Eur Cell Mater **8**(3).

Katti, K. S. (2004). "Biomaterials in total joint replacement." Colloids and Surfaces B: Biointerfaces **39**(3): 133-142.

Keane, W., G. Gekker, P. Schlievert and P. Peterson (1986). "Enhancement of endotoxin-induced isolated renal tubular cell injury by toxic shock syndrome toxin 1." The American journal of pathology **122**(1): 169.

Kessner, D., M. Chambers, R. Burke, D. Agus and P. Mallick (2008). "ProteoWizard: open source software for rapid proteomics tools development." Bioinformatics **24**(21): 2534-2536.

Kluytmans, J., A. Van Belkum and H. Verbrugh (1997). "Nasal carriage of *Staphylococcus aureus*: epidemiology, underlying mechanisms, and associated risks." Clinical microbiology reviews **10**(3): 505-520.

Knight, S. R., R. Aujla and S. P. Biswas (2011). "Total Hip Arthroplasty - over 100 years of operative history." Orthopedic Reviews **3**(2): e16.

Kobayashi, T. and M. Sokabe (2010). "Sensing substrate rigidity by mechanosensitive ion channels with stress fibers and focal adhesions." Current opinion in cell biology **22**(5): 669-676.

Koek, M. M., B. Muilwijk, M. J. van der Werf and T. Hankemeier (2006). "Microbial metabolomics with gas chromatography/mass spectrometry." Analytical chemistry **78**(4): 1272-1281.

Kreder, H. J., G. K. Berry, I. A. McMurtry and S. I. Halman (2005). "Arthroplasty in the octogenarian: quantifying the risks." The Journal of arthroplasty **20**(3): 289-293.

Kubista, M., J. M. Andrade, M. Bengtsson, A. Forootan, J. Jonák, K. Lind, R. Sindelka, R. Sjöback, B. Sjögreen and L. Strömbom (2006). "The real-time polymerase chain reaction." Molecular aspects of medicine **27**(2): 95-125.

Kung, C. (2005). "A possible unifying principle for mechanosensation." Nature **436**(7051): 647-654.

Kuroda, M., T. Ohta, I. Uchiyama, T. Baba, H. Yuzawa, I. Kobayashi, L. Cui, A. Oguchi, K.-i. Aoki and Y. Nagai (2001). "Whole genome sequencing of meticillin-resistant *Staphylococcus aureus*." The Lancet **357**(9264): 1225-1240.

Kurtz, S., K. Ong, E. Lau, F. Mowat and M. Halpern (2007). "Projections of primary and revision hip and knee arthroplasty in the United States from 2005 to 2030." The Journal of Bone & Joint Surgery **89**(4): 780-785.

Kurtz, S. M., O. K. Muratoglu, M. Evans and A. A. Edidin (1999). "Advances in the processing, sterilization, and crosslinking of ultra-high molecular weight polyethylene for total joint arthroplasty." Biomaterials **20**(18): 1659-1688.

Langer, R. and D. A. Tirrell (2004). "Designing materials for biology and medicine." Nature **428**(6982): 487-492.

Larsen, N., F. K. Vogensen, F. W. van den Berg, D. S. Nielsen, A. S. Andreasen, B. K. Pedersen, W. A. Al-Soud, S. J. Sørensen, L. H. Hansen and M. Jakobsen (2010). "Gut microbiota in human adults with type 2 diabetes differs from non-diabetic adults." PloS one **5**(2): e9085.

Learmonth, I. D., C. Young and C. Rorabeck "The operation of the century: total hip replacement." The Lancet **370**(9597): 1508-1519.

Lee, P., J. Deringer, B. Kreiswirth, R. Novick and P. Schlievert (1991). "Fluid replacement protection of rabbits challenged subcutaneous with toxic shock syndrome toxins." Infection and immunity **59**(3): 879-884.

Lidwell, O., E. Lowbury, W. Whyte, R. Blowers, S. Stanley and D. Lowe (1983). "Airborne contamination of wounds in joint replacement operations: the relationship to sepsis rates." Journal of hospital Infection **4**(2): 111-131.

Liu, Y., K. de Groot and E. B. Hunziker (2005). "BMP-2 liberated from biomimetic implant coatings induces and sustains direct ossification in an ectopic rat model." Bone **36**(5): 745-757.

Livermore, D. M. (2002). "Multiple mechanisms of antimicrobial resistance in *Pseudomonas aeruginosa*: our worst nightmare?" Clinical infectious diseases **34**(5): 634-640.

Lloyd, A. W., R. G. Faragher and S. P. Denyer (2001). "Ocular biomaterials and implants." Biomaterials **22**(8): 769-785.

Long, M. and H. Rack (1998). "Titanium alloys in total joint replacement—a materials science perspective." Biomaterials **19**(18): 1621-1639.

Lonner, J. H., P. Desai, P. E. DiCesare, G. Steiner and J. D. Zuckerman (1996). "The Reliability of Analysis of Intraoperative Frozen Sections for Identifying Active Infection during Revision Hip or Knee Arthroplasty*†." The Journal of Bone & Joint Surgery **78**(10): 1553-1558.

Loo, C.-Y., P. M. Young, W.-H. Lee, R. Cavaliere, C. B. Whitchurch and R. Rohanizadeh (2012). "Superhydrophobic, nanotextured polyvinyl chloride films for delaying *Pseudomonas aeruginosa* attachment to intubation tubes and medical plastics." Acta biomaterialia **8**(5): 1881-1890.

Lowy, F. D. (1998). "*Staphylococcus aureus* infections." New England Journal of Medicine **339**(8): 520-532.

Lu, W., B. D. Bennett and J. D. Rabinowitz (2008). "Analytical strategies for LC–MS-based targeted metabolomics." Journal of Chromatography B **871**(2): 236-242.

Lukat, G. S., B. H. Lee, J. M. Mottonen, A. M. Stock and J. Stock (1991). "Roles of the highly conserved aspartate and lysine residues in the response regulator of bacterial chemotaxis." Journal of Biological Chemistry **266**(13): 8348-8354.

Lynch, A. S. and G. T. Robertson (2008). "Bacterial and fungal biofilm infections." Annu. Rev. Med. **59**: 415-428.

Maathuis, P. G., D. Neut, H. J. Busscher, H. C. van der Mei and J. R. van Horn (2005). "Perioperative contamination in primary total hip arthroplasty." Clinical orthopaedics and related research **433**: 136-139.

Macdonald, M. L., R. E. Samuel, N. J. Shah, R. F. Padera, Y. M. Beben and P. T. Hammond (2011). "Tissue integration of growth factor-eluting layer-by-layer polyelectrolyte multilayer coated implants." Biomaterials **32**(5): 1446-1453.

Macfarlane, S. and J. F. Dillon (2007). "Microbial biofilms in the human gastrointestinal tract." J Appl Microbiol **102**(5): 1187-1196.

Mack, D., M. Nedelmann, A. Krokotsch, A. Schwarzkopf, J. Heesemann and R. Laufs (1994). "Characterization of transposon mutants of biofilm-producing Staphylococcus epidermidis impaired in the accumulative phase of biofilm production: genetic identification of a hexosamine-containing polysaccharide intercellular adhesin." Infection and immunity **62**(8): 3244-3253.

Mandel, S. and A. C. Tas (2010). "Brushite (CaHPO 4· 2H 2 O) to octacalcium phosphate (Ca 8 (HPO 4) 2 (PO 4) 4· 5H 2 O) transformation in DMEM solutions at 36.5° C." Materials Science and Engineering: C **30**(2): 245-254.

Manning, J. M., N. E. Merrifield, W. M. Jones and E. C. Gotschlich (1974). "Inhibition of bacterial growth by ß-chloro-D-alanine." Proceedings of the National Academy of Sciences **71**(2): 417-421.

Marchesi, J. R., T. Sato, A. J. Weightman, T. A. Martin, J. C. Fry, S. J. Hiom and W. G. Wade (1998). "Design and evaluation of useful bacterium-specific PCR primers that amplify genes coding for bacterial 16S rRNA." Applied and environmental microbiology **64**(2): 795-799.

Marrie, T. J., J. Nelligan and J. Costerton (1982). "A scanning and transmission electron microscopic study of an infected endocardial pacemaker lead." Circulation **66**(6): 1339-1341.

Mathews, S., R. Bhonde, P. K. Gupta and S. Totey (2011). "A novel tripolymer coating demonstrating the synergistic effect of chitosan, collagen type 1 and hyaluronic acid on osteogenic differentiation of human bone marrow derived mesenchymal stem cells." Biochem Biophys Res Commun **414**(1): 270-276.

May, J., R. Houghton and C. Perret (1964). "The effect of growth at elevated temperatures on some heritable properties of *Staphylococcus aureus*." Journal of general microbiology **37**(2): 157-169.

McKenney, D., J. Hübner, E. Muller, Y. Wang, D. A. Goldmann and G. B. Pier (1998). "The ica locus of *Staphylococcus epidermidis* encodes production of the capsular polysaccharide/adhesin." Infection and immunity **66**(10): 4711-4720.

McKevitt, A., G. Bjornson, C. Mauracher and D. Scheifele (1990). "Amino acid sequence of a deltalike toxin from *Staphylococcus epidermidis*." Infection and immunity **58**(5): 1473-1475.

McMurray, R. J., N. Gadegaard, P. M. Tsimbouri, K. V. Burgess, L. E. McNamara, R. Tare, K. Murawski, E. Kingham, R. O. Oreffo and M. J. Dalby (2011). "Nanoscale surfaces for the long-term maintenance of mesenchymal stem cell phenotype and multipotency." Nature materials **10**(8): 637-644.

Mehlin, C., C. M. Headley and S. J. Klebanoff (1999). "An inflammatory polypeptide complex from *Staphylococcus epidermidis*: isolation and characterization." The Journal of experimental medicine **189**(6): 907-918.

Mercier, C., C. Durrieu, R. Briandet, E. Domakova, J. Tremblay, G. Buist and S. Kulakauskas (2002). "Positive role of peptidoglycan breaks in lactococcal biofilm formation." Molecular microbiology **46**(1): 235-243.

Michal, G. and D. Schomburg (1999). Biochemical pathways: an atlas of biochemistry and molecular biology, Wiley New York.

Moco, S., R. J. Bino, O. Vorst, H. A. Verhoeven, J. de Groot, T. A. van Beek, J. Vervoort and C. R. De Vos (2006). "A liquid chromatography-mass spectrometry-based metabolome database for tomato." Plant Physiology **141**(4): 1205-1218.

Monday, S. R. and G. A. Bohach (1999). "Use of multiplex PCR to detect classical and newly described pyrogenic toxin genes in staphylococcal isolates." Journal of Clinical Microbiology **37**(10): 3411-3414.

Monod, J. (1949). "The growth of bacterial cultures." Annual Reviews in Microbiology **3**(1): 371-394.

Monsen, T., E. Lövgren, M. Widerström and L. Wallinder (2009). "In vitro effect of ultrasound on bacteria and suggested protocol for sonication and diagnosis of prosthetic infections." Journal of clinical microbiology **47**(8): 2496-2501.

Monton, M. R. N. and T. Soga (2007). "Metabolome analysis by capillary electrophoresis–mass spectrometry." Journal of Chromatography A **1168**(1): 237-246.

Moore, K. L., A. M. Agur and A. F. Dalley (2002). Essential clinical anatomy, Lippincott Williams & Wilkins Philadelphia:.

Morphopaedics. (2004). "Total Hip Arthroplasty." 2016, from http://morphopedics.wikidot.com/total-hip-arthroplasty.

Neuhaus, F. C. and J. L. Lynch (1964). "The Enzymatic Synthesis of D-Alanyl-D-alanine. III. On the Inhibition of D-Alanyl-D-alanine Synthetase by the Antibiotic D-Cycloserine*." Biochemistry **3**(4): 471-480.

Neut, D., J. R. van Horn, T. G. van Kooten, H. C. van der Mei and H. J. Busscher (2003). "Detection of biomaterial-associated infections in orthopaedic joint implants." Clinical orthopaedics and related research **413**: 261-268.

Nicholson, J. K., J. C. Lindon and E. Holmes (1999). "'Metabonomics': understanding the metabolic responses of living systems to pathophysiological stimuli via multivariate statistical analysis of biological NMR spectroscopic data." Xenobiotica **29**(11): 1181-1189.

Nickinson, R., T. Board, A. Gambhir, M. Porter and P. Kay (2010). "The microbiology of the infected knee arthroplasty." International orthopaedics **34**(4): 505-510.

Nitsche, M. A., W. Jaussi, D. Liebetanz, N. Lang, F. Tergau and W. Paulus (2004). "Consolidation of human motor cortical neuroplasticity by D-cycloserine." Neuropsychopharmacology: official publication of the American College of Neuropsychopharmacology **29**(8): 1573-1578.

Niwa, T. (1986). "Metabolic profiling with gas chromatography—mass spectrometry and its application to clinical medicine." Journal of Chromatography B: Biomedical Sciences and Applications **379**: 313-345.

NJR (2013) "10th annual report 2013, National joint regisrty for England, Wales and Northern Ireland." National Joint Registry report **2014**.

Nolan, T., R. E. Hands and S. A. Bustin (2006). "Quantification of mRNA using real-time RT-PCR." Nature protocols **1**(3): 1559-1582.

Novick, R. P. and T. W. Muir (1999). "Virulence gene regulation by peptides in staphylococci and other Gram-positive bacteria." Current opinion in microbiology **2**(1): 40-45.

O'Toole, G., H. B. Kaplan and R. Kolter (2000). "Biofilm formation as microbial development." Annual Reviews in Microbiology **54**(1): 49-79.

Oh, S., K. S. Brammer, Y. J. Li, D. Teng, A. J. Engler, S. Chien and S. Jin (2009). "Stem cell fate dictated solely by altered nanotube dimension." Proceedings of the National Academy of Sciences **106**(7): 2130-2135.

Oikawa, T. (2007). Alanine, Aspartate, and Asparagine Metabolism in Microorganisms. Amino Acid Biosynthesis ~ Pathways, Regulation and Metabolic Engineering. V. Wendisch, Springer Berlin Heidelberg. **5:** 273-288.

Oliveira, D. (1992). Physico-chemical aspects of adhesion. Biofilms—Science and Technology, Springer**:** 45-58.

Oliver, S. G., M. K. Winson, D. B. Kell and F. Baganz (1998). "Systematic functional analysis of the yeast genome." Trends in biotechnology **16**(9): 373-378.

Olson, M. E., H. Ceri, D. W. Morck, A. G. Buret and R. R. Read (2002). "Biofilm bacteria: formation and comparative susceptibility to antibiotics." Canadian Journal of Veterinary Research **66**(2): 86.

Organization, World Health (2001). "WHO global strategy for containment of antimicrobial resistance."

Overturf, G. D., M. P. Sherman, D. W. Scheifele and L. C. Wong (1990). "Neonatal necrotizing enterocolitis associated with delta toxin-producing methicillin-resistant *Staphylococcus aureus*." The Pediatric infectious disease journal **9**(2): 88-91.

Pagnano, M. W., L. A. McLamb and R. T. Trousdale (2003). Primary and revision total hip arthroplasty for patients 90 years of age and older. Mayo Clinic Proceedings, Elsevier.

Palmer, T. D., P. H. Schwartz, P. Taupin, B. Kaspar, S. A. Stein and F. H. Gage (2001). "Cell culture: Progenitor cells from human brain after death." Nature **411**(6833): 42-43.

Park, K. D., Y. S. Kim, D. K. Han, Y. H. Kim, E. H. B. Lee, H. Suh and K. S. Choi (1998). "Bacterial adhesion on PEG modified polyurethane surfaces." Biomaterials **19**(7-9): 851-859.

Parkinson, D., T. R. Gray and S. T. Williams (1971). "Methods for study-ing the ecology of soil micro-organisms." Methods for study-ing the ecology of soil micro-organisms.

Parvizi, J., A. D. Holiday, M. H. Ereth and D. G. Lewallen (1999). "Sudden death during primary hip arthroplasty." Clinical orthopaedics and related research **369**: 39-48.

Parvizi, J., B. G. Johnson, C. Rowland, M. H. Ereth and D. G. Lewallen (2001). "Thirty-day mortality after elective total hip arthroplasty." The Journal of Bone & Joint Surgery **83**(10): 1524-1528.

Patterson, F. and C. S. Brown (1972). "The McKee-Farrar total hip replacement." J Bone Joint Surg A **54**: 257-275.

Patti, G. J., O. Yanes and G. Siuzdak (2012). "Innovation: Metabolomics: the apogee of the omics trilogy." Nature reviews Molecular cell biology **13**(4): 263-269.

Paul, J. H. and G. I. Loeb (1983). "Improved microfouling assay employing a DNA-specific fluorochrome and polystyrene as substratum." Applied and environmental microbiology **46**(2): 338-343.

Pedersen, K. (1990). "Biofilm development on stainless steel and PVC surfaces in drinking water." Water Research **24**(2): 239-243.

Pelaez-Vargas, A., D. Gallego-Perez, M. Magallanes-Perdomo, M. Fernandes, D. Hansford, A. De Aza, P. Pena and F. Monteiro (2011). "Isotropic micropatterned silica coatings on zirconia induce guided cell growth for dental implants." dental materials **27**(6): 581-589.

Peppas, N. A. and R. Langer (1994). "New challenges in biomaterials." Science **263**(5154): 1715-1720.

Piper, K. E., M. J. Jacobson, R. H. Cofield, J. W. Sperling, J. Sanchez-Sotelo, D. R. Osmon, A. McDowell, S. Patrick, J. M. Steckelberg and J. N. Mandrekar (2009). "Microbiologic diagnosis of prosthetic shoulder infection by use of implant sonication." Journal of clinical microbiology **47**(6): 1878-1884.

Pogodin, S., J. Hasan, V. A. Baulin, H. K. Webb, V. K. Truong, T. H. P. Nguyen, V. Boshkovikj, C. J. Fluke, G. S. Watson and J. A. Watson (2013). "Biophysical model of bacterial cell interactions with nanopatterned cicada wing surfaces." Biophysical journal **104**(4): 835-840.

Politzer, I., B. Dowty and J. Laseter (1976). "Use of gas chromatography and mass spectrometry to analyze underivatized volatile human or animal constituents of clinical interest." Clinical chemistry **22**(11): 1775-1788.

Postollec, F., H. Falentin, S. Pavan, J. Combrisson and D. Sohier (2011). "Recent advances in quantitative PCR (qPCR) applications in food microbiology." Food microbiology **28**(5): 848-861.

Puleo, D. and A. Nanci (1999). "Understanding and controlling the bone–implant interface." Biomaterials **20**(23): 2311-2321.

Quirynen, M., H. C. Van Der Mei, C. M. Bollen, L. H. Van Den Bossche, G. I. Doornbusch, D. van Steenberghe and H. J. Busscher (1994). "The influence of surface-free energy on supra-and subgingival plaque microbiology. An in vivo study on implants." Journal of periodontology **65**(2): 162-167.

Raad, I., A. Alrahwan and K. Rolston (1998). "*Staphylococcus epidermidis*: emerging resistance and need for alternative agents." Clinical infectious diseases **26**(5): 1182-1187.

Rabinowitz, J., J. Purdy, L. Vastag, T. Shenk and E. Koyuncu (2011). Metabolomics in drug target discovery. Cold Spring Harbor symposia on quantitative biology, Cold Spring Harbor Laboratory Press.

Ramachandran, M. (2006). Basic orthopaedic sciences: the Stanmore guide, CRC Press.

Ramautar, R., A. Demirci and G. J. de Jong (2006). "Capillary electrophoresis in metabolomics." TrAC Trends in Analytical Chemistry **25**(5): 455-466.

Rammelt, S., T. Illert, S. Bierbaum, D. Scharnweber, H. Zwipp and W. Schneiders (2006). "Coating of titanium implants with collagen, RGD peptide and chondroitin sulfate." Biomaterials **27**(32): 5561-5571.

Ratner, B. D. (2004). Biomaterials science: an introduction to materials in medicine, Academic press.

Recsei, P., B. Kreiswirth, M. O'reilly, P. Schlievert, A. Gruss and R. Novick (1986). "Regulation of exoprotein gene expression in *Staphylococcus aureus* by agr." Molecular and General Genetics MGG **202**(1): 58-61.

Reysenbach, A.-L. and S. L. Cady (2001). "Microbiology of ancient and modern hydrothermal systems." Trends in microbiology **9**(2): 79-86.

Ribeiro, M., F. J. Monteiro and M. P. Ferraz (2012). "Infection of orthopedic implants with emphasis on bacterial adhesion process and techniques used in studying bacterial-material interactions." Biomatter **2**(4): 176-194.

Rijnaarts, H. H., W. Norde, E. J. Bouwer, J. Lyklema and A. J. Zehnder (1993). "Bacterial adhesion under static and dynamic conditions." Applied and Environmental Microbiology **59**(10): 3255-3265.

Rogers, H. J., H. R. Perkins and J. B. Ward (1980). "Microbial cell walls and membranes."

Rogers, K. L., P. D. Fey and M. E. Rupp (2009). Epidemiology of Coagulase-Negative Staphylococci and Infections Caused by These Organisms. Staphylococci in Human Disease, Wiley-Blackwell**:** 310-332.

Royet, J. and R. Dziarski (2007). "Peptidoglycan recognition proteins: pleiotropic sensors and effectors of antimicrobial defences." Nature Reviews Microbiology **5**(4): 264-277.

Ryan, K. and C. Ray (2004). "Enteroviruseses." Sherris Medical Microbiology (4th ed.). McGraw Hill: 535-537.

Sabatine, M. S., E. Liu, D. A. Morrow, E. Heller, R. McCarroll, R. Wiegand, G. F. Berriz, F. P. Roth and R. E. Gerszten (2005). "Metabolomic identification of novel biomarkers of myocardial ischemia." Circulation **112**(25): 3868-3875.

Safdar, N., L. Narans, B. Gordon and D. G. Maki (2003). "Comparison of culture screening methods for detection of nasal carriage of methicillin-resistant *Staphylococcus aureus*: a prospective study comparing 32 methods." Journal of clinical microbiology **41**(7): 3163-3166.

Salazar, O. and J. A. Asenjo (2007). "Enzymatic lysis of microbial cells." Biotechnology letters **29**(7): 985-994.

Sand, W. (1997). "Bacterial adhesion. molecular and ecological diversity. Hrsg. von Madilyn Fletcher, 361 Seiten, S/W-Abbildungen, Wiley-Liss, New York, USA 1996,£ 80.00, ISBN 0-471-02185-7." Materials and Corrosion **48**(9): 649-650.

Santavirta, S., M. Böhler, W. H. Harris, Y. T. Konttinen, R. Lappalainen, O. Muratoglu, C. Rieker and M. Salzer (2003). "Alternative materials to improve total hip replacement tribology." Acta orthopaedica Scandinavica **74**(4): 380-388.

Saran, N., R. Zhang and R. E. Turcotte (2011). "Osteogenic protein-1 delivered by hydroxyapatite-coated implants improves bone ingrowth in extracortical bone bridging." Clin Orthop Relat Res **469**(5): 1470-1478.

Sauer, K., A. K. Camper, G. D. Ehrlich, J. W. Costerton and D. G. Davies (2002). "Pseudomonas aeruginosa displays multiple phenotypes during development as a biofilm." Journal of bacteriology **184**(4): 1140-1154.

Sauer, U., D. R. Lasko, J. Fiaux, M. Hochuli, R. Glaser, T. Szyperski, K. Wüthrich and J. E. Bailey (1999). "Metabolic flux ratio analysis of genetic and environmental modulations of *Escherichia coli* central carbon metabolism." Journal of bacteriology **181**(21): 6679-6688.

Schaub, J. and M. Reuss (2008). "In vivo dynamics of glycolysis in *Escherichia coli* shows need for growth-rate dependent metabolome analysis." Biotechnology progress **24**(6): 1402-1407.

Scheuerman, T. R., A. K. Camper and M. A. Hamilton (1998). "Effects of substratum topography on bacterial adhesion." Journal of colloid and interface science **208**(1): 23-33.

Schlievert, P. M., L. M. Jablonski, M. Roggiani, I. Sadler, S. Callantine, D. T. Mitchell, D. H. Ohlendorf and G. A. Bohach (2000). "Pyrogenic toxin superantigen site specificity in toxic shock syndrome and food poisoning in animals." Infection and immunity **68**(6): 3630-3634.

Schutzbank, T. E. and N. Kahmann "Comparison of enzymes to lyse streptococcal bacteria prior to automated DNA purification on the BioRobot® M48."

Schwab, J. H., D. W. Watson and W. J. Cromartie (1955). "Further studies of group A streptococcal factors with lethal and cardiotoxic properties." The Journal of infectious diseases: 14-18.

Scottish-Arthoplasty-Project (2014). A summary of procedures and outcomes for patients undergoing arthroplasty operations during 2012-2013.

ScottishArthoplastyProject (2014). A summary of procedures and outcomes for patients undergoing arthroplasty operations during 2012-2013.

Sculco, T. (1992). "The economic impact of infected total joint arthroplasty." Instructional course lectures **42**: 349-351.

Shands, K. N., G. P. Schmid, B. B. Dan, D. Blum, R. J. Guidotti, N. T. Hargrett, R. L. Anderson, D. L. Hill, C. V. Broome and J. D. Band (1980). "Toxic-shock syndrome in menstruating women: association with tampon use and

Staphylococcus aureus and clinical features in 52 cases." New England Journal of Medicine **303**(25): 1436-1442.

Sherry, L., G. Lappin, L. O'Donnell, E. Millhouse, O. R. Millington, D. Bradshaw, A. Axe, C. Williams, C. J. Nile and G. Ramage (2016). "Viable compositional analysis of an eleven species oral polymicrobial biofilm." Frontiers in Microbiology **7**: 912.

Sigma-Aldrich (2015) "Lysing Enzymes."

Sjöström, T., A. S. Brydone, R. D. Meek, M. J. Dalby, B. Su and L. E. McNamara (2013). "Titanium nanofeaturing for enhanced bioactivity of implanted orthopedic and dental devices." Nanomedicine **8**(1): 89-104.

Sjöström, T., M. J. Dalby, A. Hart, R. Tare, R. O. Oreffo and B. Su (2009). "Fabrication of pillar-like titania nanostructures on titanium and their interactions with human skeletal stem cells." Acta Biomaterialia **5**(5): 1433-1441.

Sloot, N., M. Thomas, R. Marre and S. Gatermann (1992). "Purification and characterisation of elastase from *Staphylococcus epidermidis*." Journal of medical microbiology **37**(3): 201-205.

Smith, C. A., G. O'Maille, E. J. Want, C. Qin, S. A. Trauger, T. R. Brandon, D. E. Custodio, R. Abagyan and G. Siuzdak (2005). "METLIN: a metabolite mass spectral database." Therapeutic drug monitoring **27**(6): 747-751.

Smith, C. J. and A. M. Osborn (2009). "Advantages and limitations of quantitative PCR (Q-PCR)-based approaches in microbial ecology." FEMS microbiology ecology **67**(1): 6-20.

Soballe, K. (1993). "Hydroxyapatite ceramic coating for bone implant fixation. Mechanical and histological studies in dogs." Acta Orthop Scand Suppl **255**: 1-58.

Sochart, D. H. (2012). The Infected Implant - what Next?, Triton.

Sousa, C., P. Teixeira and R. Oliveira (2009). "Influence of surface properties on the adhesion of *Staphylococcus epidermidis* to acrylic and silicone." International journal of biomaterials **2009**.

Stepanović, S., D. Vuković, I. Dakić, B. Savić and M. Švabić-Vlahović (2000). "A modified microtiter-plate test for quantification of staphylococcal biofilm formation." Journal of Microbiological Methods **40**(2): 175-179.

Stepanović, S., D. Vuković, V. Hola, G. D. BONAVENTURA, S. Djukić, I. Ćirković and F. Ruzicka (2007). "Quantification of biofilm in microtiter plates: overview of testing conditions and practical recommendations for assessment of biofilm production by staphylococci." Apmis **115**(8): 891-899.

Stipetic, L. H., M. J. Dalby, R. L. Davies, F. R. Morton, G. Ramage and K. E. V. Burgess (2016). "A novel metabolomic approach used for the comparison of *Staphylococcus aureus* planktonic cells and biofilm samples." Metabolomics **12**(4): 1-11.

Stipetic, L. H., G. Hamilton, M. J. Dalby, R. L. Davies, R. D. Meek, G. Ramage, D. G. Smith and K. E. Burgess (2015). "Draft genome sequence of isolate

Staphylococcus aureus LHSKBClinical, isolated from an infected hip." Genome announcements **3**(2): e00336-00315.

Stock, J. B., A. M. Stock and J. M. Mottonen (1990). "Signal transduction in bacteria." Nature **344**(6265): 395-400.

Strasters, K. and K. Winkler (1963). "Carbohydrate metabolism of *Staphylococcus aureus*." Journal of general microbiology **33**(2): 213-229.

Surgeon, A. a. o. O. (2013). "Total Knee Replacement."

System, T. M. H. (2003). A Patient's Guide to Artificial Joint Replacement of the Hip. http://www.eorthopod.com/.

Tang, H., T. Cao, X. Liang, A. Wang, S. O. Salley, J. McAllister and K. Ng (2009). "Influence of silicone surface roughness and hydrophobicity on adhesion and colonization of *Staphylococcus epidermidis*." Journal of Biomedical Materials Research Part A **88**(2): 454-463.

Tautenhahn, R., C. Böttcher and S. Neumann (2008). "Highly sensitive feature detection for high resolution LC/MS." BMC bioinformatics **9**(1): 1.

Taylor, R. L., J. Verran, G. C. Lees and A. P. WARD (1998). "The influence of substratum topography on bacterial adhesion to polymethyl methacrylate." Journal of Materials Science: Materials in Medicine **9**(1): 17-22.

Teixeira, A. I., G. A. Abrams, P. J. Bertics, C. J. Murphy and P. F. Nealey (2003). "Epithelial contact guidance on well-defined micro-and nanostructured substrates." Journal of cell science **116**(10): 1881-1892.

Teufel, P. and F. Götz (1993). "Characterization of an extracellular metalloprotease with elastase activity from *Staphylococcus epidermidis*." Journal of bacteriology **175**(13): 4218-4224.

Timmerman, C., E. Mattsson, L. Martinez-Martinez, L. De Graaf, J. Van Strijp, H. Verbrugh, J. Verhoef and A. Fleer (1993). "Induction of release of tumor necrosis factor from human monocytes by staphylococci and staphylococcal peptidoglycans." Infection and immunity **61**(10): 4167-4172.

Trampuz, A., K. E. Piper, M. J. Jacobson, A. D. Hanssen, K. K. Unni, D. R. Osmon, J. N. Mandrekar, F. R. Cockerill, J. M. Steckelberg and J. F. Greenleaf (2007). "Sonication of removed hip and knee prostheses for diagnosis of infection." New England Journal of Medicine **357**(7): 654-663.

Trampuz, A., J. M. Steckelberg, D. R. Osmon, F. R. Cockerill Iii, A. D. Hanssen and R. Patel (2003). "Advances in the laboratory diagnosis of prosthetic joint infection." Reviews in Medical Microbiology **14**(1): 1-14.

Trampuz, A. and A. F. Widmer (2006). "Infections associated with orthopedic implants." Current opinion in infectious diseases **19**(4): 349-356.

Trampuz, A. and W. Zimmerli (2005). "Prosthetic joint infections: update in diagnosis and treatment." Swiss Med Wkly **135**(17-18): 243-251.

Tranter, H., S. C. Tassou and G. Nychas (1993). "The effect of the olive phenolic compound, oleuropein, on growth and enterotoxin B production by *Staphylococcus aureus*." Journal of Applied Bacteriology **74**(3): 253-259.

Tresse, O., R. de Wit, V. Cassisa, G. Le Pennec, D. Haras and M. Federighi (2008). "NATURAL BACTERIAL BlOFILMS IN THE ENVIRONMENT." Cell Differentiation Research Developments: 99.

Tsimbouri, P., N. Gadegaard, K. Burgess, K. White, P. Reynolds, P. Herzyk, R. Oreffo and M. J. Dalby (2014). "Nanotopographical effects on mesenchymal stem cell morphology and phenotype." Journal of cellular biochemistry **115**(2): 380-390.

Tsimbouri, P. M., R. J. McMurray, K. V. Burgess, E. V. Alakpa, P. M. Reynolds, K. Murawski, E. Kingham, R. O. Oreffo, N. Gadegaard and M. J. Dalby (2012). "Using nanotopography and metabolomics to identify biochemical effectors of multipotency." ACS nano **6**(11): 10239-10249.

Tunney, M. M., S. Patrick, M. D. Curran, G. Ramage, D. Hanna, J. R. Nixon, S. P. Gorman, R. I. Davis and N. Anderson (1999). "Detection of prosthetic hip infection at revision arthroplasty by immunofluorescence microscopy and PCR amplification of the bacterial 16S rRNA gene." Journal of clinical microbiology **37**(10): 3281-3290.

Vieira, F. and E. Nahas (2005). "Comparison of microbial numbers in soils by using various culture media and temperatures." Microbiological research **160**(2): 197-202.

Vitko, N. P. and A. R. Richardson (2013). "Laboratory Maintenance of Methicillin-Resistant *Staphylococcus aureus* (MRSA)." Current protocols in microbiology **0 9**: Unit-9C.2.

Vogel, V. and M. Sheetz (2006). "Local force and geometry sensing regulate cell functions." Nature reviews molecular cell biology **7**(4): 265-275.

Vollmer, W., D. Blanot and M. A. De Pedro (2008). "Peptidoglycan structure and architecture." FEMS microbiology reviews **32**(2): 149-167.

Vuong, C. and M. Otto (2002). "*Staphylococcus epidermidis* infections." Microbes Infect **4**(4): 481-489.

Walsh, C. T. (1989). "Enzymes in the D-alanine branch of bacterial cell wall peptidoglycan assembly." Journal of biological chemistry **264**(5): 2393-2396.

Wang, I. W., J. M. Anderson, M. R. Jacobs and R. E. Marchant (1995). "Adhesion of *Staphylococcus epidermidis* to biomedical polymers: contributions of surface thermodynamics and hemodynamic shear conditions." Journal of biomedical materials research **29**(4): 485-493.

Wang, T. J., M. G. Larson, R. S. Vasan, S. Cheng, E. P. Rhee, E. McCabe, G. D. Lewis, C. S. Fox, P. F. Jacques and C. Fernandez (2011). "Metabolite profiles and the risk of developing diabetes." Nature medicine **17**(4): 448-453.

Wang, W., Y. Ouyang and C. K. Poh (2011). "Orthopaedic implant technology: biomaterials from past to future." Annals of the Academy of Medicine-Singapore **40**(5): 237.

Webber, R. J., M. G. Harris and A. J. Hough (1985). "Cell culture of rabbit meniscal fibrochondrocytes: proliferative and synthetic response to growth factors and ascorbate." Journal of orthopaedic research **3**(1): 36-42.

Whalen, W. A., M. D. Wang and C. M. Berg (1985). "beta-Chloro-L-alanine inhibition of the *Escherichia coli* alanine-valine transaminase." Journal of Bacteriology **164**(3): 1350-1352.

Widmer, A. F. (2001). "New developments in diagnosis and treatment of infection in orthopedic implants." Clinical Infectious Diseases **33**(Supplement 2): S94-S106.

Wiechert, W. (2001). "13 C metabolic flux analysis." Metabolic engineering **3**(3): 195-206.

Willert, H. and G. Buchhorn (1998). "Osseointegration of cemented and noncemented implants in artificial hip replacement: long-term findings in man." Journal of long-term effects of medical implants **9**(1-2): 113-130.

Williams, J. M., M. Trope, D. J. Caplan and D. C. Shugars (2006). "Detection and Quantitation of *E. faecalis* by Real-time PCR (qPCR), Reverse Transcription-PCR (RT-PCR), and Cultivation During Endodontic Treatment." Journal of endodontics **32**(8): 715-721.

Wishart, D. S. (2008). "Metabolomics: applications to food science and nutrition research." Trends in Food Science & Technology **19**(9): 482-493.

Wishart, D. S., D. Tzur, C. Knox, R. Eisner, A. C. Guo, N. Young, D. Cheng, K. Jewell, D. Arndt and S. Sawhney (2007). "HMDB: the human metabolome database." Nucleic acids research **35**(suppl 1): D521-D526.

Wojtowicz, A. M., A. Shekaran, M. E. Oest, K. M. Dupont, K. L. Templeman, D. W. Hutmacher, R. E. Guldberg and A. J. Garcia (2010). "Coating of biomaterial scaffolds with the collagen-mimetic peptide GFOGER for bone defect repair." Biomaterials **31**(9): 2574-2582.

Wyllie, A. H. (1980). "Glucocorticoid-induced thymocyte apoptosis is associated with endogenous endonuclease activation." Nature **284**(5756): 555-556.

Xu, K. D., G. A. McFeters and P. S. Stewart (2000). "Biofilm resistance to antimicrobial agents." Microbiology **146**(3): 547-549.

Xu, L.-C. and C. A. Siedlecki (2012). "Submicron-textured biomaterial surface reduces staphylococcal bacterial adhesion and biofilm formation." Acta biomaterialia **8**(1): 72-81.

Yang, Z.-z., M. Habib, J.-b. Shuai and W.-h. Fang (2007). "Detection of PCV2 DNA by SYBR green I-based quantitative PCR." Journal of Zhejiang University Science B **8**(3): 162-169.

Yarwood, J. M., D. J. Bartels, E. M. Volper and E. P. Greenberg (2004). "Quorum sensing in *Staphylococcus aureus* biofilms." Journal of bacteriology **186**(6): 1838-1850.

Yu, J. C., W. Ho, J. Lin, H. Yip and P. K. Wong (2003). "Photocatalytic activity, antibacterial effect, and photoinduced hydrophilicity of TiO2 films coated on a stainless steel substrate." Environ Sci Technol **37**(10): 2296-2301.

Zimmerli, W., A. Trampuz and P. E. Ochsner (2004). "Prosthetic-joint infections." New England Journal of Medicine **351**(16): 1645-1654.